DETERMINATION OF ROCK JOINT SHEAR STRENGTH BASED ON ROCK PHYSICAL PROPERTIES

Rutthapol Kemthong

A Thesis Submitted in Partial Fulfillment of the Requirements for the

Degree of Master of Engineering in Geotechnology

Suranaree University of Technology

Academic Year 2006

การกำหนดกำลังรับแรงเฉือนของรอยแตกหิน
โดยใช้คุณสมบัติทางกายภาพ

รัฐพล เข็มทอง

วิทยานิพนธ์นี้เป็นส่วนหนึ่งของการศึกษาตามหลักสูตรปริญญาวิศวกรรมศาสตรมหาบัณฑิต

สาขาวิชาเทคโนโลยีธรณี

มหาวิทยาลัยเทคโนโลยีสุรนารี

ปีการศึกษา 2549

DETERMINATION OF ROCK JOINT SHEAR STRENGTH BASED ON ROCK PHYSICAL PROPERTIES

Suranaree University of Technology has approved this thesis submitted in partial fulfillment of the requirements for a Master's Degree.

Thesis Examining Committee

_____

(Asst. Prof. Thara Lekuthai)

Chairperson

_____

(Assoc. Prof. Dr. Kittitep Fuenkajorn)

Member (Thesis Advisor)

_____

(Assoc. Prof. Ladda Wannakao)

Member

_____ _____

(Assoc. Prof. Dr. Saowanee Rattanaphani) (Assoc. Prof. Dr. Vorapot Khompis)

Vice Rector for Academic Affairs Dean of Institute of Engineering

รัฐพล เข็มทอง : การกำหนดกำลังรับแรงเฉือนของรอยแตกหินโดยใช้คุณสมบัติทางกายภาพ (DETERMINATION OF ROCK JOINT SHEAR STRENGTH BASED ON ROCK PHYSICAL PROPERTIES) อาจารย์ที่ปรึกษา : รองศาสตราจารย์ ดร.กิตติเทพ เฟื่องขจร, 123 หน้า.

ชุดของการทดสอบกำลังเฉือนของรอยแตกในหินได้ดำเนินการเพื่อที่จะประเมินความสามารถในการคาดคะเนของกฎกำลังรับแรงเฉือน ที่ใช้คุณสมบัติเชิงกายภาพและค่าคงที่ที่กำหนดในภาคสนาม ตัวอย่างหินจากสิบแหล่งที่เป็นตัวแทนของหินที่พบบ่อยครั้งในอุตสาหกรรมการก่อสร้างและเหมืองแร่ในประเทศไทยได้นำมาจัดเตรียมและทดสอบในห้องปฏิบัติการ ตัวอย่างหินเหล่านี้ประกอบไปด้วย หินบะซอลต์หนึ่งชนิด หินอ่อนสองชนิด หินแกรนิตสามชนิด และหินทรายสี่ชนิด นอกจากนั้นการศึกษายังมุ่งเน้นไปที่ความน่าเชื่อถือของวิธีการที่ใช้ในภาคสนามสำหรับกำหนดค่ามุมเสียดทานพื้นฐาน (ϕ_b) ค่ากำลังกดในแกนเดียว (UCS หรือความแข็งของผนังรอยแตก) และค่าสัมประสิทธิ์ของความขรุขระ (JRC) ตัวอย่างหินที่ตัดให้มีผิวเรียบจัดเตรียมเพื่อใช้ในการทดสอบหาความสัมพันธ์ระหว่าง ϕ_b กับคุณสมบัติเชิงกลศาสตร์ และเชิงแร่วิทยาของหิน ตัวอย่างหินที่มีรอยแตกที่เกิดจากการดึงในห้องปฏิบัติการได้นำมาทดสอบเพื่อหาค่ากำลังเฉือนของรอยแตกที่มี JRC ระดับต่าง ๆ กัน และนำผลมาใช้สอบทานกฎกำลังเฉือนที่ถูกพัฒนาด้วยค่าคงที่ที่กำหนดในภาคสนาม ค่า JRC ของรอยแตกเหล่านี้ได้ถูกประเมินอย่างอิสระโดยวิศวกรสองคน ค่า UCS ได้ประเมินด้วยวิธีในภาคสนามที่แนะนำโดย ISRM (ใช้ฆ้อนธรณีและมีดพก) และได้นำมาเปรียบเทียบกับวิธีการทดสอบมาตรฐานที่ได้จากห้องปฏิบัติการที่เสนอโดย ASTM ความน่าเชื่อถือและความอ่อนไหวของค่าคงที่ทั้งสามได้ถูกตรวจสอบโดยการเปรียบเทียบค่ากำลังเฉือนที่คาดคะเนได้กับค่ากำลังเฉือนของรอยแตกผิวขรุขระที่ทดสอบได้จริงในห้องปฏิบัติการ

ผลจากการศึกษาระบุว่ากฎที่พัฒนาโดยใช้ค่าคงที่ที่กำหนดในภาคสนามสามารถคาดคะเนค่ากำลังรับแรงเฉือนของรอยแตกผิวขรุขระได้ดีสำหรับหินอ่อนและหินทรายที่นำมาจากทุกแหล่ง และจะให้ค่าสูงเกินไปเล็กน้อยสำหรับตัวอย่างหินบะซอลต์ แต่กฎนี้ไม่สามารถอธิบายกำลังเฉือนของรอยแตกในตัวอย่างหินแกรนิตได้ซึ่งอาจเกิดขึ้นจากผิวตัดเรียบของหินที่มีขนาดของผลึกแร่ใหญ่และมีความแข็งมาก (เช่น หินแกรนิต) จะมีความเรียบมากถึงแม้จะไม่มีการฝนขัด ดังนั้นจึงทำให้ค่า ϕ_b ที่ได้จากการทดสอบแรงเฉือนมีค่าต่ำเกินความเป็นจริง ผลจากการประเมินความอ่อนไหวระบุว่ากำลังรับแรงเฉือนที่คำนวณได้จากกฎของ Barton จะอ่อนไหวต่อค่า ϕ_b มากกว่าค่า UCS และ JRC ค่าของ UCS ที่ประเมินด้วยวิธีในภาคสนามของ ISRM จะสอดคล้องเป็นอย่างดีกับค่าที่ทดสอบในห้องปฏิบัติการด้วยวิธีมาตรฐาน ASTM การผันแปรของค่า UCS สำหรับหินที่มีระดับความแข็ง R2 และ R3 (ผันแปรประมาณ 25 MPa) และสำหรับหินที่มีระดับความแข็ง R4 และ R5 (ผันแปร

ประมาณ 50 MPa) จะไม่มีผลกระทบเท่าใดนักต่อค่ากำลังเฉือนที่คาดคะเนได้ สำหรับหินทรายค่า ϕ_b จะอยู่ในช่วง 25-35 องศา และจะไม่ขึ้นกับ UCS หรือวัสดุที่เชื่อมเม็ดหิน ค่า ϕ_b สำหรับหินอ่อนที่ทดสอบในงานวิจัยนี้ รวมกับหินปูนที่ทดสอบได้จากที่อื่นจะมีค่าเฉลี่ยเท่ากับ 35 ± 5 องศา และจะไม่ขึ้นกับ UCS หรือการผันแปรของแร่ประกอบหิน สำหรับหินชนิดอื่น ϕ_b จะมีแนวโน้มเพิ่มขึ้นถ้า UCS เพิ่มขึ้นโดยเฉพาะอย่างยิ่งสำหรับหินที่แข็งมาก (R5 และ R6) งานวิจัยนี้ไม่พบความสัมพันธ์ระหว่าง ϕ_b กับค่าสัมประสิทธิ์ของความยืดหยุ่นหรือกับค่ากำลังดึงสูงสุดของหิน จำนวน และความหลากหลายของตัวอย่างหินแกรนิตมีไม่เพียงพอที่จะกำหนดความสัมพันธ์ระหว่าง ϕ_b กับการผันแปรของแร่ประกอบหินถึงแม้ว่าความสัมพันธ์นั้นอาจมีอยู่จริง

สาขาวิชาเทคโนโลยีธรณี ลายมือชื่อนักศึกษา_____

ปีการศึกษา 2549 ลายมือชื่ออาจารย์ที่ปรึกษา _____

RUTTHAPOL KEMTHONG : DETERMINATION OF ROCK JOINT SHEAR STRENGTH BASED ON ROCK PHYSICAL PROPERTIES. THESIS ADVISOR : ASSOC. PROF. KITTITEP FUENKAJORN, Ph.D., P.E. 123 PP.

ROCK JOINT/SHEAR STRENGTH/ FRICTION/ROUGHNESS

A series of direct shear tests have been performed in an attempt at assessing the predictive capability of the joint shear strength criterion by using rock physical properties and field-determined parameters. Rocks from ten different source locations representing the most commonly encountered rocks in Thailand construction and mining industries are prepared and tested in the laboratory. These include basalt, two marbles, three granites and four sandstones. The investigation also concentrates on the reliability of the field methods and results for determining the basic friction angle (ϕ_b), the uniaxial compressive strength (UCS or joint wall strength), and the joint roughness coefficient (JRC). The saw-cut surface specimens are prepared to determine the relationship between ϕ_b and the mechanical and mineralogical properties of the rocks. The specimens with tension-induced fractures are tested to obtain the joint shear strength under different JRC's, for use in verification of the criterion developed from the field determined parameters. The JRC's for the rough-joint specimens are evaluated by two independent engineers. The UCS's evaluated from the ISRM-suggested field methods (i.e. using geologic hammer and pocket knife) are used in the Barton's criterion, and are compared with those tested under the relevant ASTM standard method. Reliability and sensitivity of the three parameters are examined by comparing the predicted shear strength with those actually obtained from the direct shear testing on the rough joint surfaces.

The results indicate that the criterion with the field-determined parameters can well predict the shear strength of the rough joints in marbles and sandstones from all source locations, and slightly over-predicts the shear strength in the basalt specimens. The criterion however can not describe the joint shear strengths for the granite specimens. This discrepancy is due to the fact that the saw-cut surfaces for the coarse-grained and very strong crystalline rocks (such as granites) are very smooth, even without polishing, and hence results in an unrealistically low ϕ_b from the direct shear testing. The sensitivity evaluation also suggests that the Barton's shear strength is more sensitive to ϕ_b than to UCS and JRC. The range of UCS from ISRM field-determined method agrees well with the corresponding value determined by ASTM laboratory testing. Variations of the UCS by 25 MPa for weak and medium rocks (R2 and R3) and by 50 MPa for strong and very strong rocks (R4 and R5) do not significantly affect the predicted shear strengths. For all sandstones the ϕ_b values are in the range of 25-35 degrees, and are independent of their UCS and cementing materials. The ϕ_b values for the tested marbles and for the limestone recorded elsewhere are averaged as 35±5 degrees. They are also independent of UCS and mineralogical variation. For other rock types, ϕ_b tends to increase with UCS particularly for very strong rocks (R5 and R6). No relationship between ϕ_b and elastic modulus or tensile strength has been found for any rock types. The number and diversity of the tested granites are inadequate to determine the relationship between ϕ_b and their mineralogical variations, if there is any.

School of Geotechnology Student's Signature _____

Academic Year 2004 Advisor's Signature _____

ACKNOWLEDGMENTS

The author wishes to acknowledge the funding support of Suranaree University to Technology (SUT).

Grateful thanks and appreciation are given to Assoc. Prof. Dr. Kittitep Fuenkajorn, thesis advisor, who allowed the author work independently, but gave a critical review of this research. Many thanks are also extended to Asst. Prof. Thara Lekuthai and Assoc. Prof. Ladda Wannakao, who served on the thesis committee and commented on the manuscript.

Finally, the author extends his heartfelt gratitude to his parents who put him in the path of learning.

Rutthapol Kemthong

TABLE OF CONTENTS

Page

TABLE OF CONTENTS (Continued)

Page

TABLE OF CONTENTS (Continued)

Page

TABLE OF CONTENTS (Continued)

Page

LIST OF TABLES

Table **Page**

LIST OF TABLES (Continued)

Table **Page**

LIST OF FIGURES

Figure **Page**

LIST OF FIGURES (Continued)

Figure **Page**

LIST OF FIGURES (Continued)

Figure **Page**

LIST OF FIGURES (Continued)

Figure **Page**

LIST OF FIGURES (Continued)

Figure **Page**

LIST OF FIGURES (Continued)

Figure **Page**

LIST OF SYMBOLS AND ABBREVIATIONS

ϕ	=	Friction angle
τ	=	Joint shear strength
ϕ_A	=	The estimate basic friction angle
ϕ_b	=	Basic friction angle
σ_c	=	Uniaxial compressive strength
σ_j	=	Uniaxial compressive strength
σ_n	=	Normal stress
τ_r	=	Shear strength of the intact material
ϕ_r	=	Residual friction angle
α_S	=	The angle at which sliding commences
σ_t	=	Tensile strength
a_s	=	The proportion of the discontinuity surface
c	=	Cohesive strength
d_n	=	The dilatation
E	=	Modulus of elasticity
i	=	Regular teeth inclination
JCS	=	Joint wall compressive strength
JRC	=	Joint roughness coefficient
UCS	=	Uniaxial compressive strength
V	=	The dilation rate

CHAPTER I

INTRODUCTION

1.1 Rationale and Background

Rock joint shear strength is one of the key properties used in the stability analysis and design of engineering structures in rock mass, e.g. slopes, tunnels and foundations (Hoek and Brown, 1980). The conventional method currently used to determine the joint shear strength is the direct shear testing which can be performed in the field and in the laboratory. The portable direct shear machine used in the field often can not provide sufficiently reliable results, primarily due to the limited specimen size allowed. A large scale direct machine used in the laboratory is expensive and is not widely available to the designers and field engineers. The testing process is not only costly but also time consuming, and subsequently the number of the test specimens is usually limited. The results obtained therefore can not truly represent the overall behavior of the rock mass structures. A new approach to determine the shear strength of rock joint is highly desirable, particularly, if it does not require laboratory and field testing processes.

1.2 Research objective

The objective of this research is to develop a new approach to determine the rock joint shear strength. A joint shear strength criterion is proposed with a set of parameters that can be determined in the field. The Barton's shear strength will be

defined as a function of the basic friction angle, compressive strength, joint roughness coefficient (JRC), and material constants. The basic friction angle and the rock strength will be inferred from the petrographic features of the rock (e.g., grain size, type and strength of the rock-forming minerals, and density). A mathematical relationship between these parameters will be derived. The actual JRC can be observed directly in the field. Since all parameters can be field-determined, this approach can bypass the direct shear testing process.

1.3 Research Methodology

1.3.1 Literature Review

Literature review will be carried out to study the state-of-the-art of direct shear strength testing, the shear strength criterion of rock joints, and the effects of petrography to the shear strengths (gain size, grain shape, color, compositions, etc.). These include theories, test procedures, results, analysis and applications. The sources of information are from journals, technical reports and conference papers. A summary of the literature review will be given in the thesis.

1.3.2 Sample Collection and Preparation

Rock samples will be collected from the site. The selection criteria are that the rocks should cover a large variety as much as possible, and that the sample collection should be convenient and repeatable. Ten rock types of the crystalline and clastic rocks will be collected and prepared. Sample preparation will be carried out in the laboratory at the Suranaree University of Technology. Preparation of these samples will follow the relevant ASTM standard (ASTM D4543, 1985) as much as practical.

1.3.3 Experimental Work

The prepared specimens of the ten rock types will be tested in the laboratory. The laboratory testing is divided into three main groups as follows.

1.3.3.1 Characterization Tests

The characterization tests include the uniaxial compressive strength test (ASTM D2938, 1986) and the direct shear strength test to obtain basic friction angle (ASTM D5607, 1995). The characterization tests yield data basis for use in the analysis of the rock joint shear strength.

1.3.3.2 Petrology Study

Micro-petrographic study will be performed by means of thin section analysis. A polished thin section is prepared and examined for each rock type using optical microscopy techniques. Petrologic parameters include type and percentage by volume of minerals, grain and crystal size, and orientation, and types of cementing materials. The results are used for developing the relation with the shear strength properties of the rock.

1.3.3.3 Verification Tests

A series of the direct shear strength tests of rough joints is performed to determine parameters in the proposed joint shear strength criterion for various Joint Roughness Coefficient (JRC) values. The test procedures will follow the relevant ASTM standard (ASTM D5607, 1995). The results of peak shear strength and residual shear strength will be compared with the joint shear strength from the prediction.

1.3.4 Relationships between Basic Friction Angle and Physical Properties

Determination of the relationships between basic friction angle and physical properties is divided into 2 parts: 1) using basic friction angle from characterization test, and 2) using database from a broad range of rock types. Both relationships will be compared with compressive and tensile strengths for determination of mathematical relation.

1.3.5 Prediction of Rock Joint Shear Strength and Verification

The rock joint shear strength of different JRC values will be predicted by Barton's joint strength criterion. The constants in the joint shear strengths of ten rock types will be calculated, including basic friction angle (ϕ_b), Joint Roughness Coefficient (JRC), and uniaxial compressive strength ($\sigma_{c,}$ or σ_j). The results will be compared by verification test in task 1.3.3.3.

1.3.6 Thesis Writing and Presentation

All aspects of the studies mentioned will be documented and incorporated into the thesis. The thesis will discuss the validity and potential applications of the results. It will be submitted at the end of the research.

1.4 Scope and Limitation of the Study

Ten types of rock most commonly found in the northeast of Thailand are collected and tested in the laboratory to study the petrology and the mechanical properties. The test series include the uniaxial compressive strength test (ASTM D2938, 1979) and the direct shear strength test (ASTM D5607, 1995). The analytical and experimental works assume homogeneous and isotropic conditions. The study will not include the shape and size effects. The effects of loading rate, temperature

and chemical changing will not be considered (i.e. assumed constant). The test samples will be in dry condition. No in-filling in rock joint apertures. The plastic behavior will not be considered in the analysis. The applied normal load is low (less than 50% of the rock strength).

1.5 Thesis Contents

This research thesis is divided into seven chapters. The first chapter includes problem and rationale, research objectives, scope of work, and research methodology. Chapter II presents results of the literature review on shear strength criteria, shear strength parameters, effect of petrology on mechanical properties, and shear strength testing. Chapter III describes sample collection and preparation. Chapter IV describes the experiments including 1) uniaxial compressive strength test, 2) direct shear test on saw-cut surface, 3) mineralogical study, 4) direct shear tests on rough surface, 5) rock strength estimation by manual index tests, and 6) basic friction angle by tilt test method. Chapter V presents the relationship between basic friction angles and rock strength. Chapter VI discusses the prediction of rock joint shear strength. Chapter VII provides discussions and conclusions.

Summary of uniaxial compressive strength test results is given in Appendix A. Summary of the shear stresses plotted against normal stresses is given in Appendix B. Summary of force-displacement curve of the direct shear strength tests on the rough joints is presented in Appendix C.

CHAPTER II

LITERATURE REVIEW

This chapter summarizes the results of literature review on the topics relevant to this research, including shear strength criteria, shear strength parameters, effect of petrology on mechanical properties, and shear strength testing,

2.1 Shear Strength Criteria

The mechanical rock properties are one of the most important parameters that will be used in the analysis and design of any engineering structures in rock mass. If structural mapping identifies discontinuities in rock mass on which shear type failures may take place, it will be necessary to determine the fiction angle and cohesion of the discontinuity surface in order to carry out stability analyses and design remedial work if required.

Several criteria have been proposed in the past to identify the strength of a rough rock joint. These criteria delineate the state of stress that separates pre-sliding and post-sliding of the joint. The simplest peak-shear strength model for rock joints is perhaps Patton's model (Patton, 1966). Based on the Coulomb friction law, this model characterizes the joint behavior by a single surface parameter that is the average roughness angle. More complicated joint models appeared later, accompanying the development of numerical methods. Notable among them are Ladanyi's empirical model (Ladanyi and Archambault, 1970) and Barton's emprical model (Barton, 1973).

Coulomb criterion represents the relationship between the peak shear strength and normal stress by

$$\tau = c + \sigma_n \text{ Tan } \phi \tag{2.1}$$

where τ is joint shear strength, σ_n is normal stress, c is the cohesive strength, and ϕ is angle of friction.

Patton (1966) performed a series of constant load stress direct shear tests with regular teeth inclination (i) at varying normal stresses. From these tests, he established a bilinear failure envelope - failure from an asperity sliding and asperity shearing mode.

$$\tau = \sigma_n \text{ Tan } (\phi_B + i) \tag{2.2}$$

where τ is joint shear strength, σ_n is normal stress, ϕ_B is basic friction angle, and i is regular teeth inclination.

Ladanyi and Archambault (1970) suggest the shear strength of the material adjacent to the discontinuity surfaces,

$$\tau = \frac{\sigma_n (1 - a_s)(V + \text{Tan}\phi) + a_s \cdot \tau_r}{1 - (1 - a_s) V \text{ Tan}\phi_B} \tag{2.3}$$

where τ is joint shear strength, ϕ_B is basic friction angle, a_s is the proportion of the discontinuity surface which is sheared through projections of intact material, V is the dilation rate (dv/du) at peak shear strength, and τ_r is the shear strength of the intact material.

Barton (1973) has studied the behavior of natural rock joints and proposed a criterion that is modified from Patton. It can be re-written as

$$\tau = \sigma_n \text{ Tan } \{\phi_B + \text{JRC Log}_{10} (\text{JCS}/\sigma_n)\} \quad (2.4)$$

where τ is joint shear strength, ϕ_B is basic friction angle, σ_n is normal stress, JRC is the joint roughness coefficient, and JCS is the joint wall compressive strength.

There are some constraints for the use of this criterion. Barton and Choubey (1977) recommend that the peak shear strength curves should be truncated for designing purposes at a maximum allowable shear strength given by $\text{Tan}^{-1} (\tau/\sigma_n) = 70^o$. For unfilled joints, the roughness and compressive strength of the wall are important, whereas in the case of filled joints the physical properties of the material separating the joints wall are of the primary concern. Barton criterion is only valid where joint wall is in rock-to-rock contact. Hoek and Bray (1981) report that the criterion is valid for the normal stress range, $0.01 < (\sigma_n/\text{JCS}) < 0.3$.

2.2 Shear Strength Parameters

2.2.1 Roughness

Roughness is a measurement of the inherent surface unevenness and waviness of the discontinuity related to its mean plane. It is a potentially important component of shear strength, especially in the case of dislocated and interlocked fractures (e.g. unfilled joints). Barton (1972, 1973, 1976), and Barton and Choubey (1977) have proposed a joint roughness coefficient (JRC) to describe the surface roughness scaled from zero to 20. Typical roughness profiles for entire JRC range are represented in Figure 2.1. The measurements of this index are estimated by using the direct profiling method for the joint, or by an indirect method. Barton and Bandis (1990) also have considered the scale effects of JRC and proposed JRC values for

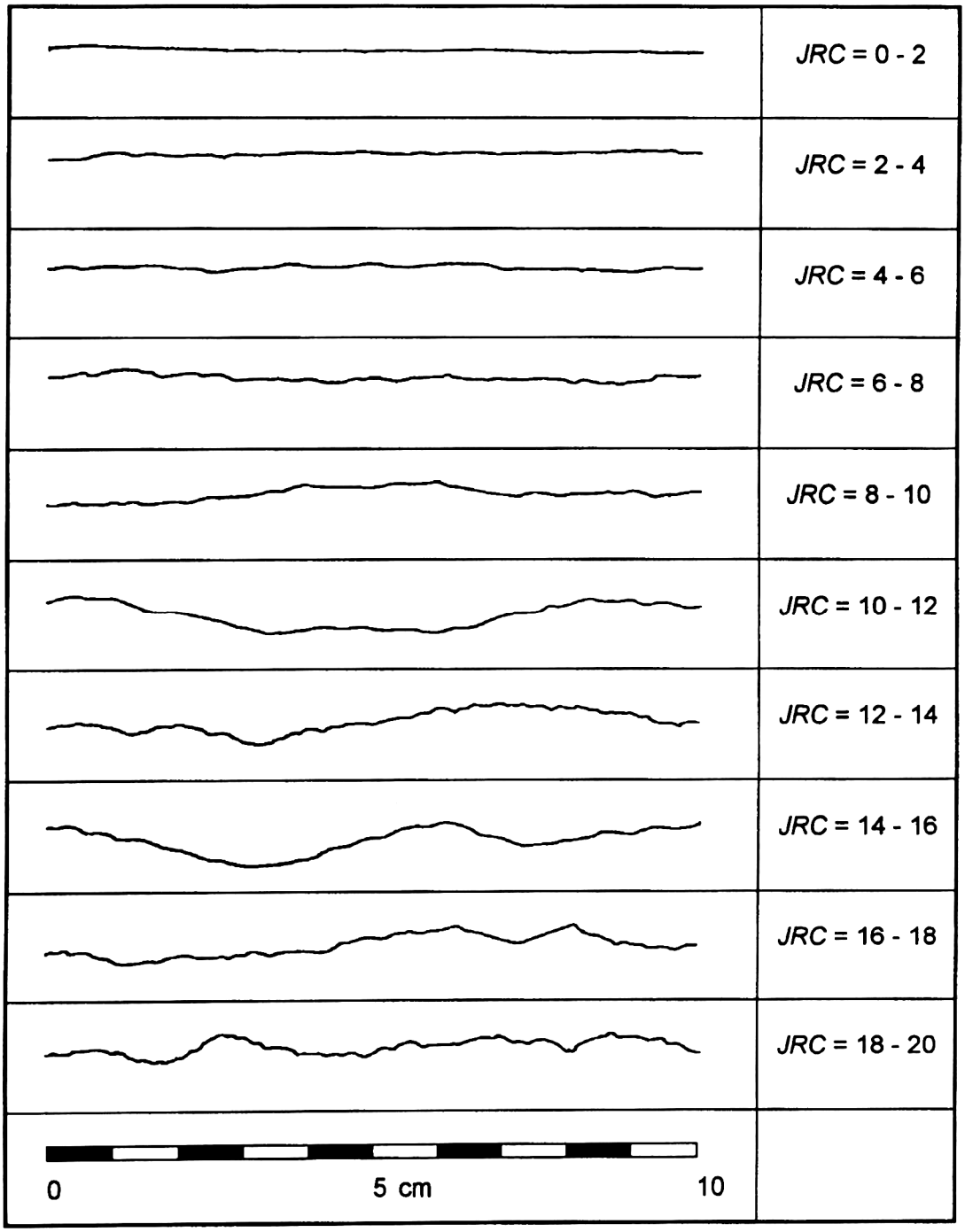

Figure 2.1 Roughness profile and corresponding JRC value (from Barton and Choubey, 1977)**.**

joints of large scale. The International Society for Rock Mechanics (ISRM) recommends that in general terms the roughness of the discontinuity walls can be characterized by waviness (large-scale undulation) and by unevenness (small-scale roughness).

Deere and Miller (1966) have proposed joint wall compressive strength (JCS). It is a very important component of shear strength and deformation, especially when the walls are in direct rock-to-rock contact as in the case of unfilled joints. Slight dislocation of joints caused by shear displacement within the rock mass can often result in small asperity contact areas with the stresses locally approaching or reaching the compression strength of the rock wall material, producing asperity damage. Brown (1981) suggests the technique for estimating JCS by Schnidt Rebound Hammer test. The technique concerns with the unit of rock, hammer orientation, and Schimidt hardness. Barton and Bandis (1993) have studied the scale effects of JSC. The results show that joint wall compressive strength decreases with increasing size sample. They also propose the scale corrections in terms of sample length and in-situ block sizes.

Zhao (1988, 1997) and Zhao and Zhou (1992) have proposed the joint matching coefficient (JMC). This rough index is based on the percentage of joint surface in contact. The conclusions demonstrate that joint matching is an important factor governing the aperture, normal closure, stiffness, shear strength, and hydraulic conductivity of the joints, when it is coupled with JRC.

The reviewed results show that the surface roughness increases the joint shear strength. JRC is an empirical index that is widely used for describing the surface roughness characteristics. This technique is easily used to measure by comparing the appearance of a discontinuity surface with standard profiles.

2.2.2 Normal Stress

Vasarhelyi (1999) has investigated the dependence of the constant normal load on the rate of the dilation. The results show that the measured dilation angle decreases with increasing normal force. Proper modeling of the shear behavior of rock discontinuities must take into account of the conditions imposed by the rock mass rigidity. In this situation, the normal stress path should be properly understood for the accurate prediction of shear strength. Such behavior is more realistically represented in the controlled normal stiffness shear test rather than in the conventional constant normal load test. Ladany and Archambault (1970) equation is correct for the cases when the Patton (1966) and Haberfield and Johnston (1994) equations fail. This means that Ladany and Archambault (1970) equation is a more general equation and it should be valid until the irregularities are not sheared off. The measured dilation-displacement curves show that after the peak stress the rate of dilation does not change for a long time.

Constant normal stiffness (CNS) is proposed for non-planer joint analysis. CNS strength parameters are more representative for design underground excavations than the conventional constant normal load (Johnston et al., 1987). The conventional constant normal load is often inappropriate for evaluating the stability analysis of the bedded mine roofs, estimation of side shear resistance of rock-socketed piles, and stability analysis of jointed strata subjected to potential toppling failures (Indraratna and Haque, 2000).

2.2.3 Cohesion

The cohesion develops discontinuity surfaces in many conditions because a small cohesive strength can have significant effect on the shear strength of

rock. It is important that this rock strength parameter is properly accounted. The following are some of the conditions in which cohesion is developed on sliding surface. For intact rock and jointed, strong rock masses with no through-going discontinuities parallel to the sliding surface, the cohesion will usually have values of several hundred kilopascals and at this high strength there little risk of shear failure. For rough rock surfaces, an apparent cohesion is developed as the asperities are sheared off when movement occurs. The magnitude of the apparent cohesion is the intercept on the shear stress axis of the tangent to the curve shear strength envelope on a Mohr diagram. The apparent cohesion will increase with increasing normal stress until residual strength of the surface is reached. For discontinuity containing infillings, the cohesion will depend on both the characteristics and thickness of the infilling (Wyllie, 1998).

In most case, the cohesion component is ignored for rock discontinuities. It should only be considered when it is certain that cohesion will contribute to shear strength. This can occur when the critical set of discontinuities (i.e. the set on which sliding is most likely to occur) is persistent such as for sliding to occur, there must be failure through intact rock. This is, however, very difficult to assess.

Wyllie (1998) has suggested that for clean planar discontinuity in rock, the cohesion will be zero and shear strength will be defined solely by the friction angle. Generally, fine grained and rock with high mica content tend to have a low friction angle, while course grained, strong rock have a high friction angle.

2.2.4 Basic and Residual Friction Angle of Rock Joint

Both angles of basic (ϕ_b) and residual (ϕ_r) friction angle represent minimum shear resistance. Conceptually, ϕ_b refers to smooth, planar surface in fresh rock and can be considered as a material constant. ϕ_r refers to the residual condition

of natural joint surface, which is attained after large shear displacement. If the natural joint surface is un-weathered, ϕ_r can be taken equal to ϕ_b.

Methods for ϕ_b characterization include direct shear test or tilt tests on saw cut surface. The values of ϕ_b depend on the rock type and the moisture conditions (Horn and Deere, 1962; Coulson, 1972). Indicative ranges for ϕ_b (dry) = 26-38^o and ϕ_b (wet) = 21-35^o, the majority of rocks falling in the 25-35^o range.

The measurement is difficult due to the very large shear displacements requirement (Xu and de Freitas, 1990). In an indirect approach, ϕ_r may be obtained by allowing for the dilatation d_n in the measurement of shear stresses during testing under very low normal stress, which also have been corrected (Hencher, 1987)

$$\sigma_{n(corr)} = (\sigma_n \cdot \cos d_n - \tau \cdot \sin d_n)\cos d_n \quad (2.5)$$

$$\tau_{(corr)} = (\tau \cdot \cos d_n - \sigma_n \cdot \sin d_n)\cos d_n \quad (2.6)$$

$$\phi_r = \arctan \tau_{(corr)} / \sigma_{n(corr)} \quad (2.7)$$

In a convenient alternative method, ϕ_r can be predicted with acceptable accuracy from the basic friction angle value ϕ_b, by using the following empirical formula (Barton and Choubey, 1977).

$$\phi_r = (\phi_b - 20) + 20(r/R) \quad (2.8)$$

where the effect of surface alteration is introduced by rebound number ratio r/R, with r and R obtained from Schmidt hammer tests on wet, weathered and dry, fresh rock surface, respectively.

Stimpson (1981) suggests the use of tilt testing of diamond core samples for the estimation of the basic friction angle. He observes that the core surfaces produced by typical core drilling procedures are precut and smooth and therefore no dissimilar to a saw cut rock surface. The following equation can then be used to estimate the basic friction angle.

$$\phi_A = \tan^{-1}(1.155 \tan \alpha_S) \quad (2.9)$$

where ϕ_A is the estimate basic friction angle and α_S is the angle at which sliding commences.

The following are typical ranges of basic friction angles for a verity of rock types and should be used as a guideline only because actual values will vary widely with site condition. Low friction angle-friction angle are from 20^o to 27^o, medium friction angle-friction angle are from 27^o to 24^o, high friction angle-friction angle are from 34^o to 40^o (Barton, 1973).

2.3 Effect of Petrology on Mechanical Properties

The effects of grain size on the engineering properties of rock have been studied by several investigators. In sandstone, rock strength is greater for finer grained rocks (Brace, 1961). Handlin and Hager (1957) note that strength increases significantly when grain size increases in limestone and marbles. Hoek (1965) suggests that a higher applied stress is needed to cause failures through grain boundaries in rock characterized by tight interlocking texture. Hartley (1974) suggests that inter-granular bonding is a significant characteristic affecting mechanical properties of sandstone. It is concluded that the number of grain contacts

and type of grains may be used as an indicator of mechanical properties. Fahy and Guccione (1979) indicate that sandstone with smaller mean grain size has higher strength values. Onodera and Asoka (1980) report that the strength decreases while the grain sizes increase in igneous rocks. They determine a linear relationship between the grain size and strength, that is, as the grain size of the granite decreases, its strength increases. Shakoor and Bonelli (1991) find that the percentage angular grain is only weakly related to strength and elastic properties. Brown (1993) reports that grain length is a good indicator for porosity.

Mineralogical composition is one of the intrinsic properties controlling the rock strength, rock containing quartz as binding material are strongest followed by calcite and ferrous mineral rocks with clayey binding material are the softest (Vutukuri et. al., 1974). The relationship between mineralogical compositions and mechanical properties of various sandstones have been previously investigated. Since the amount of feldspar, mica and rock fragments in these sandstone, when present is small, they are not involved in the correlation. Thus, these correlations are only based on quartz content (Bell, 1978; Fahy and Cuccione, 1979; Gunsallus and Kulhawy, 1984; Dobereiner and De Freitas, 1986; Shakoor and Bonelli, 1991).

Pack density or the space in a given area occupied by grains has been correlated with strength properties. Bell (1978) and Doberenier and De Fretias (1986) shows the packing density of the Fell sandstone increased, also the values of uniaxial compressive and tensile strengths and modulus of elasticity increase. Howarth and Rowlands (1986) propose a texture coefficient including packing density and report this parameter. They have a moderate correlation with mechanical properties. Doberenier and De Freitas (1986) conclude that weak sandstone is generally characterized by a low packing

density. Grain contact (instead of packing density) results in greater strength of saturated sandstone and saturated strength of 20 MPa may be served for the upper bound strength of weak rock, beyond which the failure of rock is mainly controlled by the grain fracturing instead of the rolling of grains. Moreover, it has been found that greater packing density does enable greater strength (Bell, 1978). It has been reported that the textural characteristics appear to be more important than mineral composition to the mechanical behavior of sandstone (Ulusay et al., 1994).

The moisture may also have influence on the uniaxial compressive strength (UCS) of sandstone. It has been shown that moisture can decrease the UCS of weaker sandstones (Dyke and Dobereiner, 1991 ; Hawkins and McConnell, 1992).

The strength of homogenous intact rocks obtained from laboratory testing is usually affected by the specimen size, which related to the non-uniform distribution of micro-cracks and fractures (Griffith, 1924). Rock strength tends to decrease as the specimen size increases (Evans, 1961; Jaeger and Cook, 1979; Bieniawski, 1981; Farmer, 1983). For heterogeneous rocks, the size effect also relates to the non-uniform distribution of the pores, grain sizes, grain bounding and cementing, densities, mineralogy, inclusions, welding, impurities etc.

Fuenkajorn and Daemen (1992) have constructed an empirical approach to derive a compressive failure criterion for a heterogeneous rock. An empirical failure criterion is formulated by expressing the second invariant of stress deviation at failure as a function of the first invariant of stress, key parameter and volume. The density variable included as a key parameter for this tuff minimizes the effect of heterogeneity caused by non-uniform distribution of pores, mineralogy, inclusions, welding and grain bonding.

2.4 Shear Strength Testing

2.4.1 Direct Shear Test

Direct shear tests are commonly used both in research and practice. Test sample lengths may range from 10 to 40 cm. Large apparatus is not commercially available. Tests can be run under both constant or variable normal stress, depending on the boundary conditions relevanted to the problem at hand (Bandis, 1993). Recommended procedures of this are given by International Society for Rock Mechanics suggested methods (Brown, 1981).

Hencher and Richards (1982,1989) describe a device for determining shear strength of rock. The normal load is applied by means of a dead load system and therefore remains constant throughout the test. T.he tests can be carried out accurately at relatively low stresses. Vertical displacement is measured at a single point on the level arm allowing a magnification of up to ten times providing a relatively high degree of sensitive.

Some difficulties and limitations in direct shear tests are as follows: (i) normal and shear load capabilities in common machines are generally limited; (ii) monotonic shear displacements that can be accommodated are inadequate for residual strength determinations; and (iii) rotational moments in the upper sample-half may develop, especially when testing rough joints (Bandis, 1993).

2.4.2 In-situ Direct Shear Test

Large scale in-situ test can be conducted on isolated discontinuities by adopting a test set-up such as that described by Remero (1968). Saint Simon et al. (1979) have presented the typical set up of the in-situ direct shear test in adits. The reaction for normal load is obtained from the opposite wall of the adit. Brown (1981)

suggests method for in-situ determination of direct shear strength. Two techniques are presented including the in-situ direct shear test and the torsional shear test.

The test procedure would be similar to that of the laboratory direct shear test in that a constant normal load is applied and the shear load is gradually increased until sliding takes place. The normal and shear displacements are measured operating in opposite directions, the sample can be reset after each test, in order to conduct tests at a number of different normal loads and obtain value of both the peak and residual strengths (Wyllie, 1998).

This test is expansive and only to perform where critically locating, thin, weak, continuous seams exist within relatively strong adjacent rock. In such cases, conservative lower bound estimated of shear strength seldom provides adequate assurance against instability. The relatively large surface area tested is an attempt to address unknown scale effect. However, the question of how large a specimen is large enough still remains. The test, as performed on thin, fine grained, clay seam, is considered to be an in-drained test.

2.4.3 Field Direct Shear Test

Portable direct shear test is one of simpler and cheaper testing system. This technique is described by Ross-Brown and Walton (1975) and Hoek and Bray (1981). The portable shear box can accept specimens up to a size of about a 140 mm cube. The idea is to select a specimen from a rock face or borehole core containing a single discontinuity suitable for testing, trim the specimen to size and then wire or tape it together to protect the discontinuity surface texture (Priest, 1993). Ross-Brown and Walton (1975) discuss a number of methods for recording surface geometry, including visual description, mechanical profilometry, photogrammetry

and the use of rubber impressions. Priest (1975) has studied shear displacement and shear stress on chalk. The tests are conducted using a portable shear box test at five different effective stresses in the range 0.24 to 1.2 MPa.

Although the portable shear box is widely used for routine testing, it does have a number of disadvantages when precise control over testing conditions is required. The use of manually operated jacks can make it difficult to control shear displacement and maintain a constant normal stress throughout the test. There is tendency for the upper half of the shear box to tilt over at large shear displacement on rough specimens, making it difficult to interpret measurements of shear and normal displacement. Many workers now prefer to use a shear testing apparatus based on the conventional soil shear box. This apparatus is, however, limited to laboratory use, can only apply normal stresses up to about 2 MPa and can cope with only a limited degree of discontinuity surface roughness. There are many investigators who develop the technique that can reduce that limit. (e.g. Skinas et al.,1990; Archambault et al, 1990).

2.4.4 Triaxial Test

The triaxial cell is sometimes used to investigate the shear behavior of discontinuities. Specimens are prepared from cored containing discontinuities inclined at 25-40^{o} to the specimen axis. A specimen is set up in the triaxial cell and the axial loads are successively applied. The triaxial cell is well suited to testing discontinuities in presence of water. Tests may be either drained or undrained, preferably with known level of joint water pressure being imposed and maintained throughout the test (Brady and Brown, 1993).

It is assumed that slip on the discontinuity occurs. Mohr circle plots are made of the total or effective stresses at slip at a number of values of minimum

principal stress and the points on these circles giving the stresses on the plane of the discontinuity are identified. The required shear strength envelope is then drawn through these points. This requires that a number of tests be carried out on s discontinuities (Brady and Brown, 1993).

The triaxial technique for determining shear strength is developed by Rosengren (1988) who determined the correction required to allow for the influence of friction and change of contact area. His analysis has been re-presented by Goodman (1976). Brady and Brown (1993) successfully use this technique on specimens with 150-mm diameter at confining pressures of up to 70 MPa. Ramamurthy (2001) has conducted the axisymmetric triaxial compression tests on intact rock and jointed rock. The triaxial result is used to develop the new shear strength criterion involving only two different strength parameters that are cohesion and angle of shearing.

CHAPTER III

SAMPLE PREPARATION

3.1 Sample Collection

Rock samples used in this research have been collected from ten different source locations, representing the most commonly-encountered rocks in the construction and mining industries in Thailand. They can be categorized here into four groups: basalt, two marbles, three granites and four sandstones. The main selection criteria are the availability, the freshness and the mechanical homogeneity while aiming at the mineralogical diversity among different rock types. The locations where some rock samples are collected are shown in Figures 3.1 and 3.2.

3.2 Sample Preparation

There are four groups of specimen preparation for different laboratory test methods, 1) uniaxial compressive strength tests, 2) direct shear tests on saw-cut surfaces, 3) direct shear tests on rough joints, and 4) mineralogical study.

3.2.1 Sample Preparation for Uniaxial Compressive Strength Tests

The process including coring, cutting and grinding (Figures 3.3 through 3.5). The core specimens have been drilled from the blocks of each rock type with NX-size bit (54 mm). Ten specimens are prepared to have nominal length to diameter ratio (L/D) equal to 2.5. Preparation of these samples follows, as much as practical,

Figure 3.1 Sandstone block are collected from a quarry in Klong Phai district, Nakhon Ratchasrima province.

Figure 3.2 Quarry in Burirum province where basalt samples have been collected.

Figure 3.3 Drilling machine (model SBEL 1150) is used to drill core specimens with 54 mm diameter.

Figure 3.4 Core sample is cut to obtain the desired length.

Figure 3.5 Grinding of core sample for smooth and parallel end surfaces.

the ASTM standard practice (ASTM D4543). Some rock specimens prepared for uniaxial compressive strength testing are shown in Figure 3.6 through 3.9.

3.2.2 Sample Preparation for Direct Shear Tests on Saw-cut Surface

Direct shear testing is carried out on the saw cut surfaces of rock specimens to determine their basic friction angle. Three specimens are prepared for each rock type. The tested fracture area is 10×10 cm. Some saw-cut surface specimens are shown in Figures 3.10 through 3.12.

3.2.3 Sample Preparation for Direct Shear Tests on Rough Joint

In order to obtain shear strength of rough joints, tensile fractures are induced in rock blocks with a dimension of 10×10×20 cm. Line load is applied at the mid-section of the specimen until splitting tensile failure occurs (Figure 3.13). This results in a clean, rough and perfectly matched fracture (Figure 3.14). Three pairs of specimens are prepared for each rock type.

3.2.4 Sample Preparation for Mineralogical Study

Petrographic analysis is a process used to determine the mineral compositions of rock samples. Ten thin sections of representative samples are prepared from each rock type. The specimen size is 2x3 cm with a thickness of less than 1 mm. The results of this study will be presented and discussed in the next chapter.

Figure 3.6 Basalt specimens prepared for uniaxial compressive strength testing with 54 mm diameter and L/D ratio equal to 2.5.

Figure 3.7 Granite specimens prepared for uniaxial compressive strength testing with 54 mm diameter and L/D ratio equal to 2.5.

Figure 3.8 Marble specimens prepared for uniaxial compressive strength testing with 54 mm diameter and L/D ratio equal to 2.5.

Figure 3.9 Sandstone specimens prepared for uniaxial compressive strength testing with 54 mm diameter and L/D ratio equal to 2.5.

Figure 3.10 Saw-cut surface specimens of granite prepared for direct shear test with block size 10×10×7.5 cm.

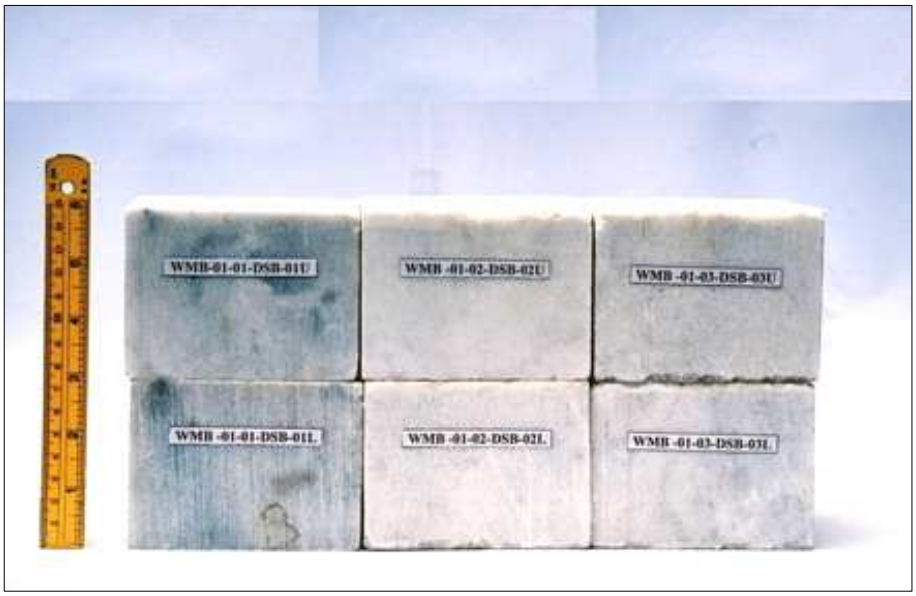

Figure 3.11 Saw-cut surface specimens of marble prepared for direct shear test with block size 10×10×7.5 cm.

Figure 3.12 Saw-cut surface specimens of sandstone prepared for direct shear test with block size 10×10×7.5 cm.

Figure 3.13 Splitting tensile fractures of marble specimens prepared for direct shear testing.

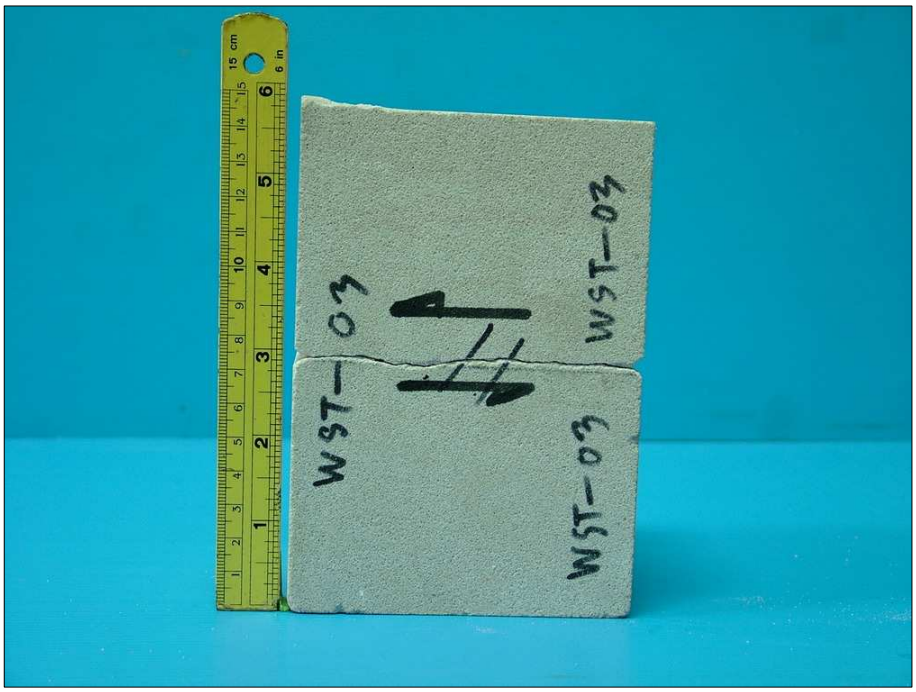

Figure 3.14 Phra Wihan sandstone specimen with a rough joint prepared for direct shear test.

CHAPTER IV

LABORATORY TESTS

The primary objectives of the laboratory tests are to determine basic mechanical rock properties and the shear strengths of smooth and rough joint surfaces. The laboratory test program is divided into six main groups; 1) uniaxial compressive strength tests, 2) mineralogical study, 3) direct shear tests on saw-cut surface, 4) direct shear tests on rough surface, 5) rock strength estimation by manual index tests, and 6) basic friction angle by tilt test method.

4.1 Uniaxial Compressive Strength Tests

The uniaxial compressive strength (UCS) or the rock strength on the joint walls is required for applications of the Barton's criterion. Test procedure for the laboratory determination of the UCS strictly follows the American Society for Testing and Materials standard (ASTM D2938) and suggested method by ISRM (International Society of Rock Mechanics) (Brown, 1981).

Core specimens with a nominal diameter of 54 mm and length-to-diameter ratio of 2.5 are axially loaded to failure (Figure 4.1). Ten specimens have been tested for each rock type. The UCS of the specimen is calculated by dividing the maximum load by the original cross-sectional area. The tangent Young's modulus is also calculated from the stress-strain curves at 50% of the maximum stress level.

Figure 4.1 Uniaxial compressive strength test on 54 mm diameter specimen with L/D raito equal to 2.5. The specimen is loaded axially in compression machine model ELE-ADR2000.

All results are summarized in Table 4.1 and the details of each specimen are shown in Appendix A (Tables A.1 through A.10). The stress-strain curves of all specimens are shown in Appendix A (Figure A.1 through A.10).

4.2 Mineralogical Study

Ten thin sections of representative samples are prepared from each rock type to determine the mineral compositions. Table 4.2 gives the results, including rock names, brief mineral compositions, rock description, the geologic formation or unit to which they belong, and the location from which they are obtained.

4.3 Direct Shear Tests on Saw-Cut Surfaces

Direct shear testing is carried out on the saw cut surfaces of rock specimens to determine their basic friction angle. The test procedure follows as much as practical the ASTM D5607 standard practice. Three specimens are tested for each rock type. The tested surface area is 10×10 cm. Shear force is continuously applied and monitored until a total shear displacement of 1 cm is obtained. The shearing rate is about 1 mm/minute. Each block specimen is sheared 5 times (forward-backward-forward-backward-forward) with the normal stresses between from 500 pounds to 4,500 pounds.

The peak shear stress is calculated and plotted against the corresponding normal stress. Figure 4.2 shows the test arrangement of saw-cut surface specimen used in the direct shear testing with direct shear machine model SBEL-DR44, capacity of 10,000 pounds normal load and 30,000 pounds shear force.

Table 4.1 Uniaxial compressive strength and elastic modulus of the tested rock specimens.

Rock Types	σ_c (MPa)	E (GPa)
Crystalline Rocks		
1. Burirum Basalt	188.1 ± 26.3	33.2 ± 3.4
2. Vietnamese Granite	138.1 ± 18.9	34.5 ± 4.3
3. Tak Granite	119.4 ± 8.8	32.4 ± 4.6
4. Chinese Granite	119.3 ± 18.3	34.0 ± 8.0
5. Saraburi Marble	78.7 ± 14.6	21.3 ± 4.4
6. Lopburi Marble	74.4 ± 12.6	28.7 ± 2.4
Clastic Rocks		
7. Phu Kradung Sandstone	72.8 ± 5.7	12.2 ± 0.7
8. Phu Phan Sandstone	72.4 ± 8.5	18.4 ± 1.1
9. Phra Wihan Sandstone	71.3 ± 9.0	13.9 ± 2.0
10. Sao Khua Sandstone	67.5 ± 4.6	11.5 ± 0.5

Table 4.2 Description of rock samples obtained from ten source locations.

Rock Type	Code	Mineral Compositions	Description	Rock Unit / Location
Aphanitic Basalt	BA	50% Pyroxene (0.5-1 mm) and 50% plagioclase (0.3-0.8 mm)	Aphanitic basalt, very dark grey to black in colour, densed with a few vesicles (less than 1%), no olivine crystal observed	Burirum Basalt Unit / Burirum Province
Limestone Marble	YME	100% Calcite (1-5 mm)	Meta-sedimentary rock, appearing yellowish brown, non granular, non foliated, showing original texture of limestone with metamorphosed fossils and rock fragments, strongly reacts with HCL without powdering Discusssion: The rock should have been overcome the low grade metamorphism according to undestroyed original texture. Calcite is still retained. Original rock was moderately abundant fossiliferous limestone, containing 40% fossils, 10% intraclasts with micrite matrix, also called “sparce biomicrite”	Saraburi Group / Saraburi Province
Limestone Marble	WMB	100% Calcite (1-2 mm)	Granular marble, appearing white, calcite grains can be seen by eye, average size of 2 mm, equidimensional, mineral grains crumbled by hand, strongly reacts with HCL without powdering Discussion: The original rock can be any limestone but it was overcome low-high temperature-intermediate pressure metamorphism. Calcite is still retained in the rock which reacts strongly with HCL. Though shape of calcite crystals are interlocking and changed to be more rounded. It is easy to be crumbled by hand	Saraburi Group / Lopburi Province

Table 4.2 Description of rock samples obtained from ten source locations (cont.).

Rock Type	Code	Mineral Compositions	Description	Rock Unit / Location
Quartz Syenite	RGR	75% Orthoclase (0.3-2 cm), 10% quartz (2-5 mm), 10% plagioclase (1-3 mm), and 5% amphibole (1-2 mm)	Felsic phaneritic granite, appearing pink, crystals of minerals can be seen by naked eyes, fine grained with average size of 2-5 mm in length, quartz is generally smaller than feldspar, orthoclase phynocryst (> 1cm) also present	"Unknown" / Vietnam
Plagiogranite	GGR	40% Plagioclase (0.5-1 mm), 30% quartz (2-5 mm), 5% orthoclase (3-5 mm), 3% amphibole (1-2 mm), and 2% biotite (1-2 mm)	Felsic phaneritic granite, appearing grey with black and white spotted, crystals of minerals can be seen by eyes, fine grained with average size of 4-5 mm., quartz and feldspar are equally of the same size	Tak Batholith / Tak Province
Quartz Monzonite	WGR	70% Plagioclase (0.5-2 cm), 15% quartz (3-5 mm), 7% orthoclase (2-3 mm), 5% amphibole (1-2 mm), and 3% biotite (2-3 mm)	Intermediate phaneritic granite, appearing white with scattered black, crystals of minerals can be seen by eyes, coarse grained, quartz and feldspar generally of equal size, average size of more than 5 mm, plagioclase crystals reach 1 cm, showing striations	"Unknown" / China

Table 4.2 Descriptions of rock samples obtained from ten source locations (cont.).

Rock Type	Code	Mineral Compositions	Description	Rock Unit / Location
Calcareous Lithic Sandstone	GST	70% Lithic fragment (0.1-0.3 mm), 18% quartz (0.1-0.5 mm), 7% mica (0.1-0.5 mm), 3% feldspar (0.1-0.5 mm), and 2% other (0.1-0.8 mm)	Fine grained sandstone, grayish green, lithic fragment and quartz dominated with less mica, well sorted, angular, slightly reacts with HCL	Phu Kradung Formation / Nakhon Ratchasima Province
Quartz Sandstone	YST	72% Quartz (0.2-0.8 mm), 20% feldspar (0.1-0.8 mm), 3% mica (0.1-0.3 mm), 3% rock fragment (0.5-2mm), and 2% other (0.5-1 mm)	Fine grained sandstone, brownish yellow, quartz and feldspar dominated with a few mica, well sorted, angular, not react with HCL Discussion: Brownish yellow colour may originate from limonite, Fe-oxide mineral	Phu Phan Formation / Nakhon Ratchasima Province
White Quartz Sandstone	WST	75% Quartz (0.1-0.5 mm), 15% feldspar (0.2-0.5 mm), 7% mica (0.1-0.5 mm), and 3% lithic fragment (0.1-1 mm)	Fine grained sandstone, brownish white with scattered black, quartz and feldspar dominated with less mica, well sorted, angular, not react with HCL	Phra Wihan Formation / Nakhon Ratchasima Province
Arkosic Feldspathic Sandstone	RST	70% Feldspar (0.1-0.5 mm), 18% quartz (0.1-0.5 mm), 7% mica (0.1-0.2 mm), 3% rock fragment (0.1-0.3 mm), and 2% other (0.1-0.3 mm)	Fine grained sandstone, appearing red, feldspar and quartz dominated with less mica, well sorted, angular, not react with HCL. Discussion: Red colour may point to occurrence of oxidization by Fe-oxide	Sao Khua Formation / Nakhon Ratchasima Province

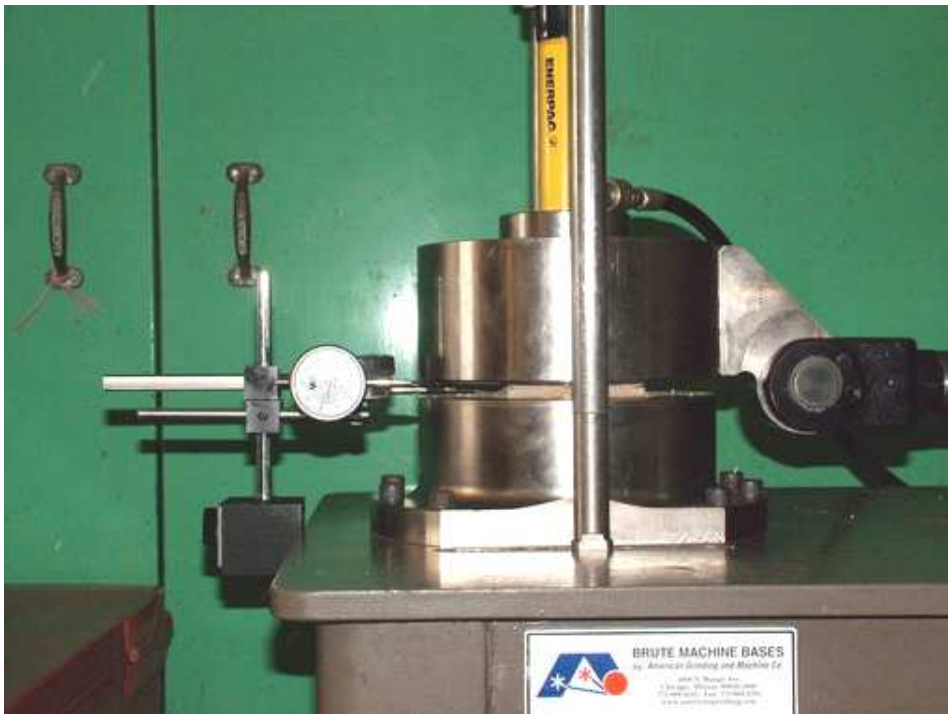

Figure 4.2 Test arrangement of saw-cut surface specimen used in the direct shear test with direct shear machine model SBEL DR440.

Linear relationship between the shear and normal stresses is obtained for all tests which are plotted in Appendix B (Figures B.1 through B.10). The basic friction angle (ϕ_b) is calculated from the shear-normal stress slopes. Table 4.3 lists the ϕ_b values for the ten rock types.

4.4 Direct Shear Tests on Rough Surface

A series of direct shear strength tests on rough joints have been conducted on ten rock types. The sample preparation and test procedure follow the applicable ASTM standard (ASTM 5607) and the ISRM suggested method (Brown, 1981), as mush as practical. Three pairs of specimens are prepared and tested for each rock type. A shear direction is then pre-defined. Six engineers independently determine the JRC along the shear direction. Their results agree reasonably well; usually 5 out of 6 give the same range of JRC. Table 4.4 summarizes the JRC's for each pair of the rock specimens.

Series of direct shear tests are performed on the specimens with the tension-induced fractures (Figure 4.3). The selected normal stresses are 1.08, 1.29 and 1.95 MPa. Each specimen is sheared only once for each normal stress using a constant shearing rate of 1 mm/minute. Shear force is continuously applied until a total shear displacement of 1 cm is reached. Figure 4.4 shows the measurement of displacement dial gages. The peak and residual shear loads are monitored. Table 4.4 lists the peak shear stresses calculated for the ten rock types. As expected, the greater the normal stress applied, the greater the peak shear stress obtained. The peak shear strength (τ_p) and residual shear strength (τ_r) are calculated by the equations;

Table 4.3 Basic friction angles from direct shear test on saw-cut surfaces.

Rock Types	ϕ_b No.1 (degrees)	ϕ_b No.2 (degrees)	ϕ_b No.3 (degrees)	ϕ_b Average (degrees)
Crystalline Rocks				
1. Burirum Basalt	36	37	33	35.3 ± 2.08
2. Vietnamese Granite	17	20	18	18.3 ± 1.53
3. Tak Granite	24	25	25	24.7 ± 0.58
4. Chinese Granite	26	26	25	25.7 ± 0.58
5. Saraburi Marble	34	34	35	34.3 ± 0.58
6. Lopburi Marble	34	37	36	35.7 ± 1.53
Clastic Rocks				
7. Phu Kradung Sandstone	32	35	34	33.7 ± 1.53
8. Phu Phan Sandstone	29	33	33	31.7 ± 2.31
9. Phra Wihan Sandstone	29	34	32	31.7 ± 2.52
10. Sao Khua Sandstone	27	32	33	30.7 ± 3.21

Table 4.4 Results of the direct shear strength tests on rough joints.

Rock Types	Specimen No.	JRC	Normal Load (lbs)	Normal Stress (kPa)	Peak Shear Strength (kPa)	Residual Shear Strength (kPa)
Crystalline Rocks						
1. Burirum Basalt	BA-01	8-10	2500	1655	1986	1589
	BA-02	8-10	4500	2986	3185	2256
	BA-03	8-10	5500	3636	3305	2974
2. Vietnamese Granite	RGR-01	10-12	2500	1068	3204	1197
	RGR-02	10-12	4500	1922	3588	1643
	RGR-03	8-10	5500	2378	4150	1837
3. Tak Granite	GGR-01	12-14	2500	1051	1555	1177
	GGR-02	8-10	4500	1932	2833	1631
	GGR-03	10-12	5500	2291	4581	2156
4. Chinese Granite	WGR-01	12-14	2500	1080	2938	1123
	WGR-02	14-16	4500	1950	3293	1647
	WGR-03	14-16	5500	2386	3557	1822
6. Saraburi Marble	YMB-01	8-10	2500	1078	1250	1034
	YMB-03	8-10	3000	1588	2146	1588
	YMB-02	12-14	4500	1934	2450	1891
5. Lopburi Marble	WMB-01	8-10	2500	1060	1230	763
	WMB-03	10-12	3000	1255	1589	1255
	WMB-02	10-12	4500	1893	2861	2020
Clastic Rocks						
7. Phu Kradung Sandstone	GST-01	6-8	2500	1076	1076	904
	GST-03	6-8	3000	1282	1367	1111
	GST-02	6-8	4500	1939	1852	1465
8. Phu Phan Sandstone	YST-01	6-8	2500	1075	1333	1161
	YST-03	6-8	3000	1288	1545	1116
	YST-02	8-10	4500	1932	2704	1889
9. Phra Wihan Sandstone	WST-01	6-8	2500	1078	1380	1078
	WST-03	6-8	3000	1292	1464	1205
	WST-02	8-10	4500	1945	2075	1599
10. Sao Khua Sandstone	RST-01	4-6	2500	1069	1197	727
	RST-03	6-8	3000	1271	1356	932
	RST-02	6-8	4500	1943	1900	1598

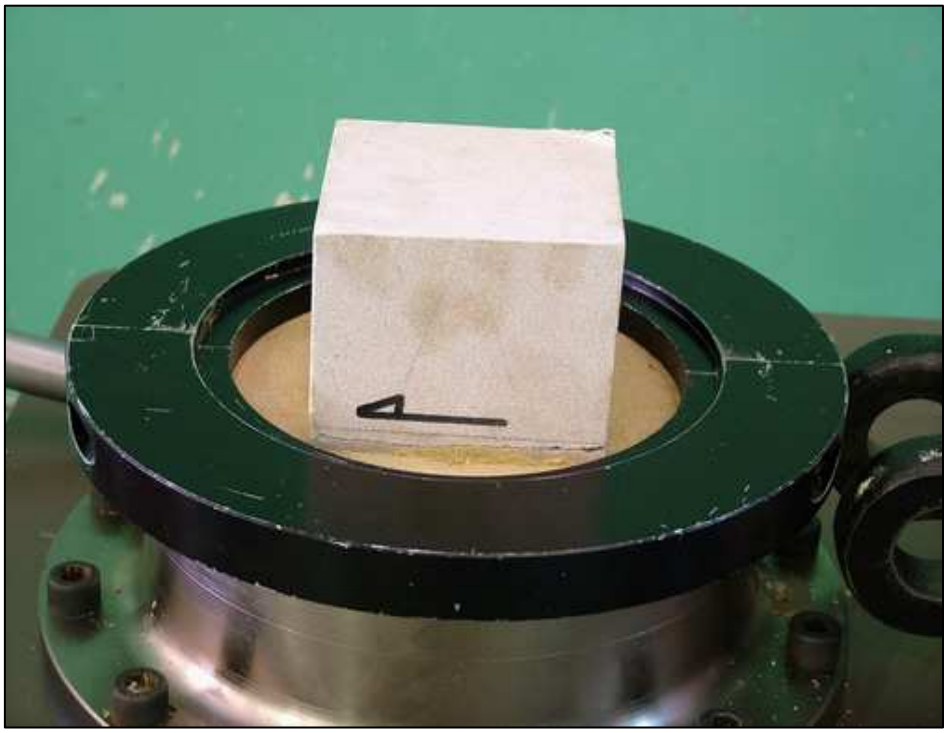

Figure 4.3 Direct shear strength test on rough joint with 10x10 cm of contact area.

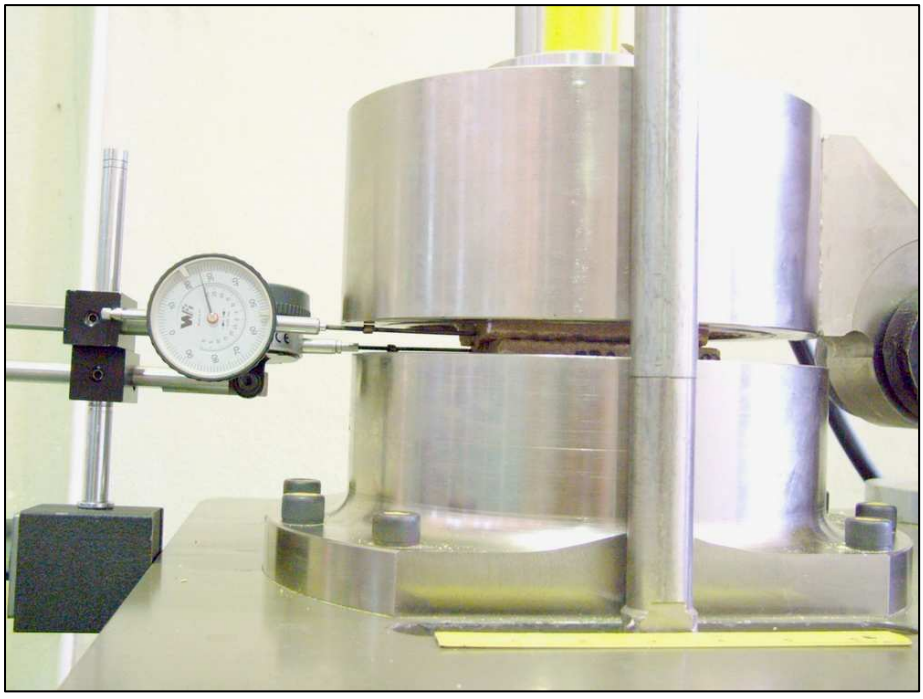

Figure 4.4 Upper and lower specimens are attached with displacement dial gages.

$$\tau_p = P_p / A \quad (4.1)$$

$$\tau_r = P_r / A \quad (4.2)$$

where P_p is the maximum shear force, P_r is the residual shear force, and A is the contact area between both specimens. It is assumed here that since the total displacement is small (less than 1 cm), the contact area (A) is taken as constant during the shear test. The force-displacement curves are given in Appendix C (Figures C.1 through C.30).

4.5 Rock Strength by Field Determination Method

The field identification of the UCS follows the ISRM suggested method given by Brown (1981). Two engineers independently identify the grade for each rock type using mainly the geologic hammer and pocket knife. The nominal specimen sizes are 10×10×5 cm. The grades for the selected rock specimens are identified to be either R4 or R5. The strength results obtained by the two engineers coincide, and agree well with the UCS from the uniaxial compression test (Table 4.5). This suggests that the range of the rock strength identified by the field method may be reliable and adequate for use in the Barton's criterion.

4.6 Basic Friction Angle by Tilt Test Method

The basic friction angles are measured by a simple tilting apparatus. The tilt test apparatus is a self-weight tilt testing device used for measuring the basic friction angle (ϕ_b) (Chryssanthakis, 2003). The objective of the tilt test is to compare the results with direct shear tests on saw-cut surface.

Table 4.5 Classification of the strength rating obtained from the ISRM field-identification.

Rock Types	Engineer No.1		Engineer No.2	
	Strength Rating by ISRM	σ_c (MPa)	Strength Rating by ISRM	σ_c (MPa)
Crystalline Rocks				
1. Burirum Basalt	R4	50-100	R5	100-250
2. Vietnamese Granite	R6	>250	R5	100-250
3. Tak Granite	R5	100-250	R5	100-250
4. Chinese Granite	R5	100-250	R5	100-250
5. Saraburi Marble	R2	5-25	R4	50-100
6. Lopburi Marble	R3	25-50	R4	50-100
Clastic Rocks				
7. Phu Kradung Sandstone	R6	>250	R4	50-100
8. Phu Phan Sandstone	R4	50-100	R4	50-100
9. Phra Wihan Sandstone	R4	50-100	R4	50-100
10. Sao Khua Sandstone	R5	100-250	R5	100-250

A series of tilt tests have been performed on ten rock types. Three pairs of specimens are prepared and tested for each rock type. The results of tilt test on saw-cut surfaces specimens and the comparison with direct shear test are shown in Table 4.6. The values of basic friction angle from tilt tests are in the range of those obtained from direct shear test on saw-cut surface.

Table 4.6 Results of basic friction angle from tilt test.

Rock types	Friction angle, ϕ_b (degrees)	
	Tilt test	Direct shear test
1. Burirum Basalt	26	35.3
2. Vietnamese Granite	34	18.3
3. Tak Granite	30	24.7
4. Chinese Granite	25	25.7
5. Saraburi Marble	25	34.3
6. Lopburi Marble	28	35.7
7. Phu Kradung Sandstone	33	33.7
8. Phu Phan Sandstone	31	31.7
9. Phra Wihan Sandstone	34	31.7
10. Sao Khua Sandstone	34	30.7

CHAPTER V

DISCUSSIONS ON BASIC FRICTION ANGLES

5.1 Introduction

The objective of this chapter is to determine whether there is any relationship between the basic friction angle and other physical and mechanical properties of the rocks. The basic friction angles of smooth surfaces of rock joint obtained elsewhere are also complied and used to assist in determining such relationship.

5.2 Basic Friction Angle and Intact Rock Properties

An attempt has been made here at correlating the ϕ_b with the intact rock strength. The UCS and ϕ_b for various rock types obtained elsewhere (Goodman, 1989; Grasselli and Egger, 2003; Hoek and Bray, 1981; Waltham, 1994) has been compiled and compared with the results obtained here. Surprisingly publications reporting both UCS and ϕ_b tested for the same rocks are rare, particularly those providing the detailed rock descriptions or the source locations. Table 5.1 gives the summary of data from this research and other researches.

The tested aphanitic basalt has ϕ_b equal 35 ± 2 degrees which agrees well with those obtained elsewhere (Figure 5.1). The number and diversity of the specimens are however inadequate to determine or discuss about the relationship between the ϕ_b and mineral or mechanical properties of the basalts.

Table 5.1 Mechanical rock properties from the other research.

Rock type	Location/ Name	σ_c MPa	E GPa	σ_t MPa	ϕ_b Degrees	Sources
Amphibolite	N/A	N/A	N/A	N/A	32	Hoek and Bray (1981)
Aplite	N/A	N/A	N/A	N/A	31-35	Duzgun et al. (2002)
Basalt	N/A	N/A	N/A	N/A	31-38	Hoek and Bray (1981)
	N/A	250	90	15	50	Waltham (1994)
	Nevada	148	N/A	N/A	31	Goodman (1989)
	Burirum	188	33.2	N/A	33-37	*obtained here
Chalk	N/A	N/A	N/A	N/A	30	Hoek and Bray (1981)
	N/A	15	6	0.3	25	Waltham (1994)
Clay	N/A	2	0.2	2	20	Waltham (1994)
Conglomerate	N/A	N/A	N/A	N/A	35	Hoek and Bray (1981)
Dolomite	N/A	N/A	N/A	N/A	27-31	Hoek and Bray (1981)
	Hasmark	N/A	N/A	N/A	35	Goodman (1989)
Gneiss	N/A	160	45.9	3.5	36	Grasselli and Egger (2003)
	N/A	60	21.1	N/A	36	
	N/A	N/A	N/A	N/A	23-29	Hoek and Bray (1981)
	N/A	N/A	N/A	N/A	26-30	Duzgun et al. (2002)
	N/A	150	45	10	30	Waltham (1994)
Granite	Tarn	173	48.4	8.8	34	Grasselli and Egger (2003)
	N/A	N/A	N/A	N/A	29-35	Hoek and Bray (1981)
	N/A	N/A	N/A	N/A	31-35	
	N/A	200	75	15	55	Waltham (1994)
	Stone mountain	N/A	N/A	N/A	51	Goodman (1989)

Table 5.1 Mechanical rock properties from the other research (cont.).

Rock type	Location/ Name	σ_c MPa	E GPa	σ_t MPa	ϕ_b Degrees	Sources
Granite	N/A	N/A	N/A	N/A	31-35	Duzgun et al. (2002)
	Inada	N/A	N/A	N/A	47	Goodman (1989)
	Vietnamese	138	34.5	N/A	17-20	*obtained here
	Tak	119	32.4	N/A	24-25	
	Chinese	119	34	N/A	25-26	
Greywacke	N/A	180	60	15	45	Waltham (1994)
Gypsum	N/A	25	20	1	30	Waltham (1994)
Hornfels	N/A	250	80	N/A	40	Waltham (1994)
	N/A	N/A	N/A	N/A	31-35	Duzgun et al. (2002)
Limestone	Wolf camp	N/A	N/A	N/A	34	Goodman (1989)
	Magny	25	14.9	2.4	36	Grasselli and Egger (2003)
	Port du gard	5	3.6	1	37	
	N/A	100	60	10	35	Waltham (1994)
	N/A	25	15	2	35	
	Indiana	N/A	N/A	N/A	42	Goodman (1989)
	N/A	N/A	N/A	N/A	31-37	Duzgun et al. (2002)
Marble	Carrara	87	29.6	9.2	37	Grasselli and Egger (2003)
	N/A	100	30	30	35	Waltham (1994)
	Georgia	N/A	N/A	N/A	25	Goodman (1989)
	Saraburi	79	21	N/A	34-35	*obtained here
	Lopburi	74	29	N/A	34-37	
Micaschist	N/A	N/A	N/A	N/A	26	Duzgun et al. (2002)

Table 5.1 Mechanical rock properties from the other research (cont.).

Rock type	Location/ Name	σ_c MPa	E GPa	σ_t MPa	ϕ_b Degrees	Sources
Mudstone	N/A	40	10	1	30	Waltham (1994)
	N/A	N/A	N/A	N/A	20-25	Duzgun et al. (2002)
Quartzite	Sioux	N/A	N/A	N/A	48	Goodman (1989)
	N/A	N/A	N/A	N/A	30	Duzgun et at. (2002)
Sandstone	N/A	10	25.4	0.7	37	Grasselli and Egger (2003)
	N/A	N/A	N/A	N/A	25-35	Hoek and Bray (1981)
	N/A	70	30	5	45	Waltham (1994)
	N/A	20	4	1	40	
	Berea	N/A	N/A	N/A	27	Goodman (1989)
	Bartlesville	N/A	N/A	N/A	37	
	Pottsville	N/A	N/A	N/A	45	
	N/A	N/A	N/A	N/A	31-33	Duzgun et at. (2002)
	N/A	N/A	N/A	N/A	31-33	
	N/A	N/A	N/A	N/A	26-32	
	Phu Kradung	73	12	N/A	32-35	* obtained here
	Phu Phan	72	18	N/A	29-33	
	Phra Wihan	71	14	N/A	29-34	
	Sao Khua	67	11	N/A	33-37	
Schist	N/A	60	20	2	25	Waltham (1994)
Serpentinite	N/A	166	76.8	6	39	Grasselli and Egger (2003)
	N/A	74	39.4	16.3	39	
Shale	N/A	N/A	N/A	N/A	27	Hoek and Bray (1981)

Table 5.1 Mechanical rock properties from the other research (cont.).

Rock type	Location/ Name	σ_c MPa	E GPa	σ_t MPa	ϕ_b Degrees	Sources
Shale	N/A	20	2	0.5	25	Waltham (1994)
	N/A	N/A	N/A	N/A	14	Goodman (1989)
	Stockton	N/A	N/A	N/A	22	
	Edmonton	N/A	N/A	N/A	7	
Siltstone	N/A	N/A	N/A	N/A	27-31	Hoek and Bray (1981)
	Repetto	N/A	N/A	N/A	32	Goodman (1989)
	N/A	N/A	N/A	N/A	25-33	Duzgun et al. (2002)
Slate	N/A	N/A	N/A	N/A	25-30	Hoek and Bray (1981)
	N/A	90	30	10	25	Waltham (1994)
	N/A	N/A	N/A	N/A	25-30	Duzgun et al. (2002)
Soapstone	N/A	N/A	N/A	N/A	20	Duzgun et al. (2002)
Tuff	N/A	N/A	N/A	N/A	21	Duzgun et al. (2002)

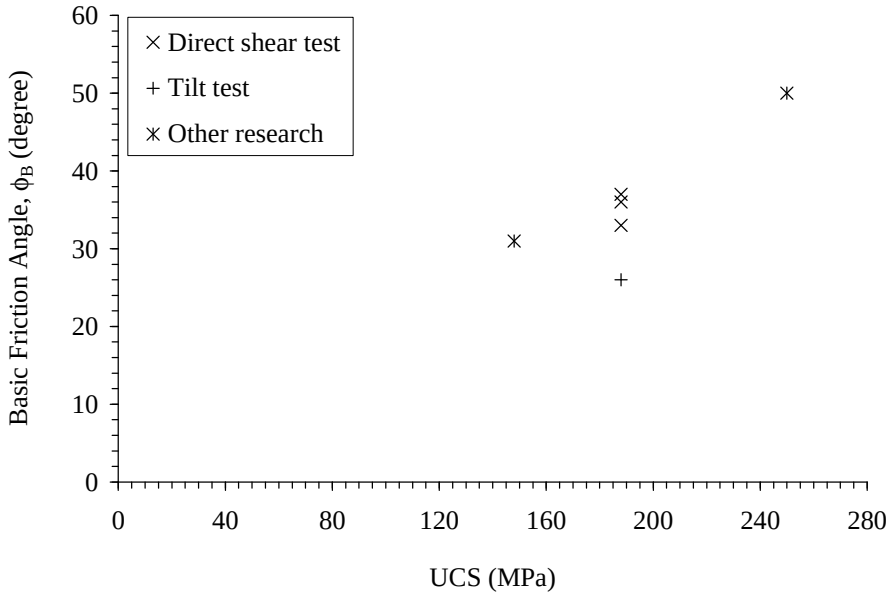

Figure 5.1 Relationship between UCS and basic friction angles of basalt.

The ϕ_b values for the tested quartz syenite, plagiogranite and quartz monzonite are 18 ± 2, 25 ± 1, and 26 ± 1 degrees, which are notably lower than those obtained for the granites elsewhere (Figure 5.2). Most granite and gneiss have ϕ_b about 30 degrees. This is probably due to the fact that the saw-cut surfaces for the coarse-grained and very strong crystalline rocks (such as granites) are very smooth, even without polishing, and hence results in an unrealistically low ϕ_b from the direct shear testing. This also implies that rock cutting process and equipment can govern the characteristics of the cut surfaces, and hence affects ϕ_b as well.

Figure 5.3 plots ϕ_b as a function of UCS for the marble tested here and the marble and limestone tested elsewhere. From the available information, ϕ_b appears to be independent of UCS and grain size. The average ϕ_b is 35 ± 3 degrees.

For sandstones from all source locations, ϕ_b is averaged as 33 ± 8 degrees (Figure 5.4). The averaged ϕ_b for the quartz sandstones (pure sandstone) is 32 ± 3 degrees. The averaged ϕ_b for the arkosic feldspathic sandstone is slightly lower (31 ± 3 degrees), and for the calcareous lithic sandstone is slightly greater (34 ± 2 degrees). This suggests that for the tested fine-grained sandstones, the cementing materials may have some influence on ϕ_b. The UCS however may not be appropriate for use as an indicator of ϕ_b, as it shows significantly high standard variation (over 10%) for all tested sandstones.

Figure 5.5 plots ϕ_b as a function of UCS for various rock types, except sandstone, limestone and marble. It seems that for strong rocks (ISRM-designated R4 & R5), ϕ_b increases with UCS. A liner fit shows a mathematical relation as

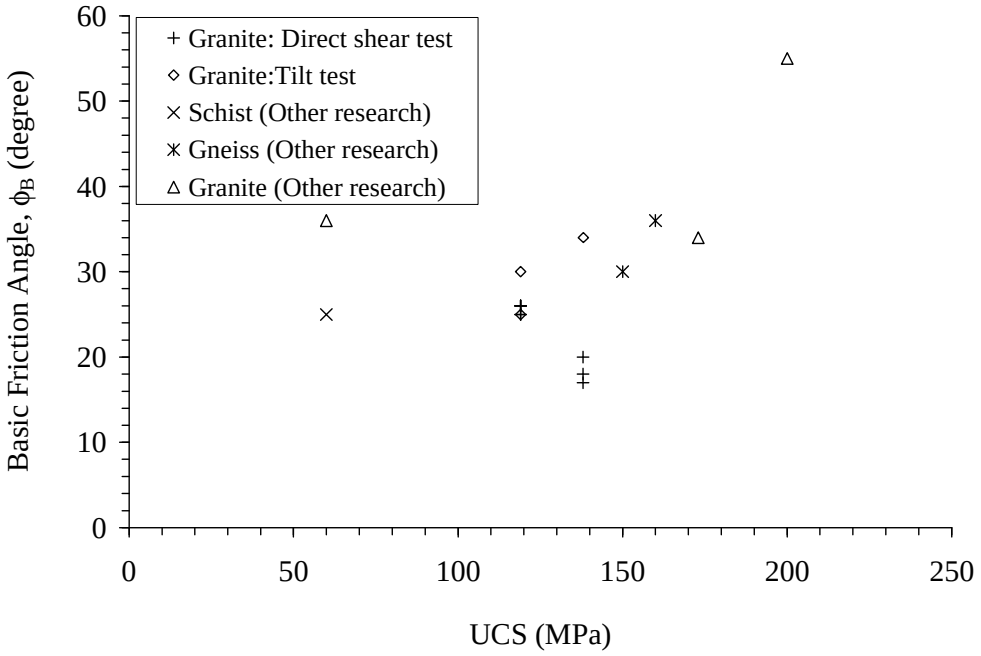

Figure 5.2 Relationship between UCS and basic friction angles of crystalline rocks.

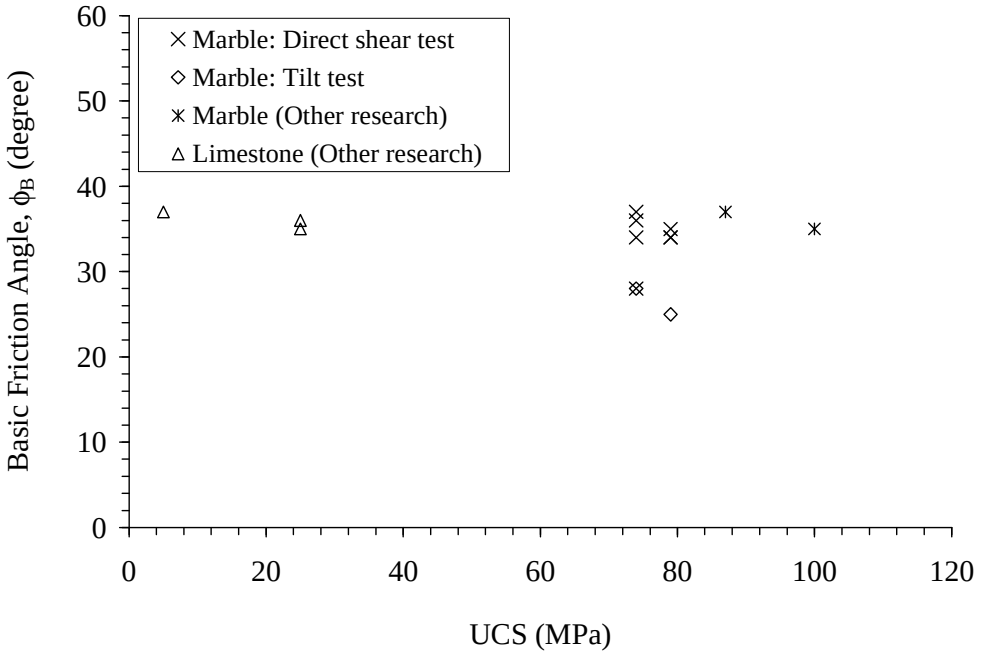

Figure 5.3 Relationship between UCS and basic friction angles of marbles and limestone.

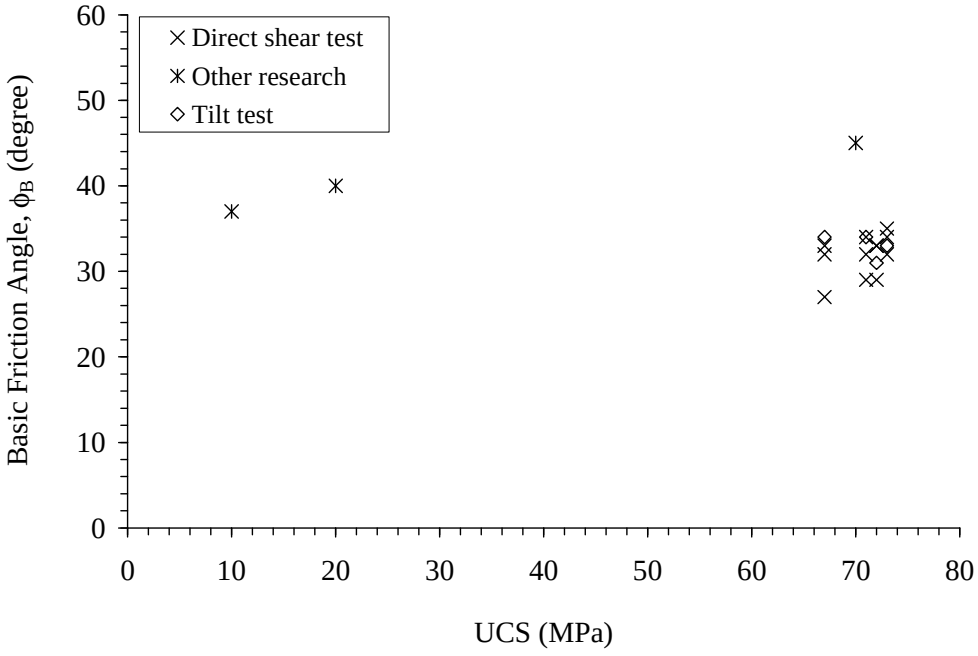

Figure 5.4 Relationship between UCS and basic friction angles of sandstones.

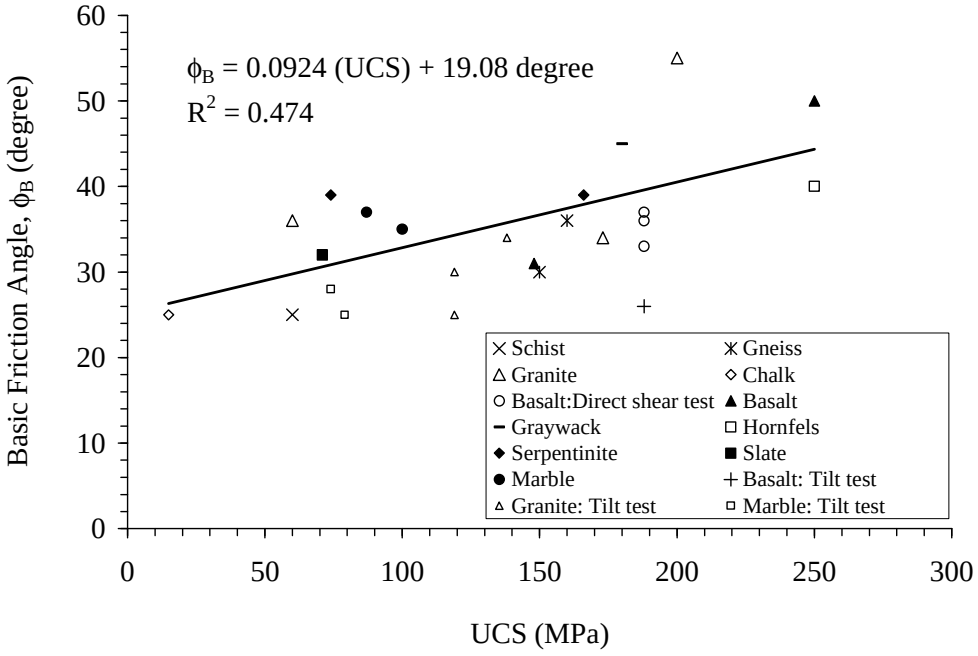

Figure 5.5 Relationship between UCS and basic friction angles for various rock types.

$$\phi_b = 0.0924\ UCS + 19.08;\ (R^2 = 0.474) \quad (5.1)$$

where ϕ_b is in degree and UCS is in MPa.

Extreme care should be taken when applying the above equation for other rocks. The available data are widely scattered, and are not truly sufficient to support the dependency of ϕ_b on UCS, as reflecting by the low coefficient of correlation. It is believed that ϕ_b does not always depend on the UCS. The real factors governing the ϕ_b for the crystalline rocks are probably the crystal size, mineral compositions, the cutting process, and the strength of cementing materials. For all rock types, no relationship has been found between ϕ_b and elastic modulus of the rocks.

CHAPTER VI

PREDICTION OF ROUGH JOINT SHEAR STRENGTHS

6.1 Introduction

The objective of this chapter is to compare and analyze between the predicted and the measured shear strengths of rough joints. Barton's criterion is used to calculate (predict) the shear strengths for the specimens with tension-induced fractures. The calculations use several combinations of the maximum and minimum values for the JRC, the UCS obtained from the ISRM field-identification, and the UCS determined by the ASTM standard method. For all calculations the actual ϕ_b is used. This is primarily to assess the predictive capability of the criterion, the adequacy of the field-identified UCS, and the sensitivity of the JRC and UCS on the Barton's shear strength.

6.2 Comparison of the Results

Table 6.1 compares the predicted shear strength with those actually tested for the rough joints. The actual values of joint shear strength are show in Figure 6.1 through 6.10.

The criterion using field-determined parameters satisfactorily predicts the shear strength to the rough joints in marbles and sandstones from all source locations, and slightly over-predicts the shear strength in the basalt specimens. It drastically

Table 6.1 Predicted and actual shear strengths for 3 rough joints from each rock type.

Rock Type	JRC Range	Predicted Shear Strength (kPa)						Actual Shear Strength (kPa)	Normal Stress (kPa)
		Actual UCS		UCS Min.		UCS Max.			
		JRC Min.	JRC Max.	JRC Min.	JRC Max.	JRC Min.	JRC Max.		
Burirum Basalt	8-11	2076	2413	1921	2181	2152	2528	1986	1655
	8-11	3483	3961	3225	3590	3607	4145	3185	2986
	8-11	4140	4677	3834	4241	4287	4891	3305	3636
Vietnamese Granite	10-12	868	1008	826	950	951	1123	3204	1068
	10-12	1440	1645	1368	1550	1581	1834	3588	1922
	8-10	1477	1688	1414	1602	1598	1854	4150	2378
Tak Granite	12-14	1237	1434	1198	1380	1421	1670	1555	1051
	8-10	1582	1795	1548	1748	1733	2009	2833	1932
	10-12	2074	2338	2020	2266	2322	2678	4581	2291
Chinese Granite	12-14	1310	1519	1269	1461	1507	1805	2938	1080
	14-16	2410	2743	2321	2624	2841	3343	3293	1950
	14-16	2818	3182	2714	3046	3315	3863	3557	2386

Table 6.1 Predicted and actual shear strengths for 3 rough joints from each rock type (cont.).

Rock Type	JRC Range	Predicted Shear Strength (kPa)						Actual Shear Strength (kPa)	Normal Stress (kPa)
		Actual UCS		UCS Min.		UCS Max.			
		JRC Min.	JRC Max.	JRC Min.	JRC Max.	JRC Min.	JRC Max.		
Saraburi Marble	8-10	1237	1413	1169	1315	1273	1466	1250	1078
	12-14	1738	1959	1644	1826	1788	2032	2146	1588
	8-10	2598	2928	2384	2640	2718	3094	2450	1934
Lopburi Marble	8-10	1297	1483	1236	1393	1347	1557	1230	1060
	10-12	1709	1951	1607	1806	1793	2074	1589	1255
	10-12	2416	2714	2274	2518	2533	2879	2861	1893
Phu Kradung Sandstone	6-8	1077	1225	1041	1169	1109	1273	1076	1076
	6-8	1532	1721	1480	1644	1577	1788	1367	1282
	6-8	1833	2046	1771	1954	1886	2126	1852	1939
Phu Phan Sandstone	6-8	1001	1137	968	1088	1031	1183	1333	1075
	6-8	1180	1333	1141	1275	1215	1387	1545	1288
	8-10	1903	2124	1821	2010	1981	2234	2704	1932
Phra Wihan Sandstone	6-8	1002	1138	971	1091	1034	1186	1380	1078
	6-8	1181	1334	1144	1279	1219	1391	1464	1292
	8-10	1911	2132	1832	2021	1992	2246	2075	1945
Sao Khua Sandstone	4-6	841	955	826	930	862	991	1197	1069
	6-8	1118	1261	1088	1217	1160	1324	1356	1271
	6-8	1643	1831	1600	1767	1705	1922	1900	1943

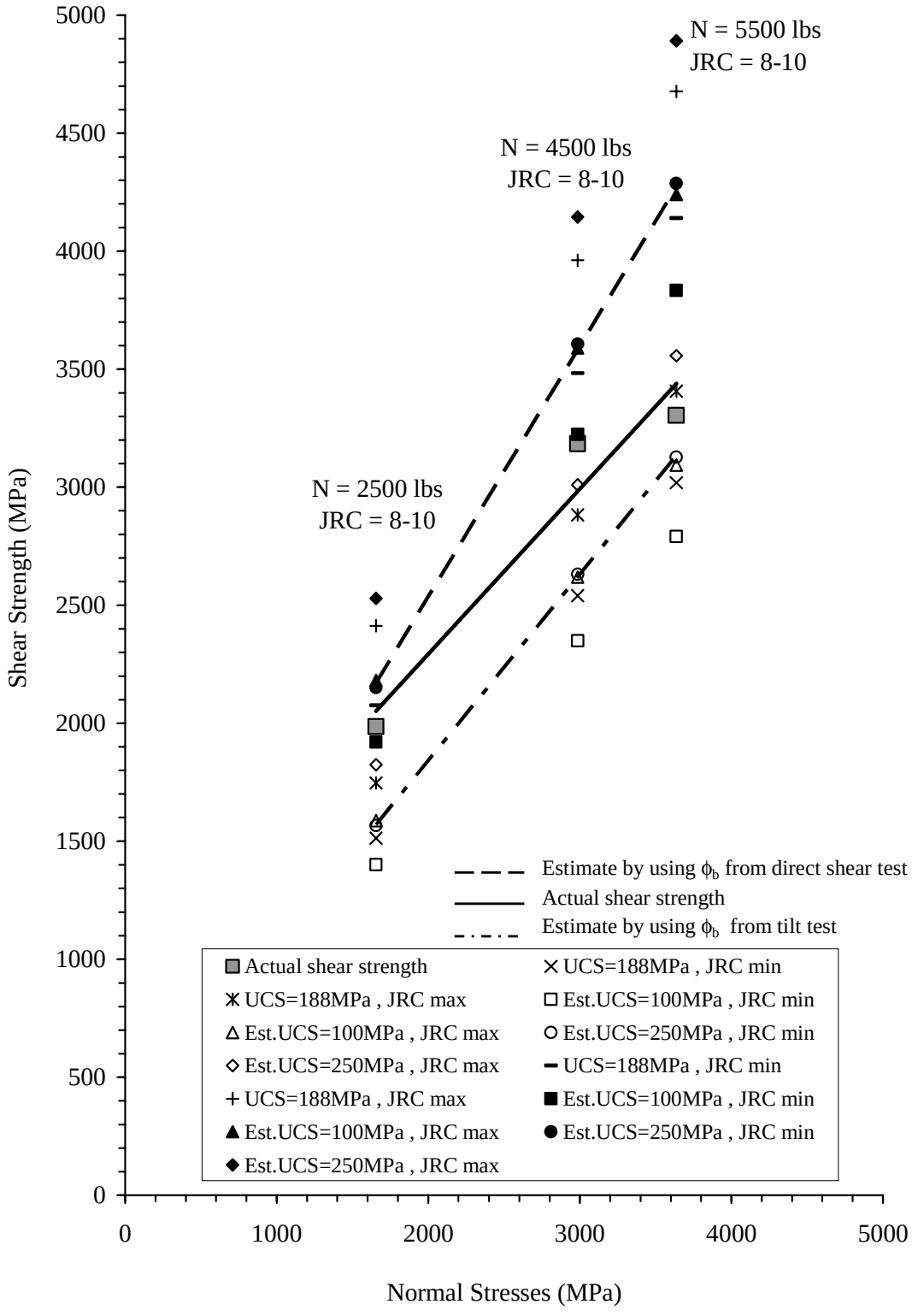

Figure 6.1 Comparison of predicted and actual joint shear strength for Burirum basalt.

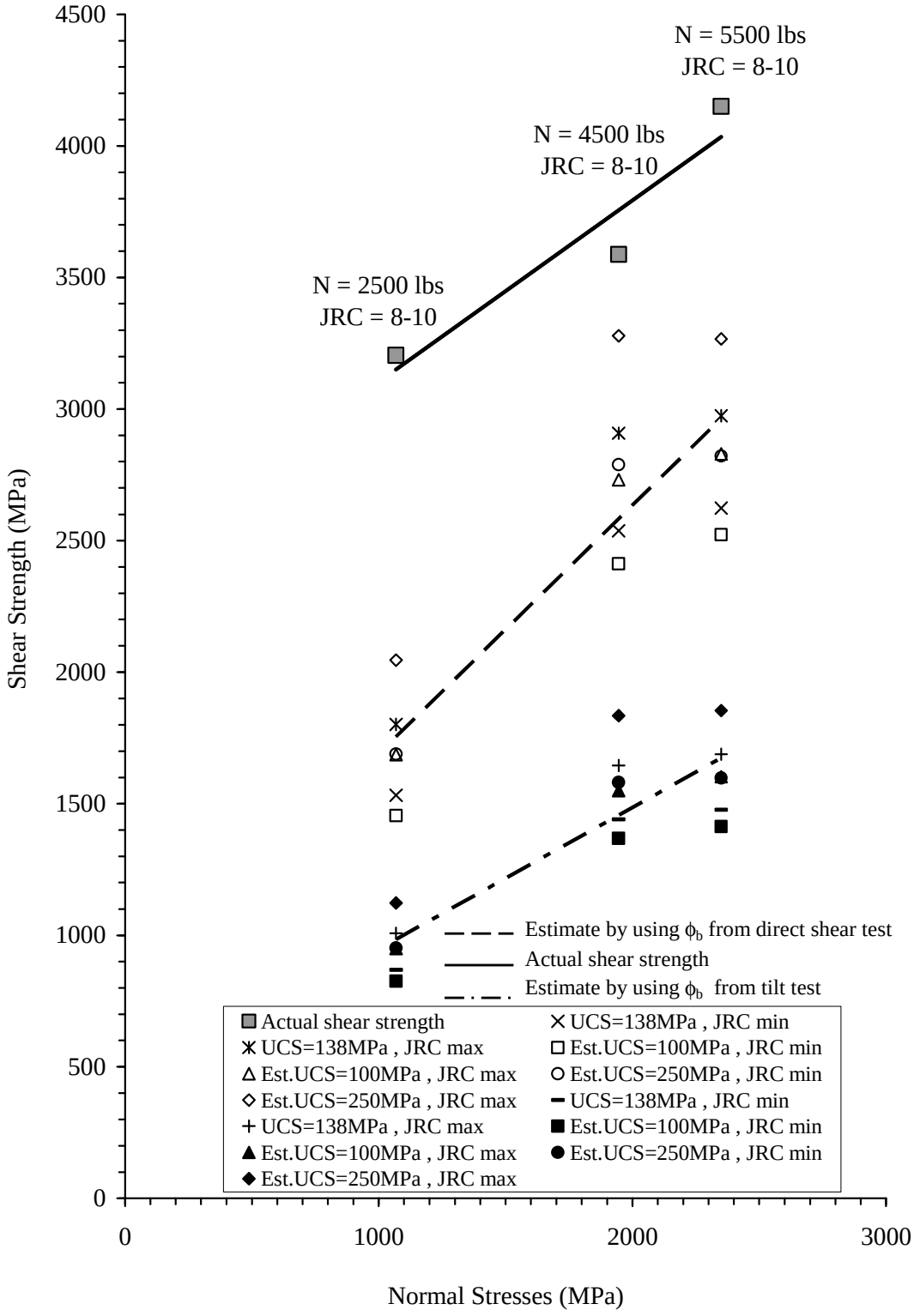

Figure 6.2 Comparison of predicted and actual joint shear strength for Vietnamese granite.

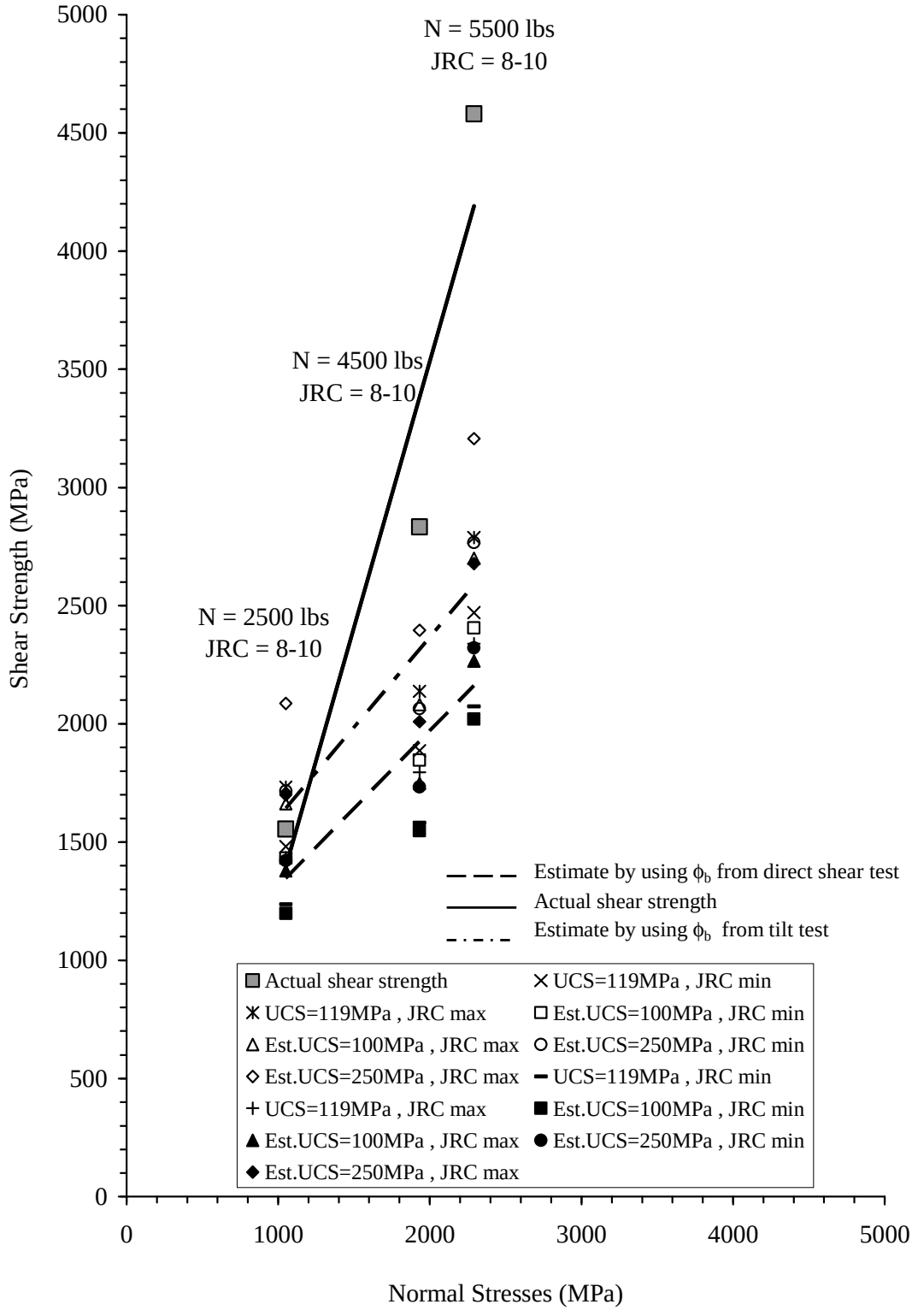

Figure 6.3 Comparison of predicted and actual joint shear strength for Tak granite.

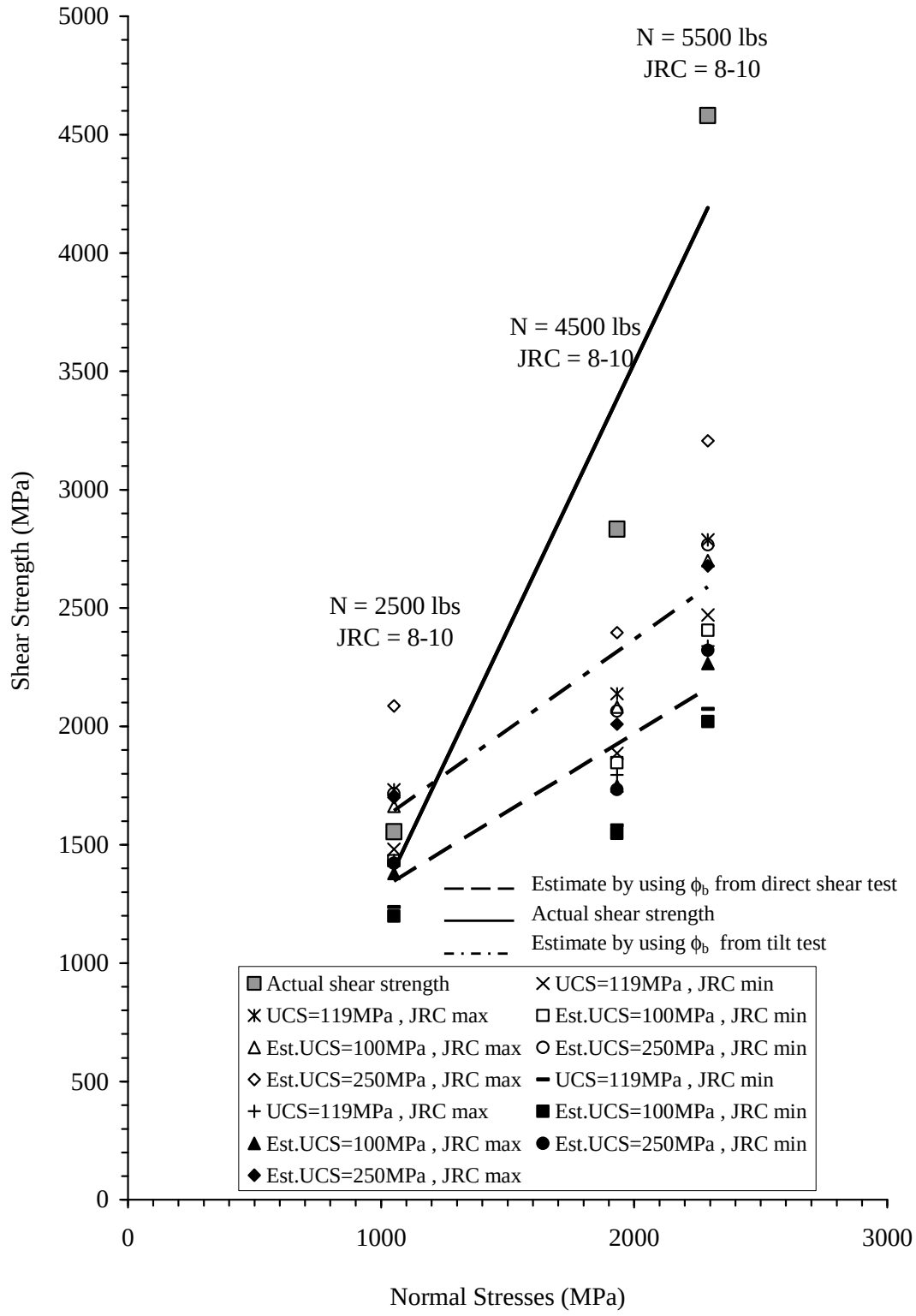

Figure 6.4 Comparison of predicted and actual joint shear strength for Chinese granite.

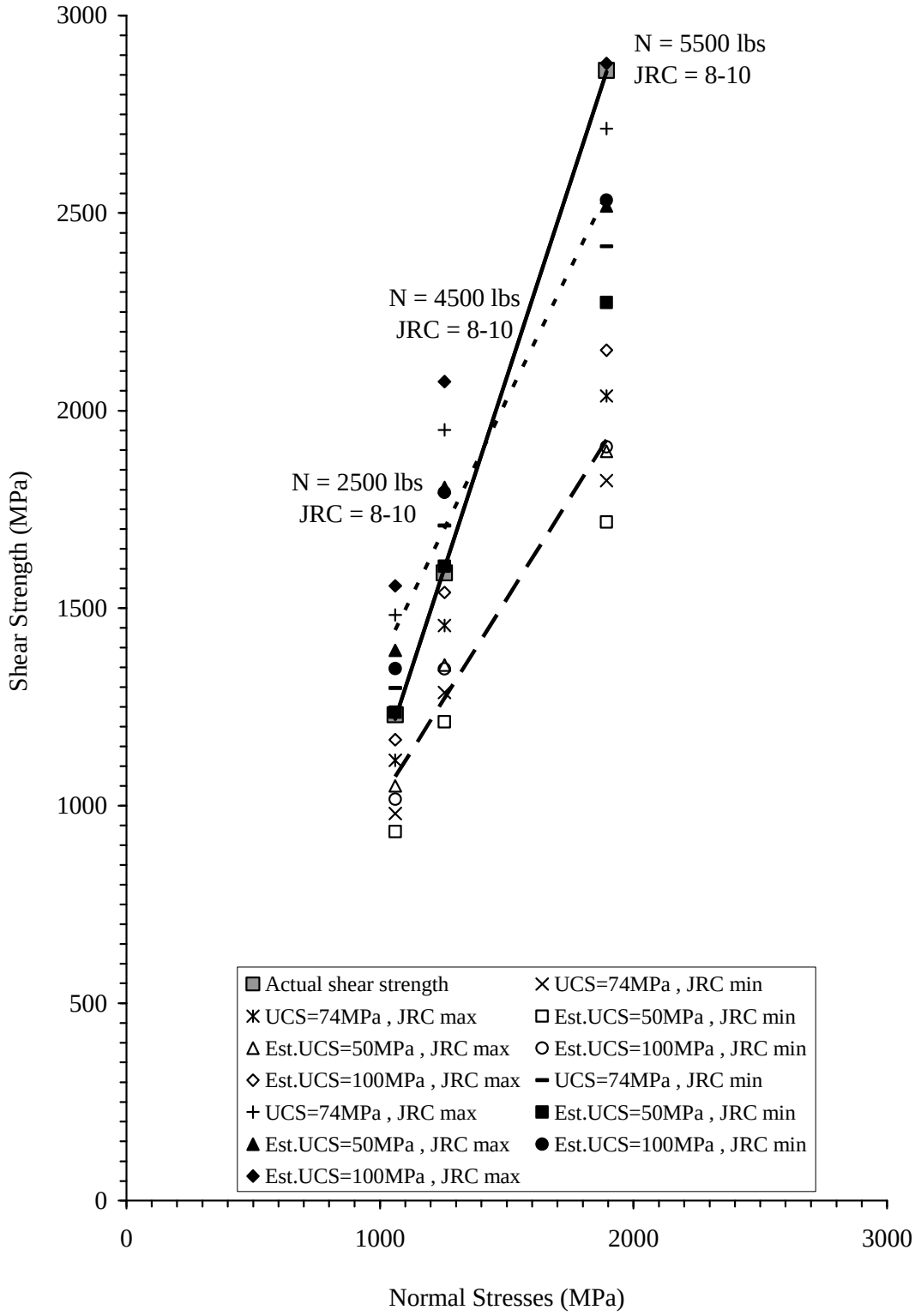

Figure 6.5 Comparison of predicted and actual joint shear strength for Saraburi marble.

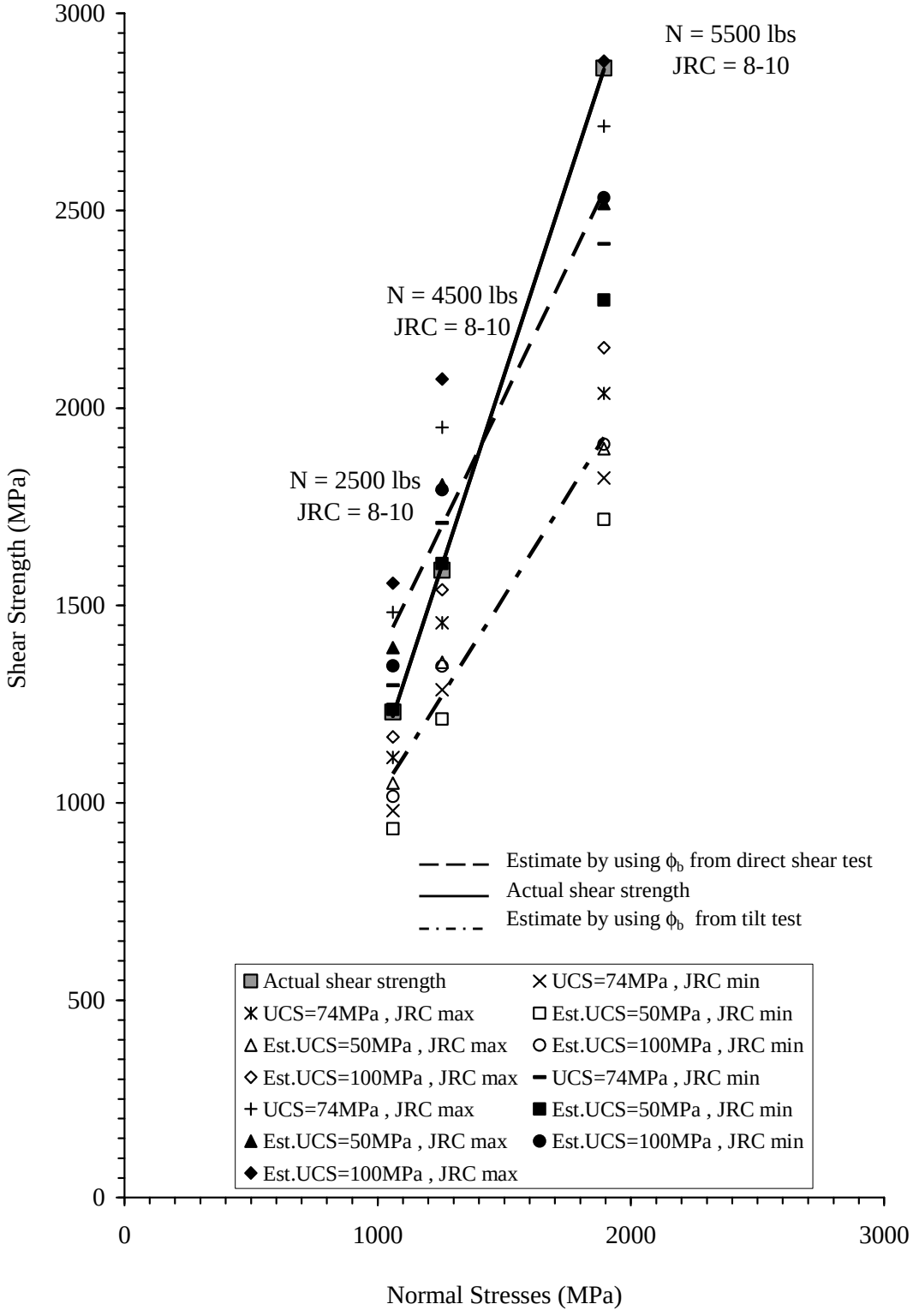

Figure 6.6 Comparison of predicted and actual joint shear strength for Lopburi marble.

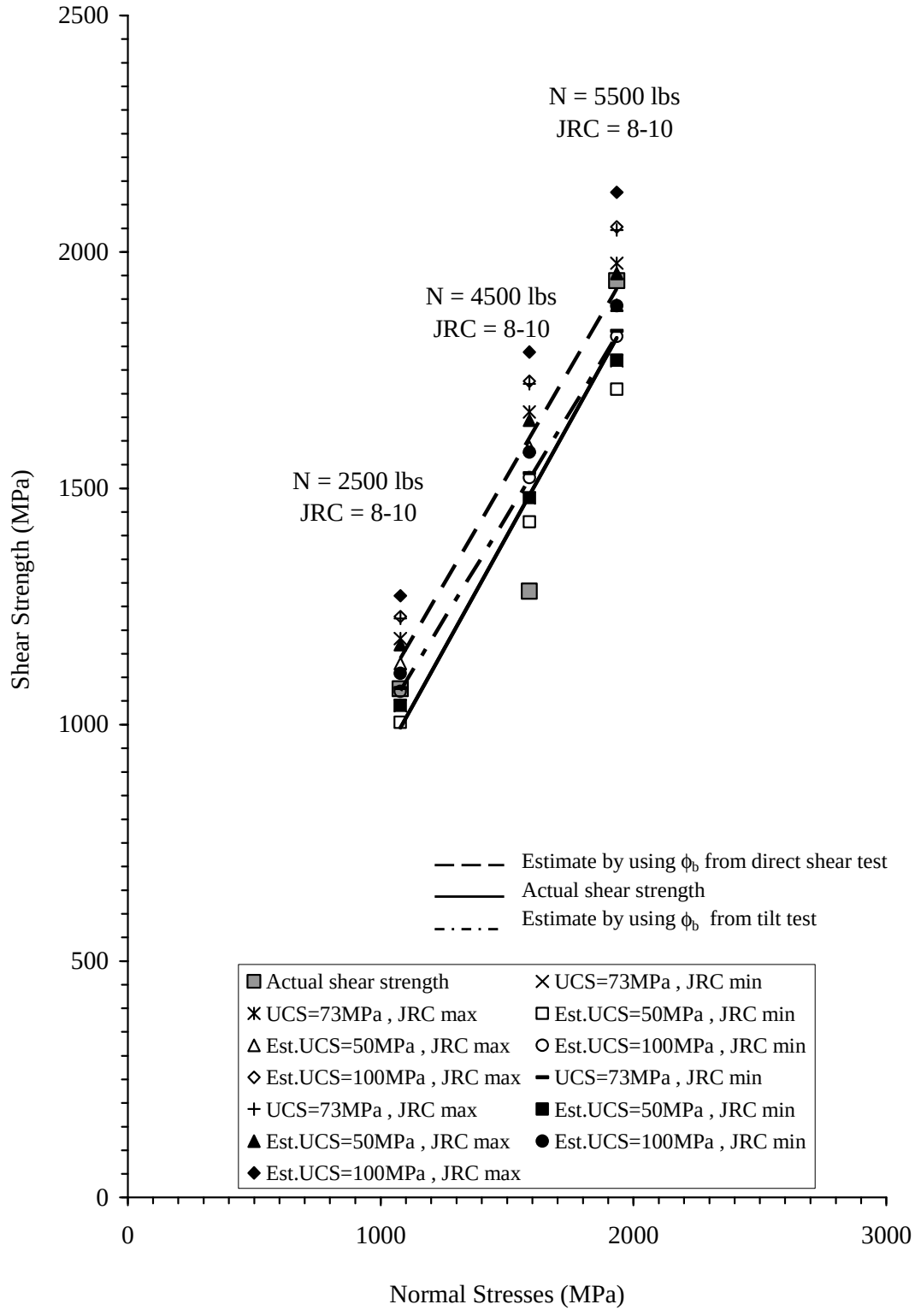

Figure 6.7 Comparison of predicted and actual joint shear strength for Phu Kradung sandstone.

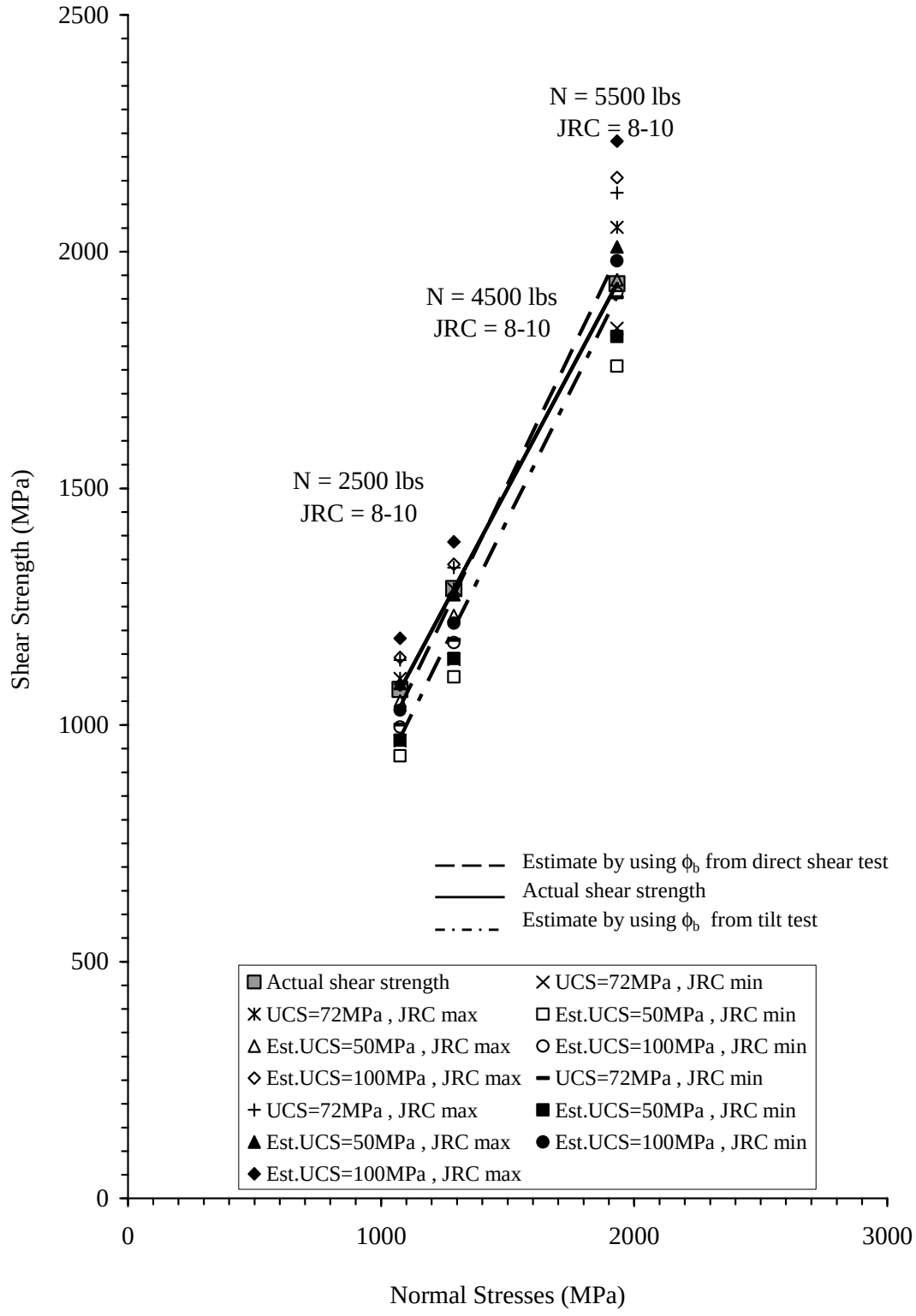

Figure 6.8 Comparison of predicted and actual joint shear strength for Phu Phan sandstone.

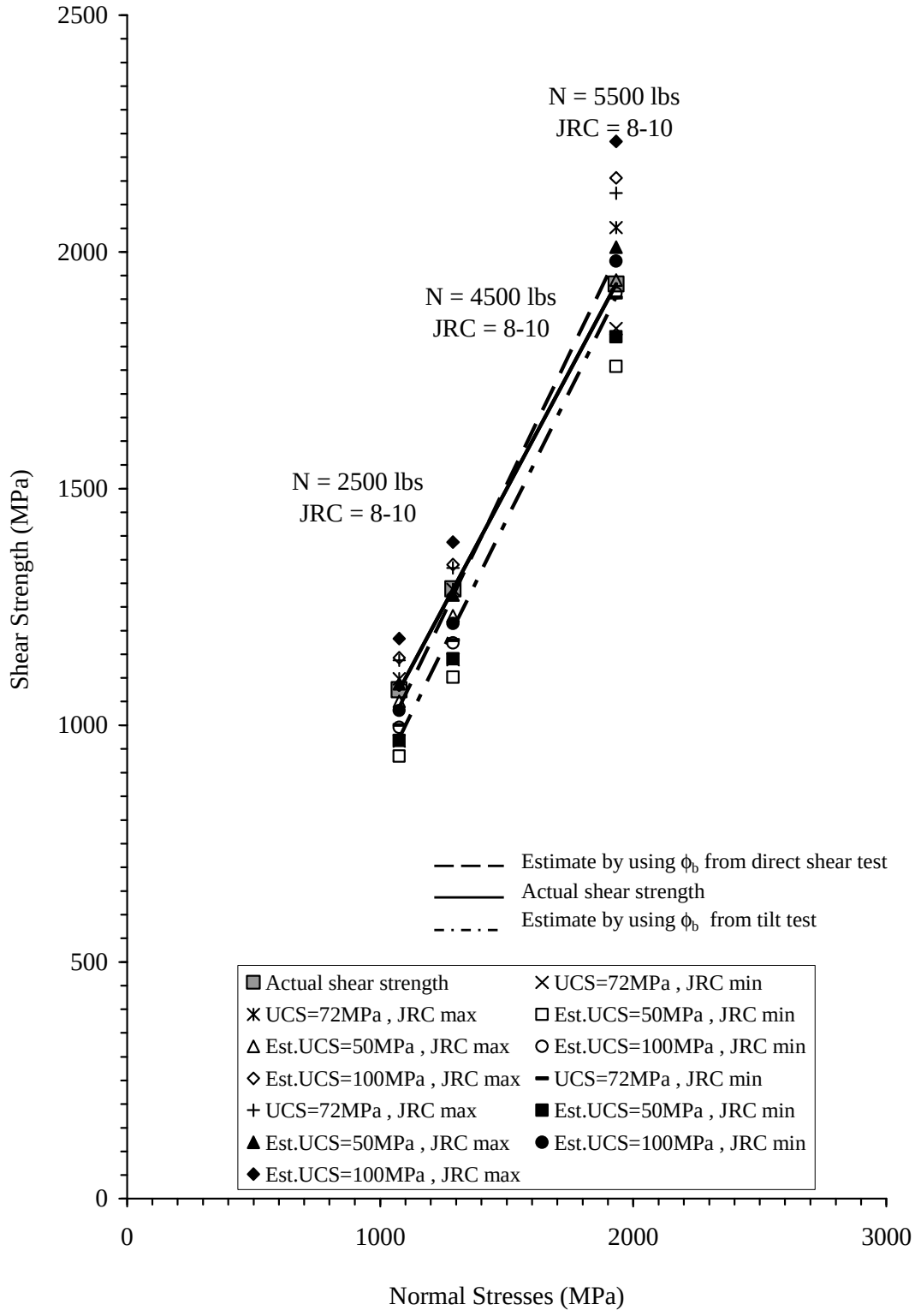

Figure 6.9 Comparison of predicted and actual joint shear strength for Phra Wihan sandstone.

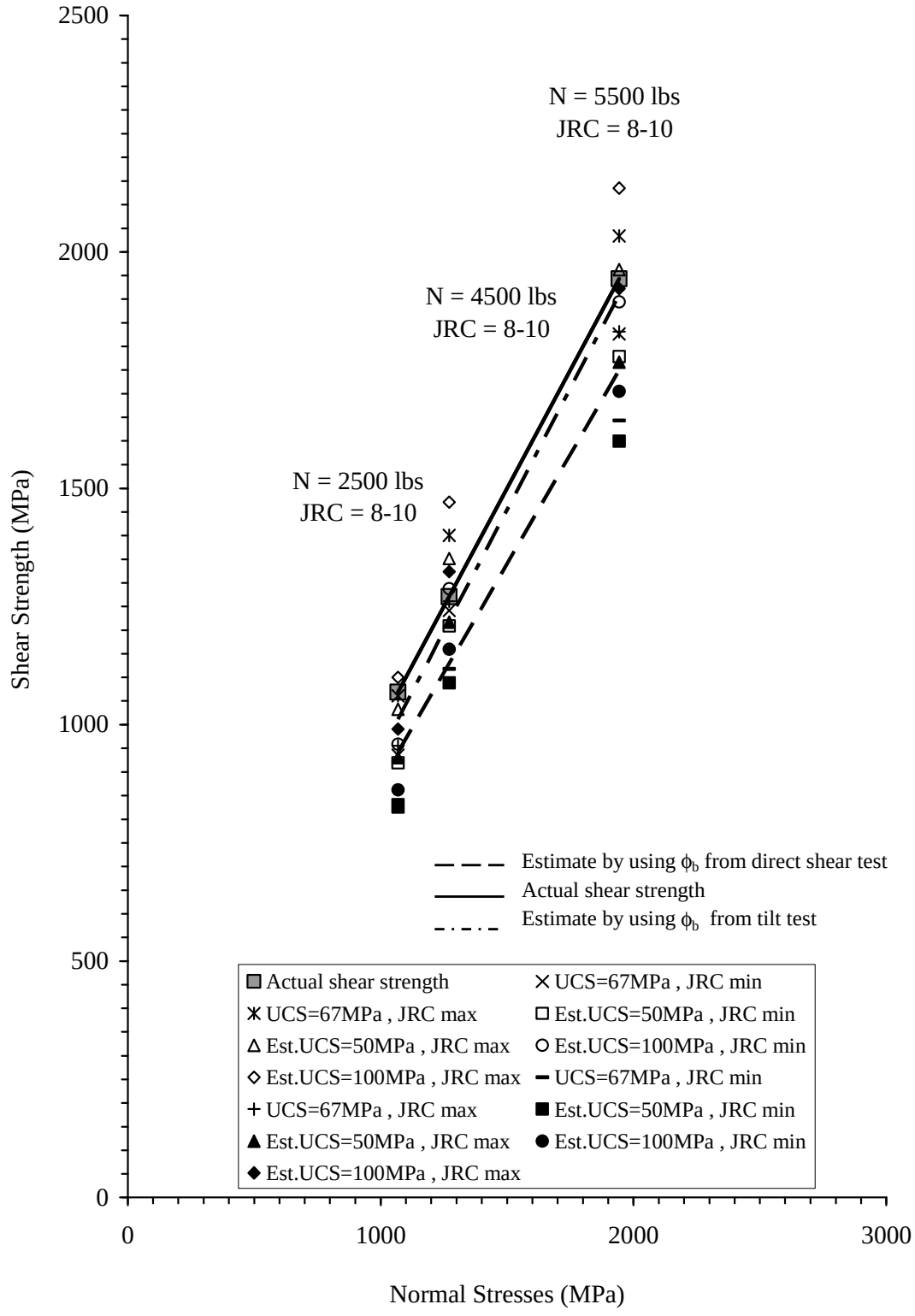

Figure 6.10 Comparison of predicted and actual joint shear strength for Sao Khua sandstone.

underestimates the shear strength of granite specimens from all locations. This is due to the face that ϕ_b from direct shear testing on the smooth saw-cut surfaces in granite is lower than the actual values.

The sensitivity evaluation also suggests that the Barton's shear strength is more sensitive to ϕ_b than to UCS and JRC. For all rock types, the range of UCS from ISRM field-identified method agrees well with the corresponding value determined by ASTM laboratory testing. Variations of the UCS by 25 MPa for weak and medium rocks (R2 and R3) and by 50 MPa for strong and very strong rocks (R4 and R5) do not significantly affect the predicted shear strengths. The range of JRC determined by six engineers, though it shows some subjectivity, provides appropriate values for the strength predictions.

CHAPTER VII

DISCUSSIONS AND CONCLUSIONS

The objective of this research is to seek the relationship between the joint shear strength of rocks and their physical and mechanical properties. Barton's criterion is used here to describe the shear strength of the joints. Ten rock types that are commonly found in Thailand are selected as rock samples. The petrographic properties and uniaxial compressive strengths of these samples are determined. Series of direct shear testing are performed on saw-cut surfaces and tension induced fractures of these rock samples to determine the basic friction angles (ϕ_b), cohesion (c) and friction angle of rock fractures. The ISRM field method is used to determine the intact rock strengths. All tested fractures are clean, tight and perfectly matched. The effects of joint aperture, dilation and filling materials are excluded from this study.

The results indicate that the Barton's criterion satisfactorily predicts the shear strength of rough joints in marbles and sandstones from all source locations, and slightly over-predicts the shear strength in the basalt specimens. It can not describe the joint shear strengths for the granite specimens, probably due to the fact that the saw-cut surfaces for the coarse-grained and very strong crystalline rocks (such as granites) are very smooth, even without polishing, and hence results in an unrealistically low ϕ_b from the direct shear testing.

The values of basic friction angles from the direct shear tests and the tilt tests are compared. Both tests yield similar results for the clastic rocks. For crystalline

rocks, the ϕ_b from direct shear tests is indicated smaller values for granite and larger for basalt and marble.

Barton's shear strength is more sensitive to ϕ_b than to UCS and JRC. The value of basic friction angle for the tested fine-grained sandstones is averaged as 33 ± 8 degrees. The cementing materials may have some influence on ϕ_b. For the tested marbles and for the limestone recorded elsewhere, ϕ_b is averaged as 35 ± 5 degrees, and appears to be independent of UCS. For other strong rocks (ISRM-designated R4 & R5), ϕ_b apparently increases linearly with UCS. This relationship remains inconclusive due to insufficient information.

Based on the observation, the real factors governing the ϕ_b for the crystalline rocks are probably the crystal size, mineral compositions, and the cutting process, and for the clastic rocks are the grain size and shape, and the bond strength of cementing materials. The number and diversity of the basalt and granite specimens are not adequate to determine the relationship between ϕ_b and the mineralogical variations, even if there is any. For some igneous or metamorphic rocks in particular, e.g., granite, diorite and gneiss, it may be virtually impossible to determine the relationship between ϕ_b and their mineralogy due to the infinite combinations of the rock compositions and textures on the fracture surfaces.

More testing is required. For clastic rocks, specimens with significantly different grain sizes and cementing materials are desirable. For the strong crystalline rocks, the effects of the cutting process should be investigated on roughness of the saw-cut surfaces.

Even though some uncertainties remain, as described above, the findings from this research still provide a quick and useful approach for determining the Barton's shear strength of clean, tight and rough joints. The ISRM field-identification seems adequate to determine the necessary parameters used in the Barton's criterion.

REFERENCES

Archambault, G., Fortin, M., Gill, D. E., Aubertin, M., and Ladanyi, B. (1990). Experimental investigations for an algorithm simulating the effect of variable normal stiffness on discontinuities shear strength. In Barton and Stephansson (eds.). **Rock Joint** (pp. 141-148). Rotterdam: A.A. Balkema.

ASTM D2938. Standard test methods for unconfined compressive strength of intact rock core specimens. In **Annual Book of ASTM Standards** (Vol. 04.08). Philadelphia: American Society for Testing and Materials.

ASTM D5607. Standard test methods for performing laboratory direct shear strength tests of rock specimens. In **Annual Book of ASTM Standards** (Vol. 04.08). Philadelphia: American Society for Testing and Materials.

Balazs, V. (1998). Shear failure in rock using different constant normal load. **Periodica Polytechnica Ser**. **Civ**. **Eng**. 43(2): 179-186.

Baliga, B. D. and Singh, V. K. (1992). Geotechnical investigation and appraisal of face stability in jointed rock mass in copper open-pit Rajasthan. In **Regional Symposium on Rock Slopes** (pp. 27-33). India: Oxford & IBH.

Bandis, S. C. (1993). Engineering properties and characterization of rock discontinuities. **Comprehensive Rock Engineerin** (Vol. I, pp. 155-184).

Barton, N. R. (1972). A model study of rock joint deformation. **International Journal of Rock Mechanics and Mining Sciences**. 9: 579-602.

Barton, N. R. (1973). Review of a new shear strength criterion for rock joints. **Engineering Geology**. 7: 287-332.

Barton, N. R. (1976). The shear strength of rock and rock joints. **International Journal of Rock Mechanics and Mining Sciences & Geomechanics Abstracts**. 13: 255-279.

Barton, N. R. and Bandis, S. (1982). Effect of block size on the shear behavior of jointed rock. In **Proceedings of the 23rd US Symposium on Rock Mechanics** (pp. 739-760). Berkeley: SME.

Barton, N. R. and Bandis, S. (1990). Review of predictive capabilities of JRC-JCS model in engineering practice. In **Proceedings of the International Conference on Rock Joints** (pp. 603-610). Norway: Leon.

Barton, N. R. and Choubey, V. (1977). The shear strength of rock joints in theory and practice. **Rock Mechanics**. 10: 1-54.

Beer, A. J., Stead, D., and Coggan, J. S. (2002). Technical note estimation of the joint roughness coefficient (JRC) by Visual Comparison. **Rock Mechanics Rock Engineering**. 35(1): 65-74.

Bell, F. G. (1978). The physical and mechanical properties of the fell sandstones Northumberland England. **Engineering Geology**. 12: 1-29.

Bieniawski, Z. T. (1981). Improved design of coal pillars for mining conditions. In **Proceedings of the 1st Annual Conference on Ground Control in Mining** (pp. 12-22). West Virgina University.

Brace, W. F. (1961). Dependence of fracture strength of on grain size. In **Proceeding of the 4th Symposium on Rock Mechanics** (pp.99-103). Pensylvania University.

Brady, B. H. G. and Brown, E. T. (1993). **Rock Mechanics for Underground Mining**. London: Chapman & Hall.

Brown, C. E. (1993). Use of principal-component, correlation and stepwise multiple-regression analyses to investigation selected physical and hydraulic properties of carbonate-aquifers. **Journal of Hydrology**. 147: 169-195.

Brown, E. T. (1981). **Rock Characterization, Testing and Monitoring - ISRM Suggested Methods**. Oxford: Pergamon.

Bye, A. R. and Bell, F. G. (2001). Stability assessment and slope design at Sandstones open pit, South Africa. **International Journal of Rock Mechanics and Mining Sciences & Geomechanics Abstracts**. 38: 449-466.

Chryssanthakis, P. (2003). **Forsmark Site Investigation Borehole : KFM01A Results of Tilt Testing**. Oslo: Morwegian Geotechnical Institute.

Coulson, J. M. (1972). Shear strength of flat surfaces in rock: stability of slopes. In **Proceedings of the 13th US Symposium on Rock Mechanics** (pp. 77-105). New York: ASCE.

Deere, D. U. and Miller, R. P. (1966). Engineering classification and index properties of intact rock. Technical Report No. AFWL-TR-65-11. New Maxico: Kirkland Airforce Base.

Dobereiner, L. and De Fretias, M. S. (1986). Geotechnical properties of weak sandstone. **Geotechnique**. 36(1): 79-94.

Duzgun, H. S. N., Yucemen, M. S., and Karpuz, C. (2002). A probabilistic model for the assessment of uncertainties in the shear strength of rock discontinuities. **International Journal of Rock Mechanics and Mining Sciences & Geomechanics Abstracts**. 39: 743-754.

Dyke, C. G. and Dobereiner, L. (1991). Evaluating the strength and deformability of sandstones. **Quarterly Journal of Engineering Geology**. 24: 123-134.

Evans, I. (1961). The tensile strength of coal. **Colliery Engineering**. 38: 428-434.

Fahy, M. P. and Guccione, M. J. (1979). Estimating strength sandstone using petrographic thin-section data. **Engineering Geology**. 16: 467-485.

Fairhurst, C. (1964). On the validity of the brazilian test for brittle materials. **International Journal of Rock Mechanics and Mining Sciences & Geomechanics Abstracts**. 1: 535-546.

Farmer, I. W. (1983). **Engineering Behavior of Rock** (2nd ed.). New York: Chapman and Hall.

Fasching, A. (2002). Rock mass characterization in an early stage of a tunnel project. Short Course on Geotechnics for Tunnel Design and Construction (pp. 43-48). Bangkok, Thailand

Fuenkajorn, K. (2003). **Fundamentals of Rock Mechanics**. Bangkok: Eson Paint Product.

Fuenkajorn, K. (2003). **Fundamental of Rock Mechanics.** Bangkok: Eason Paint Product.

Fuenkajorn, K. and Daemen, J. J. K. (1988). Boreholes closure in salt, Technical Report Prepared for the US Nuclear Regulatory Commission, Report No. NUREG/CR-5243 RW, University of Arizona.

Fuenkajorn, K. and Daemen, J. J. K. (1992). An empirical strength criterion for heterogeneous tuff. **An International Journal Engineering Geology**. 32: 209-223.

Giraud, A., Rochet, L., and Antoine, P. (1990). Processes of slope failure in crystallophyllian formation. **Engineering Geology**. 29: 241-253.

Goodman, R. E. (1976). **Method of Geological Engineering**. St. Paul, MN: West publishing company.

Goodman, R. E. (1989). **Introduction to Rock Mechanics** (2rd ed.). Canada: John Wiley & Sons.

Grasselli, G. and Egger, P. (2000). 3D Surface characterization for the prediction of shear strength of rock joint. **In Proceedings of the Eurock 2000** (pp. 281-286). Balkema, Germany: Essen.

Grasselli, G. and Egger, P. (2003). Constitutive law for the shear strength of rock joints based on three-dimensional surface parameters. **International Journal of Rock Mechanics and Mining Sciences & Geomechanics Abstracts**. 40: 25-40.

Griffith, A. A. (1924). Theory of rupture. In **Proceedings of the 1st Congression of the Applied Mechanics** (pp. 55-63). Delft: Technische Bockhandel en Drukkerij.

Gunsallus, K. L. and Kulhawy, F. H. (1984). A comparative evaluation of rock strength measures. **International Journal of Rock Mechanics and Mining Sciences & Geomechanics Abstracts**. 21: 233-248.

Haberfield, C. M. and Johnston, I. W. (1994). A mechanistically-based model for rough rock joints. **International Journal of Rock Mechanics and Mining Sciences & Geomechanics Abstracts**. 31(4): 279-292.

Handlin, J. and Hager, R. V. (1957). Experimental deformation of sedimentary rock under a confining pressure. **Journal of the American Association for Petroleum Geology**. 41: 1-50.

Hartley, A. (1974). A review of geological factors influencing the mechanical properties of road surface aggregation. **Quaternary Journal of Engineering Geology**. 7: 69-100.

Hawkins, A. B. and McConnell, B. J. (1992). Sensitivity of sandstone strength and deformability to changes in moisture content. **Quarterly Journal of Engineering Geology**. 25: 115-130.

Hencher, S. R. (1987). The implications of joints and structures for slope stability. In **Proceedings of the Slope Stability** (pp. 145-185). New York: John Wiley & Sons.

Hencher, S. R. and Richards, L. R. (1982). The basic frictional resistance of sheeting joints in Hong Kong Granite. **Hong Kong Engineer**. 11(2): 21-25.

Hencher, S. R. and Richards, L. R. (1989). Laboratory Direct Shear Testing of Rock Discontinuities. **Ground Engineering**. 22(2): 24-31.

Hoek, E. (1965). **Rock Fracture under Static Stress Conditions**. Ph.D. Thesis, University of Cape Town, South Africa.

Hoek, E. and Bray, J. W. (1981). **Rock Slope Engineering** (3rd ed.). London: The Institution of Mining and Metallurgy.

Hoek, E. and Brown, E. T. (1980). **Underground Excavations in Rock**. London: The Institution of Mining and Metallurgy.

Horn, H. M. and Deere, D. U. (1962). Friction characteristics of minerals. **Geotechnique**. 12: 319-335.

Howarth, D. F. and Rowlands, J. C. (1986). Development of an index to quantify rock texture for qualitative assessment of intact rock properties. **Geotechnical Testing Journal**. 9: 169-179.

Indraratna, B. and Haque, A. (2000). **Shear Behavior of Rock Joints**. Rotterdam: A.A. Balkema.

ISRM. (1981). **Suggested Method for Rock Characterization, Testing and Monitoring**. Oxford: Pergamon.

Jaeger, J. C. (1959). The frictional properties of joints in rocks. **Geofis pura appl**. 43: 148-158.

Jaeger, J. C. (1971). Friction of rocks and stability of rock slopes. **Geotechnique**. 21(2): 97-143.

Jaeger, J. C. and Cook, N. G. W. (1979). **Fundamentals of Rock Mechanics** (3rd ed.). London: Chapman and Hall.

Johnston, I. W., Lam, T. S. K., and Williams, A. F. (1987). Constant normal stiffness direct shear testing for socketed pile design in weak rock. **Geotechnique**. 37(1): 83-89.

Kawamura, K. and Ogawa, S. (1997). Slope failure in major tertiary mudstone zone. **Deformation and Progressive Failure in Geomechanics** (pp. 701-706). Japan.

Kitagawa, R. (1999). Weathering mechanism and slope failures of granitic rocks in Southwest Japan-Effect of hydrothermal activities. In **Proceedings of the International Symposium on Slope Stability Engineering** (pp. 109-113). Rotterdam: A.A. Balkema.

Kitamura, H., Aoki, M., Nishikawa, T., Suzuki, M., and Umezaki, T. (1999). Investigation of cut slope consisting of serpentinite and schist. In **Proceedings of the International Symposium on Slope Stability Engineering** (pp. 103-107). Rotterdam: A.A. Balkema.

Kumsar, H., Akgun, M., and Aydan, Ö. (1998). A back analysis of circular slope failure at Pamukkale-Golemezli irrigation canal in Turkey. In **Regional Symposium on Sedimentary Rock Engineering** (pp. 197-203). Taiwan: Press.

Ladanyi, B. and Archambault, G. (1970). Simulation of shear behavior of jointed rock mass. In **Proceedings of the 11th Symposium on Rock Mechanics: Theory and Practice** (pp. 105-125). New York: AIME.

Landanyi, B. and Archambault, G. (1972). Evaluation de la resistance au cisaillement d'un massif rocheux fragmente. In **Proceedings of the 24th International Geological Congress** (pp. 249-260). Montreal.

Maharaj, R. J. (1999). Site investigation of weathered expansive mudrock slopes: Implications for slope instability and slope stabilization. In **Proceedings of the International Symposium on Slope Stability Engineering** (pp. 115-120). Rotterdam: A.A. Balkema.

Murrell, S. A. F. (1965). The effects of triaxial stress systems on the strength of rocks at atmospheric temperatures. **Geophys**. **J**., R. Astron. Soc. 10(3): 231-81.

Onodera, T. F. and Asoka, K. H. M. (1980). Relation between texture and mechanical properties of crystalline rocks. **Bulletin of the International Association for Engineering Geology**. 22: 173-177.

Patton, F. D. (1966). **Multiple Mode of Shear Failure in Rock and Related Material**. Ph.D. Thesis, University of Illinois, USA.

Patton, F. D. (1966). Multiple modes of shear failure in rock. In **Proceedings of the 1st Congress on International Society Rock Mechanics** (pp. 509-513). Lisbon.

Priest, S. D. (1975). **Geomechanical Aspects of Tunneling in Discontinuous Rock with Particular Reference to the Lower Chalk**. Ph.D. Thesis, University of Durham.

Priest, S. D. (1993). **Discontinuity Analysis for Rock Engineering**. London: Chapman & Hall.

Ramamurthy, T. (2001). Shear strength response of some geological materials in triaxial compression. **International Journal of Rock Mechanics and Mining Sciences & Geomechanics Abstracts**. 38: 683-697.

Riedmuller, G. and Schubert, W. (2002). Project and rock mass specific investigation for tunnels. Short Course on Geotechnics for Tunnel Design and Construction (pp. 56-74). Bangkok, Thailand.

Riedmuller, G., Franz, J.B., Klima, K., and Medley, W. (2002). Engineering geological characterization of brittle faults and classification of fault rocks. Short Course on Geotechnics for Tunnel Design and Construction (pp. 13-33). Bangkok, Thailand.

Romero, S. U. (1968). In situ direct shear tests on irregular surface joints filled with clayey material. In **Proceedings of the International Symposium on Rock Mechanics** (pp. 189-194). Madrid: ISRM.

Ross-Brown, D. M. and Walton, G. (1975). A portable shear box for testing rock joints. **Rock Mechanics**. 7: 129-153.

Saint Simon, P. G. R., Solymar, Z. V., and Thompson, W. J. (1979). Damsite investigation in soft rocks of Place River Valley. In **Proceedings of the 4th International Conference on Rock Mechanics** (pp. 553-560). Canada: Montreux.

Schubert, W. and Riedmuller, G. (2002). Tunnelling in fault zones- state of the art in investigation and construction. Short Course on Geotechnics for Tunnel Design and Construction (pp. 7-15). Bangkok, Thailand.

Seidel, J. P. and Haberfield, C. M. (1995). The application of energy principles to the determination of sliding resistance of rock joints. **Rock Mechanics Rock Engineering**. 28(4): 211-226.

Selley, R. C. (1994). **Applied sedimentology**. London: Academic Press Limited.

Shakoor, A. and Bonelli, R. E. (1991). Relationship between petrographic characteristics, engineering index properties, and mechanical properties of selected sandstone. **Bulletin of the International Association for Engineering Geologists**. 28: 55-71.

Simsons, N., Menzies, B., and Matthews, M. (2001). **Soil and Rock Slope Engineering**. Great Britain: MPG Books.

Skinas, C. A., Bandis, S. C., and Demiris, C. A. (1990). Experimental investigations and modeling of rock joint behavior under constant normal stiffness. In Barton and Stephansson (eds.). **Rock Joint** (pp. 301-307). Rotterdam: A.A. Balkema.

Stavros, C. and Bandis, S. (1998). Engineering properties and characterization of rock discontinuiies. In J.A. Hudson (ed). **Comprehensive Rock Engineering Principles**, **Practice & Projects** (pp.155-183). Oxford: Pergamon.

Stimpson, B. (1981). A suggested technique for determining the basic friction angle of rock surfaces using core. **International Journal of Rock Mechanics and Mining Sciences & Geomechanics Abstracts**. 18: 63-65.

Tisa, A. and Kovari, K. (1984). Continuous failure state direct shear tests. **Rock Mechanics Rock Engineering**. 17(2): 83-95.

Tse, R. and Cruden, D. M. (1979). Estimating joint roughness coefficients. **International Journal of Rock Mechanics and Mining Sciences & Geomechanics Abstracts**. 16: 303-307.

Ulusay, R., Tureli, K., and Ider, M. H. (1994). Prediction of engineering properties of a selected litharenite sandstone from it's petrographic characteristics using correlation and multivariate statistical techniques. **Engineering Geology**. 37: 135-157.

Vasarhelyi, B. (1999). Shear failure in rock using different constant normal load. **Periodica Polytechnica Ser**. **Civ**. **Eng**. 43(2): 179-186.

Vutukuri, V. S., Lama, R. D., and Saluja, S. S. (1974). **Handbook on Mechanical Properties of Rocks** (Vol. 1). Clausthal-Zellerfeld: Trans Tech Publications.

Waltham, A. C. (1994). **Foundations of Engineering Geology**. Glasgow: Blackie Academic & Professional.

Wyllie, D. C. (1998). **Foundation on Rock**. London: E&FN Spon.

Xu, S. and De Fretias, M. H. (1990). The complete shear stress versus shear displacement behavior of clean and infilled rough joint. In **Proceedings of the International Conference on Rock Joint** (pp. 341-348). Rotterdam: A.A. Balkema.

Yang, Z. Y., Di, C. C., and Lo, S. C. (2001). Reassessing the joint roughness coefficient (JRC) estimation using Z_2. **Rock Mechanics Rock Engineering**. 34(3): 243-251.

Yang, Z. Y., Di, C. C., and Lo, S. C. (2001). Two-dimensional Hurst index of joint surface. **Rock Mechanics Rock Engineering**. 34(4): 323-345.

Zhao, J. (1988). The joint matching coefficient (JMC) of rock joints. In **Proceedings of the International Symposium on Tunneling for Water Resources and Power Projects** (pp. 21-27). New Delhi.

Zhao, J. (1997). Joint surface matching and shear strength Part B. JRC-JMC shear strength criterion. **International Journal of Rock Mechanics and Mining Sciences & Geomechanics Abstracts**. 34: 179-185.

Zhao, J. and Zhou, Y. (1992). Influence of joint matching characteristics in rock slope stability. In **Proceedings of the ISRM Regional Symposium on Rock Slope** (pp.139-146). New Delhi.

APPENDIX A

RESULTS OF UNIAXIAL COMPRESSIVE STRENGHT TEST

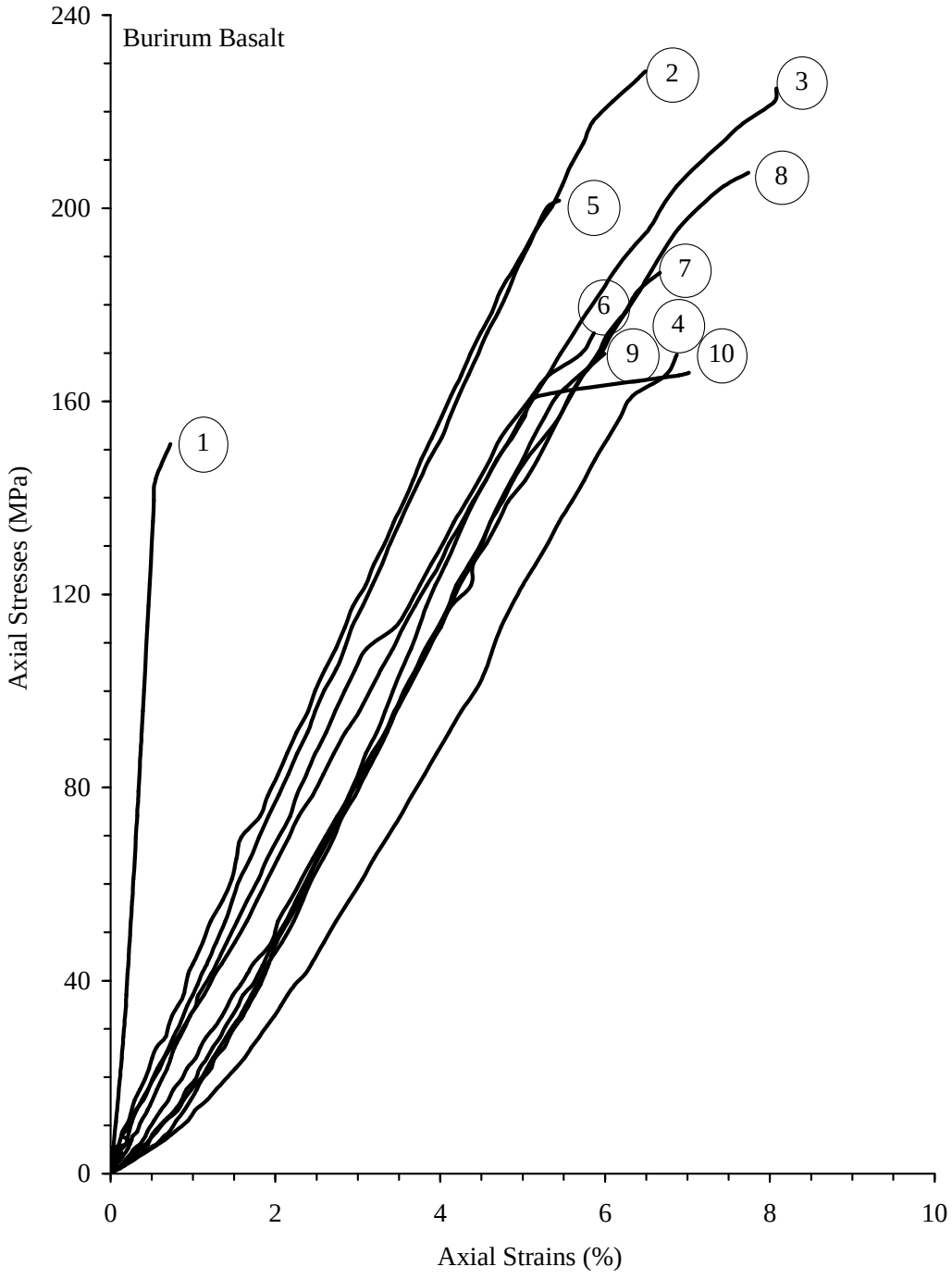

Figure A.1 The axial stress-strain curves for uniaxial compressive strength tests of Burirum basalt.

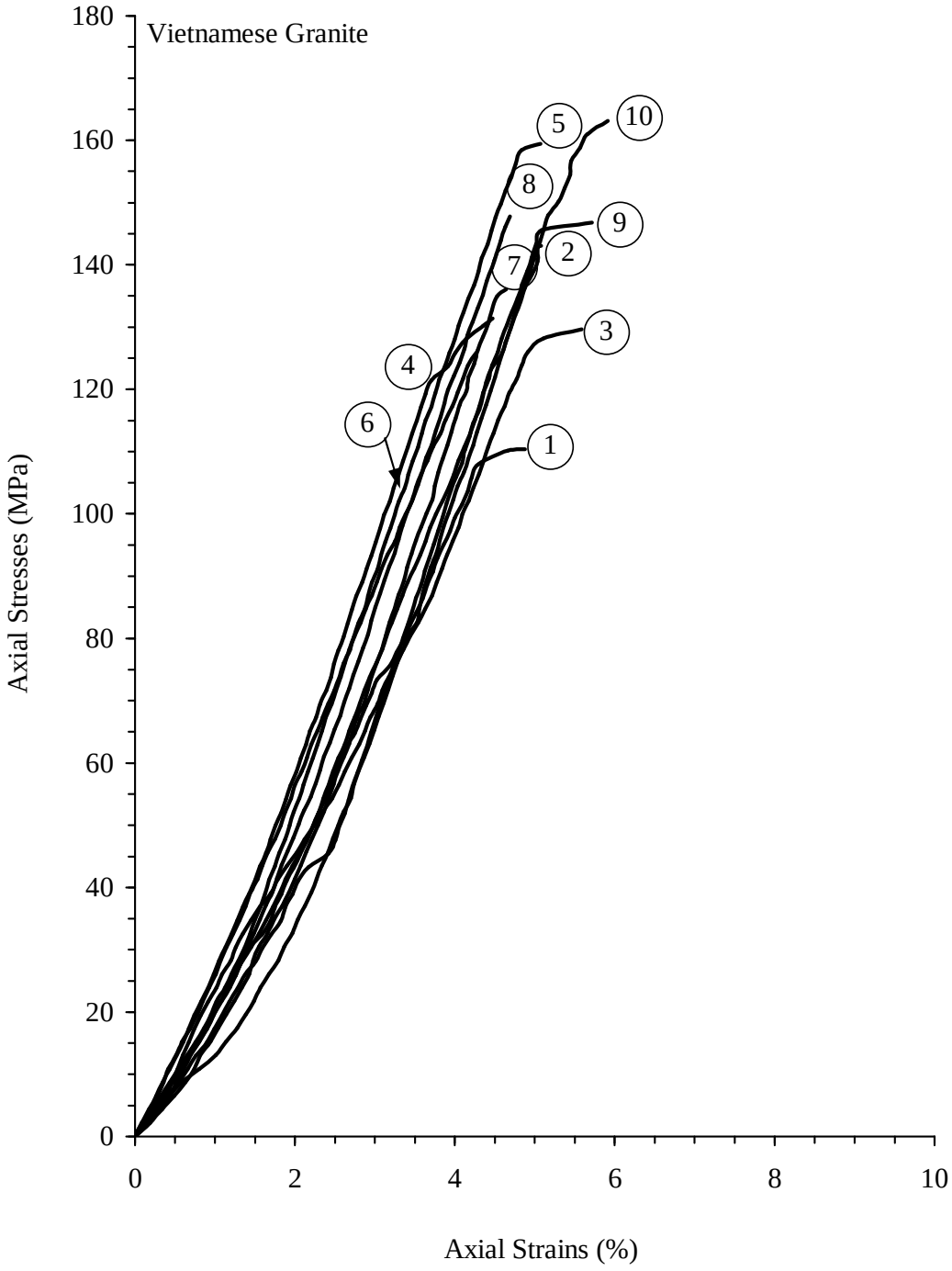

Figure A.2 The axial stress-strain curves for uniaxial compressive strength tests of Vietnamese granite.

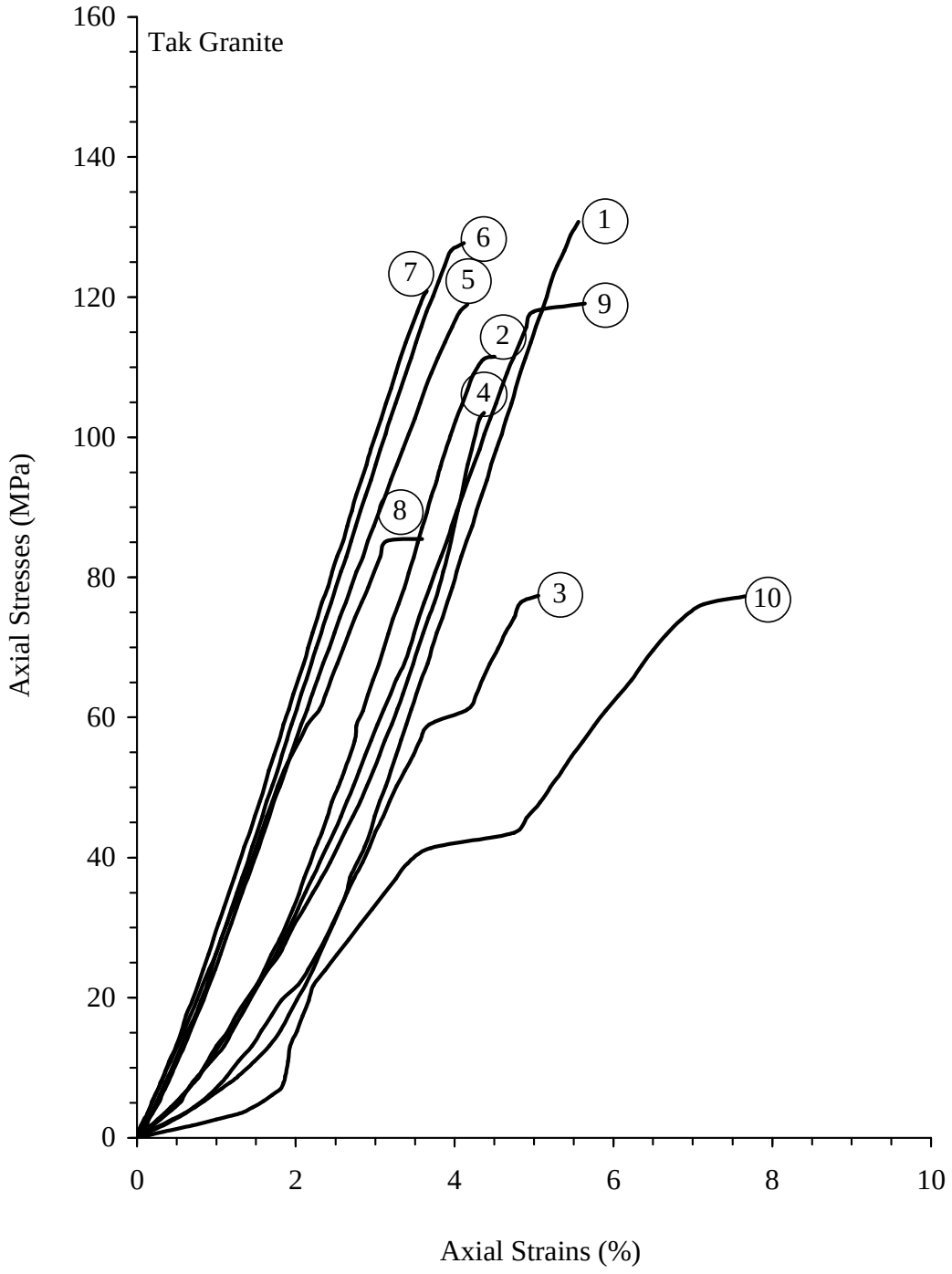

Figure A.3 The axial stress-strain curves for uniaxial compressive strength tests of Tak granite.

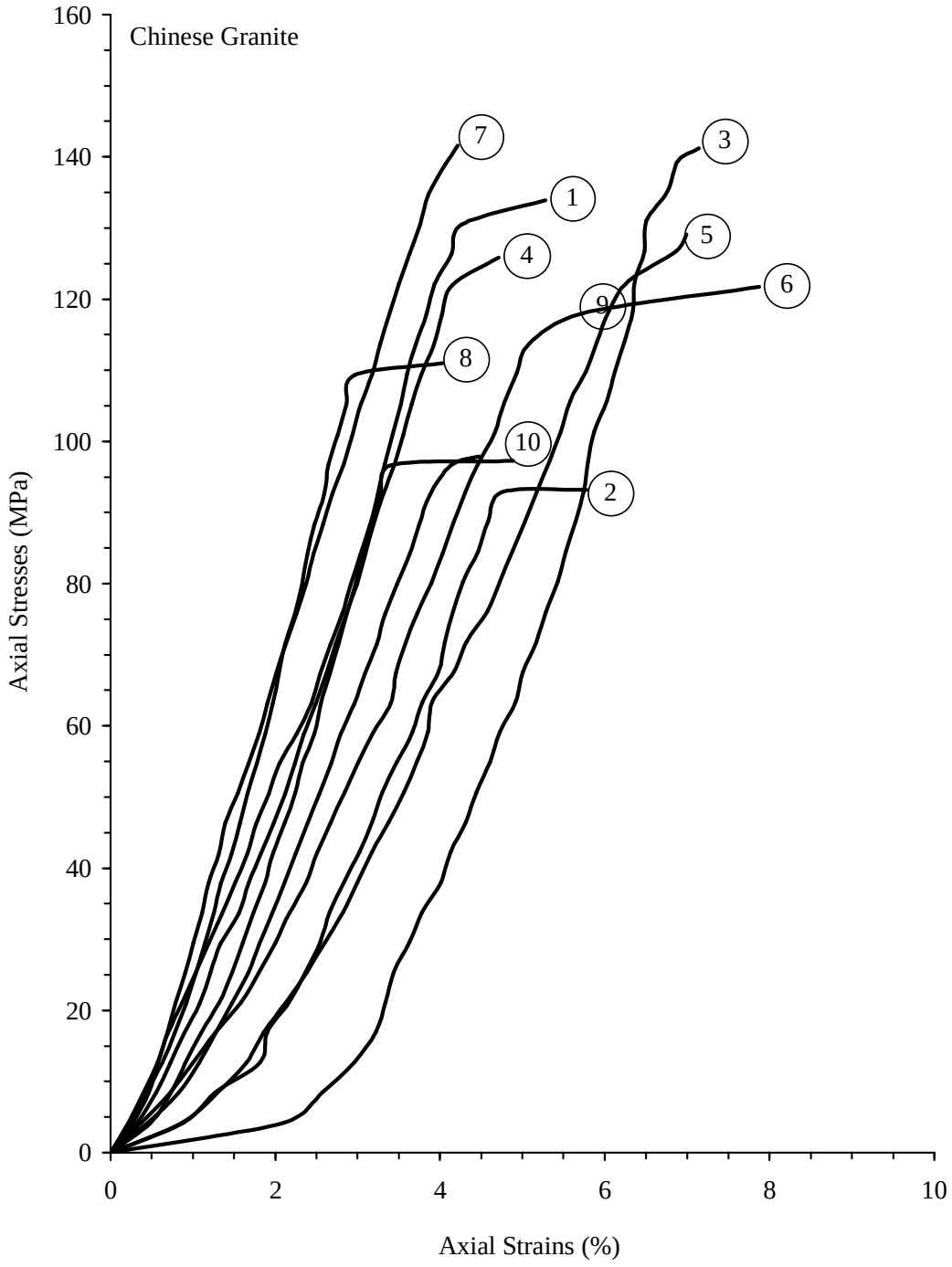

Figure A.4 The axial stress-strain curves for uniaxial compressive strength tests of Chinese granite.

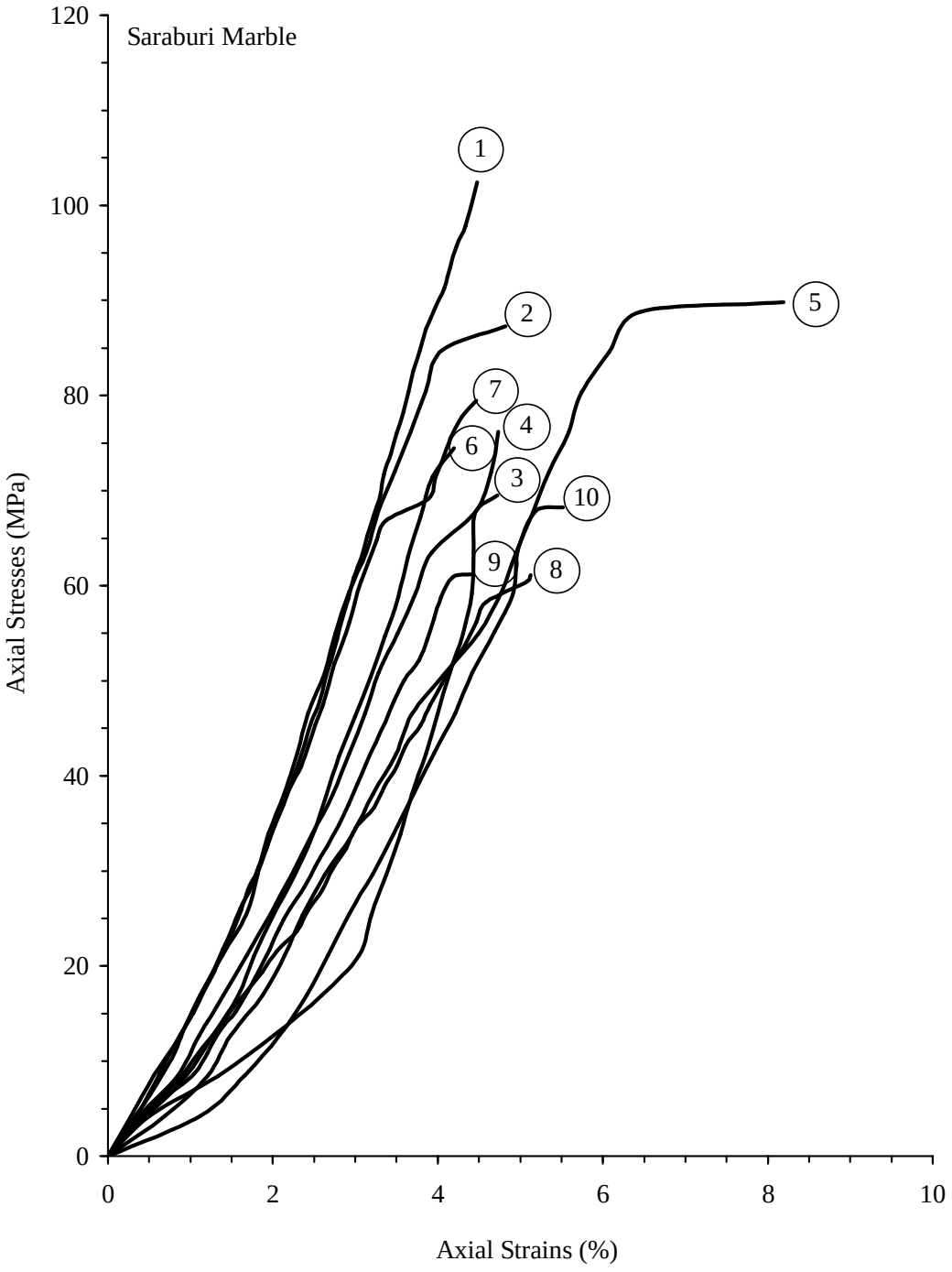

Figure A.5 The axial stress-strain curves for uniaxial compressive strength tests of Saraburi marble.

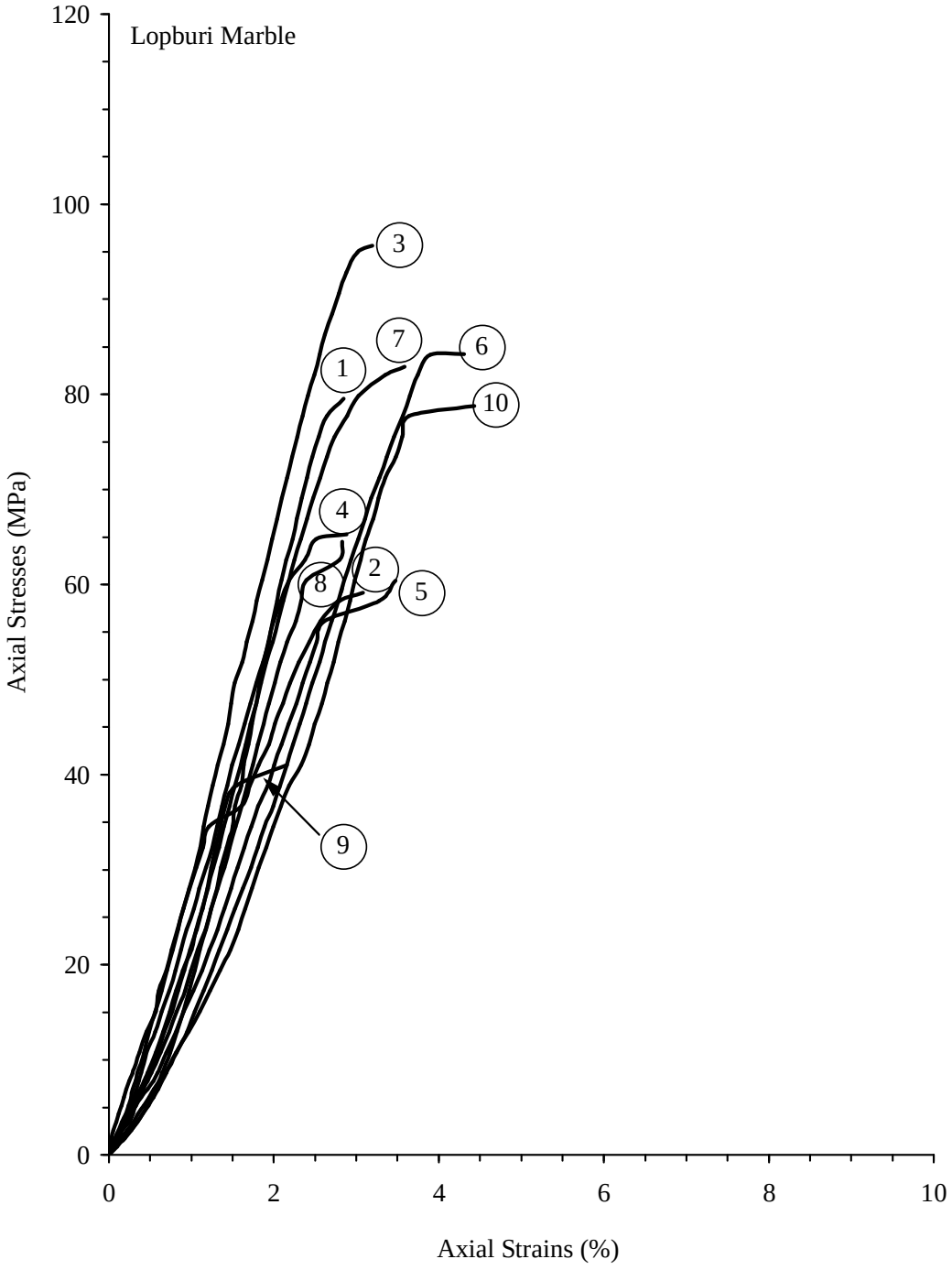

Figure A.6 The axial stress-strain curves for uniaxial compressive strength tests of Lopburi marble.

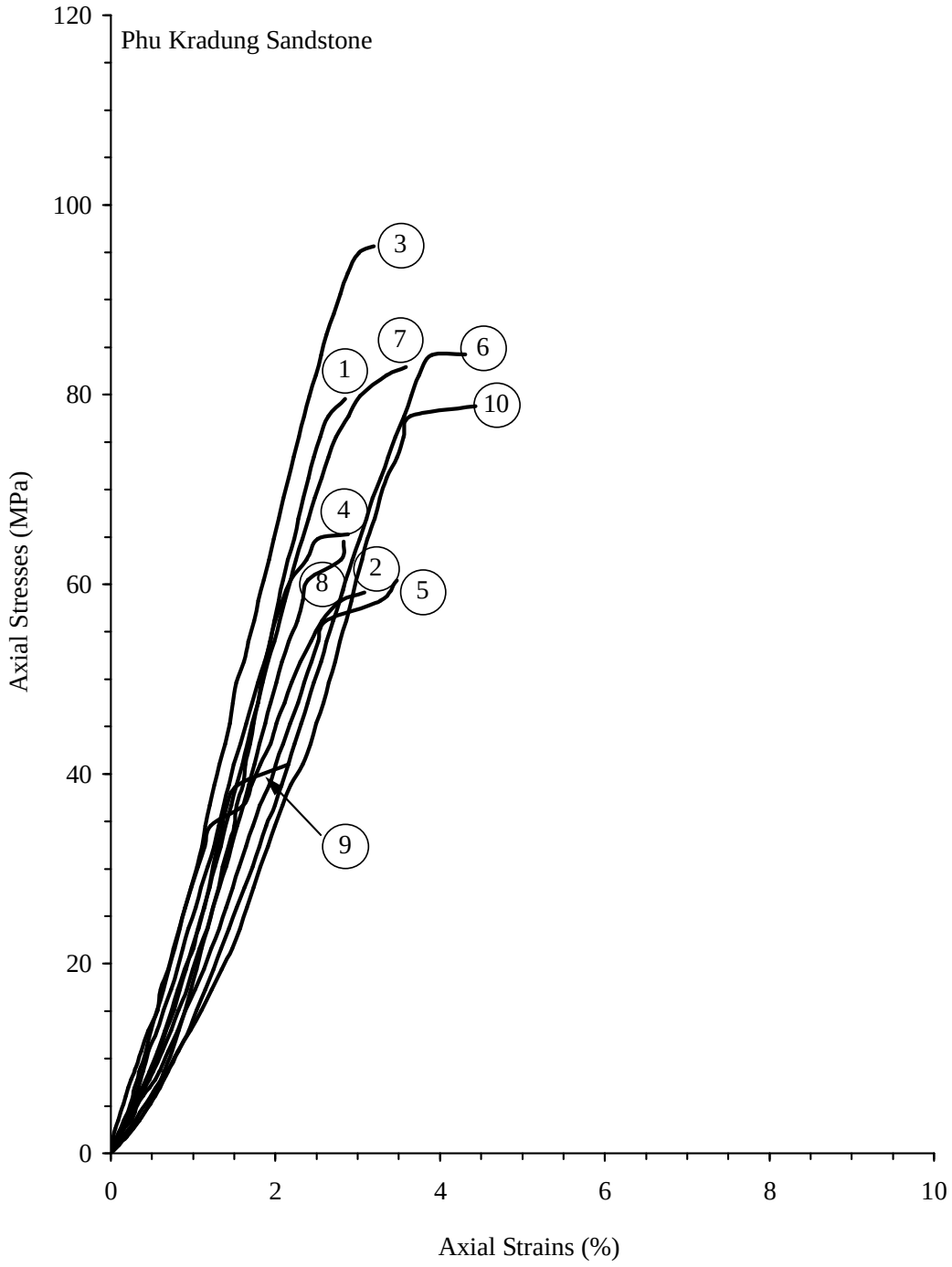

Figure A.7 The axial stress-strain curves for uniaxial compressive strength tests of Phu Kradung sandstone.

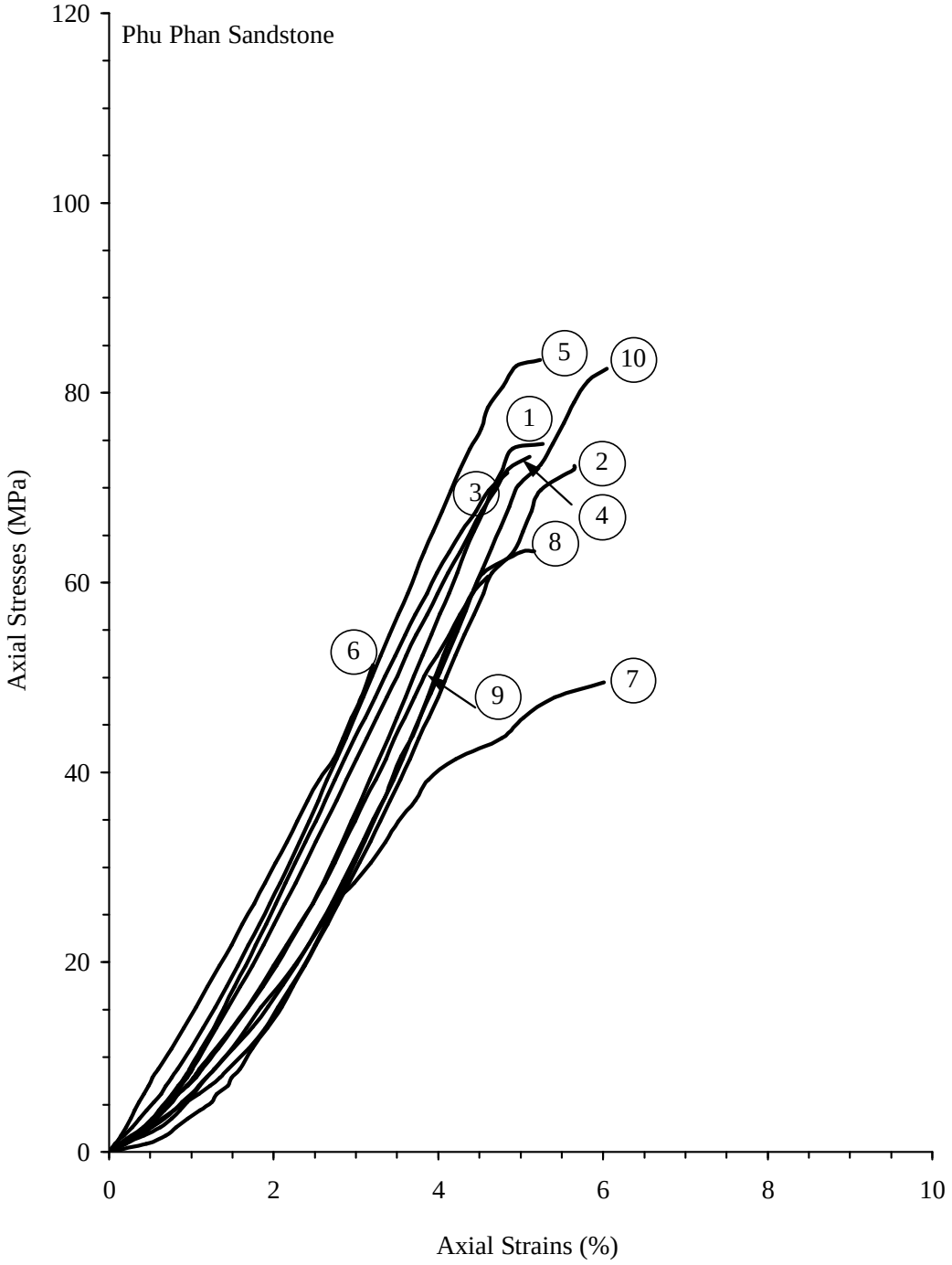

Figure A.8 The axial stress-strain curves for uniaxial compressive strength tests of Phu Phan sandstone.

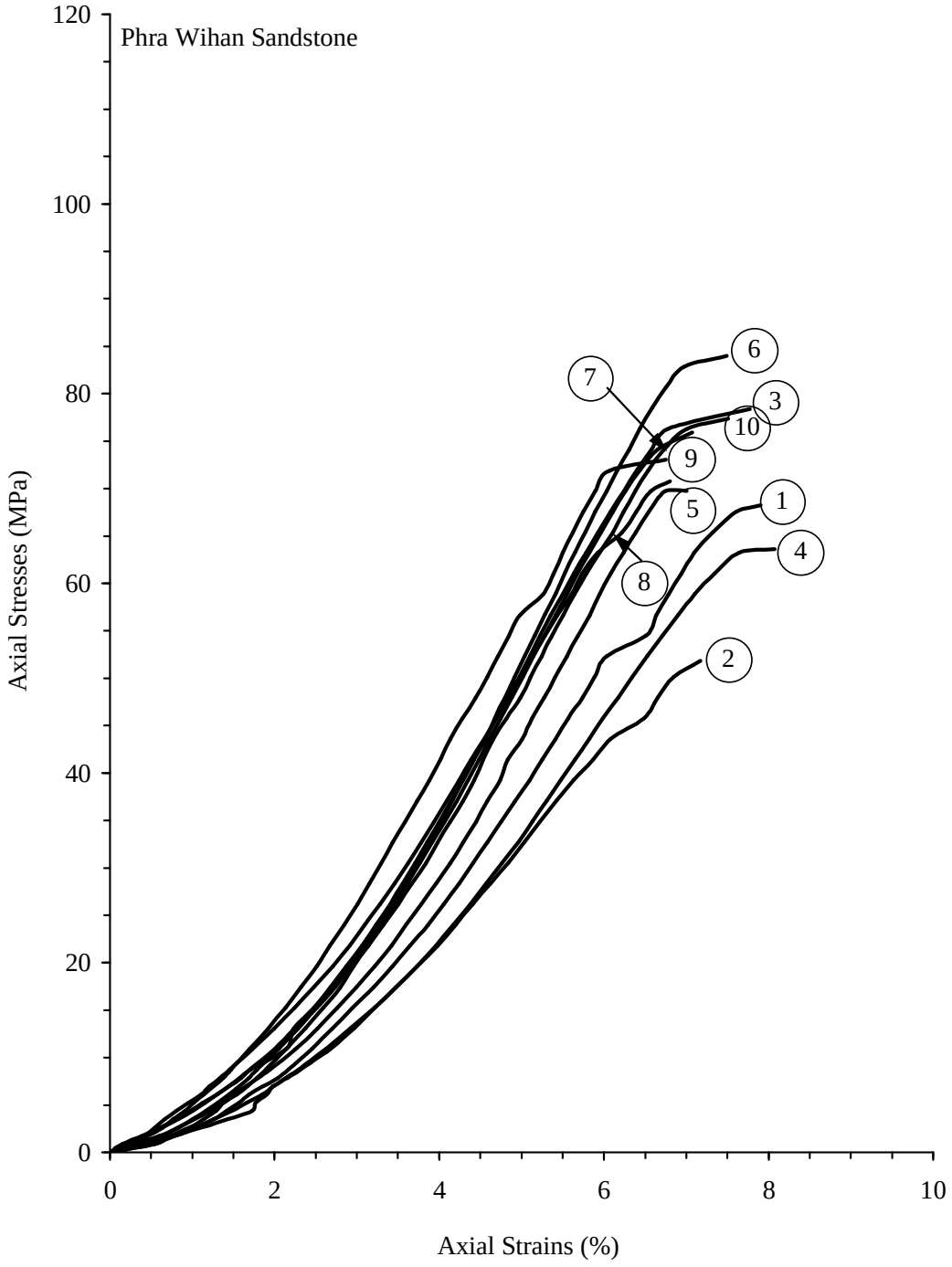

Figure A.9 The axial stress-strain curves for uniaxial compressive strength tests of Phra Wihan sandstone.

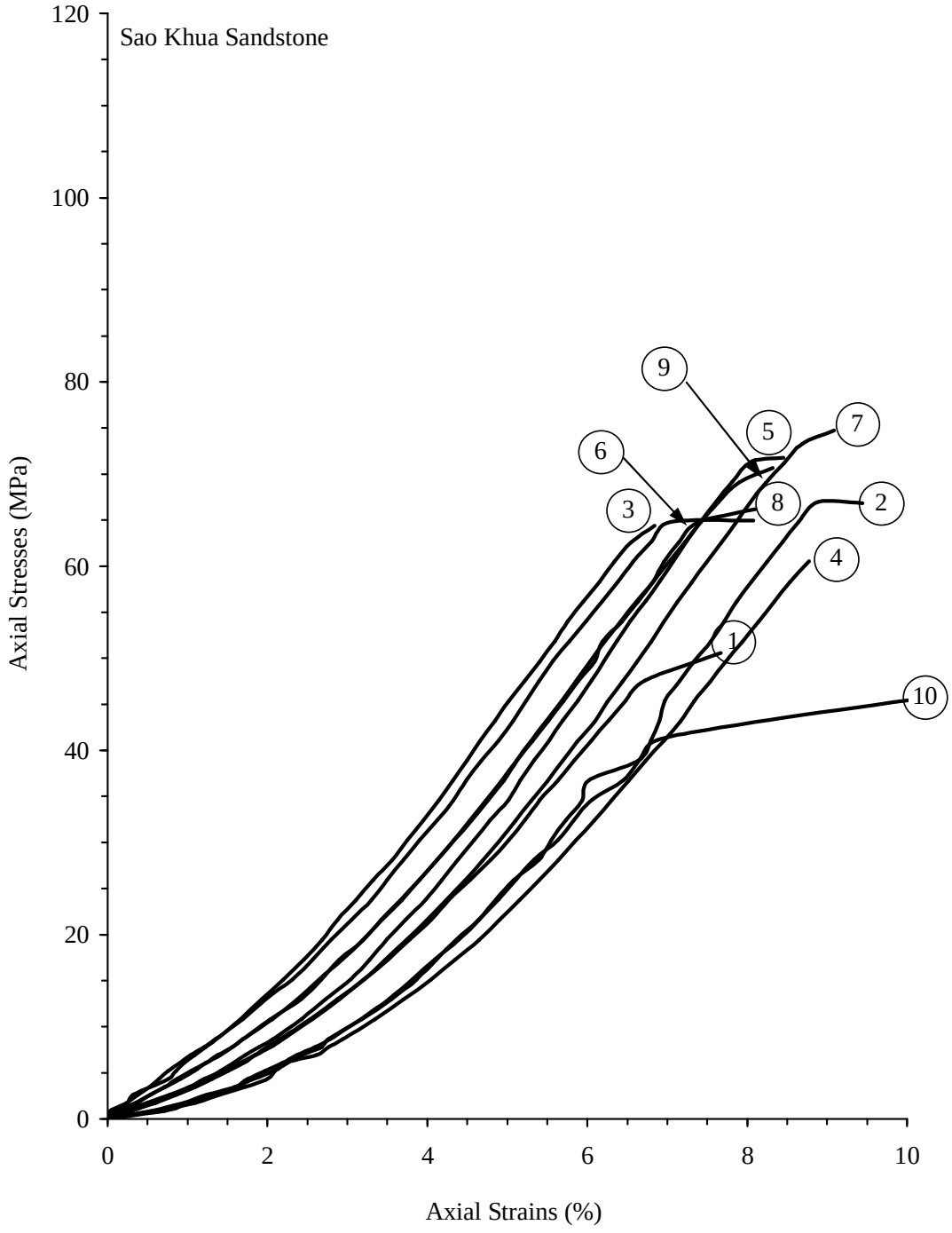

Figure A.10 The axial stress-strain curves for uniaxial compressive strength tests of Sao Khua sandstone.

Table A.1 Results of uniaxial compressive strength tests of Burirum basalt.

Specimen No.	Average Diameter D (mm)	Average Length L (mm)	Density ρ (g/cc)	Failure Stress σ_c (MPa)	Elastic Modulus E (GPa)
BA-22-UCS-01	53.51	137.70	2.81	151.13	32.00
BA-22-UCS-02	53.53	137.18	2.82	228.38	38.00
BA-22-UCS-03	53.55	136.78	2.77	224.77	32.00
BA-22-UCS-04	53.51	137.69	2.81	169.90	30.00
BA-22-UCS-05	53.55	137.32	2.81	201.61	38.00
BA-22-UCS-06	53.52	137.26	2.81	174.58	38.00
BA-22-UCS-07	53.53	137.21	2.81	186.76	31.00
BA-23-UCS-08	53.54	137.40	2.82	207.48	31.00
BA-23-UCS-09	53.54	137.07	2.81	169.90	31.00
BA-23-UCS-10	53.53	137.26	2.81	166.03	31.00
Average Uniaxial Compressive Strength			188.06 ± 26.30 MPa		
Average Elastic Modulus			33.20 ± 3.36 GPa		

Table A.2 Results of uniaxial compressive strength tests of Vietnamese granite.

Specimen No.	Average Diameter D (mm)	Average Length L (mm)	Density ρ (g/cc)	Failure Stress σ_c (MPa)	Elastic Modulus E (GPa)
RGR-01-01-UCS-01	53.75	141.47	2.60	97.42	28.00
RGR-01-02-UCS-02	53.72	141.03	2.63	143.05	38.00
RGR-01-03-UCS-03	53.60	139.41	2.62	129.68	28.50
RGR-01-04-UCS-04	53.60	140.48	2.62	125.90	31.00
RGR-01-05-UCS-05	53.62	141.01	2.61	159.48	37.50
RGR-01-06-UCS-06	53.63	138.35	2.62	131.39	37.50
RGR-01-07-UCS-07	53.55	137.90	2.62	136.06	38.00
RGR-01-08-UCS-08	53.50	138.64	2.63	147.83	37.50
RGR-01-09-UCS-09	53.60	139.47	2.62	146.80	31.00
RGR-01-10-UCS-10	53.55	139.32	2.62	163.09	37.50
Average Uniaxial Compressive Strength				138.07 ± 18.86 MPa	
Average Elastic Modulus				34.45 ± 4.26 GPa	

Table A.3 Results of uniaxial compressive strength tests of Tak granite.

Specimen No.	Average Diameter D (mm)	Average Length L (mm)	Density ρ (g/cc)	Failure Stress σ_c (MPa)	Elastic Modulus E (GPa)
GG-SR-UN-01	53.55	135.06	2.62	124.47	-
GG-SR-UN-02	53.52	135.26	2.62	111.43	35.90
GG-SR-UN-03	53.46	134.53	2.62	77.33	23.93
GG-SR-UN-04	53.51	135.36	2.62	103.21	39.18
GG-SR-UN-05	53.53	133.83	2.62	118.57	31.25
GG-SR-UN-06	53.52	135.73	2.61	127.34	34.68
GG-SR-UN-07	53.49	135.58	2.62	120.68	35.53
GG-SR-UN-08	53.53	135.15	2.62	85.18*	28.12
GG-SR-UN-09	53.48	136.02	2.62	118.92	30.54
GG-SR-UN-10	53.53	135.66	2.62	130.31	32.08
Average Uniaxial Compressive Strength				119.37 ± 8.75 MPa	
Average Elastic Modulus				32.36 ± 4.58 GPa	

Table A.4 Results of uniaxial compressive strength tests of Chinese granite.

Specimen No.	Average Diameter D (mm)	Average Length L (mm)	Density ρ (g/cc)	Failure Stress σ_c (MPa)	Elastic Modulus E (GPa)
WGR-01-01-UCS-01	38.53	77.52	2.63	97.26	32
WGR-01-02-UCS-02	38.43	79.40	2.65	93.20	27
WGR-01-03-UCS-03	38.43	78.53	2.65	141.20	38
WGR-01-04-UCS-04	38.52	78.28	2.64	125.87	36
WGR-01-05-UCS-05	38.43	79.37	2.63	129.12	18
WGR-01-06-UCS-06	38.48	77.87	2.64	121.70	28
WGR-01-07-UCS-07	38.50	78.27	2.63	141.55	39
WGR-01-08-UCS-08	38.52	78.28	2.64	111.11	44
WGR-01-09-UCS-09	38.53	77.40	2.63	97.85	33
WGR-01-10-UCS-10	38.50	78.02	2.64	133.89	43
Average Uniaxial Compressive Strength				119.27 ± 18.34 MPa	
Average Elastic Modulus				34.00 ± 7.97 GPa	

Table A.5 Results of uniaxial compressive strength tests of Saraburi marble.

Specimen No.	Average Diameter D (mm)	Average Length L (mm)	Density ρ (g/cc)	Failure Stress σ_c (MPa)	Elastic Modulus E (GPa)
YMB-01-01-UCS-01	38.37	77.92	2.58	68.26	16
YMB-01-02-UCS-02	38.38	77.58	2.60	87.26	25
YMB-01-03-UCS-03	38.42	77.07	2.61	69.52	26
YMB-01-04-UCS-04	38.40	77.70	2.61	76.18	21
YMB-01-05-UCS-05	38.42	77.88	2.58	89.82	17
YMB-01-06-UCS-06	38.53	77.52	2.56	74.48	24
YMB-01-07-UCS-07	53.77	139.98	2.54	79.49	26
YMB-01-08-UCS-08	53.77	136.63	2.58	61.14	15
YMB-01-09-UCS-09	53.57	140.31	2.57	61.25	18
YMB-01-10-UCS-10	53.58	139.59	2.60	102.42	25
Average Uniaxial Compressive Strength				78.69 ± 14.57 MPa	
Average Elastic Modulus				21.30 ± 4.42 GPa	

Table A.6 Results of uniaxial compressive strength tests of Lopburi marble.

Specimen No.	Average Diameter D (mm)	Average Length L (mm)	Density ρ (g/cc)	Failure Stress σ_c (MPa)	Elastic Modulus E (GPa)
MB-SR-UN-01	53.77	133.38	2.71	79.51	29.38
MB-SR-UN-02	53.78	133.72	2.72	59.09	28.78
MB-SR-UN-03	53.78	133.38	2.72	95.57	32.36
MB-SR-UN-04	53.73	135.04	2.72	65.32	29.70
MB-SR-UN-05	53.78	132.95	2.72	60.32	25.02
MB-SR-UN-06	53.76	133.93	2.73	84.21	25.46
MB-SR-UN-07	53.79	133.32	2.72	82.80	30.25
MB-SR-UN-08	53.78	134.25	2.72	64.43	27.81
MB-SR-UN-09	53.77	133.61	2.71	39.86	31.14
MB-SR-UN-10	53.78	133.68	2.72	78.71	27.40
Average Uniaxial Compressive Strength				74.44 ± 12.62 MPa	
Average Elastic Modulus				28.73 ± 2.35 GPa	

Table A.7 Results of uniaxial compressive strength tests of Phu Kradung sandstone.

Specimen No.	Average Diameter D (mm)	Average Length L (mm)	Density ρ (g/cc)	Failure Stress σ_c (MPa)	Elastic Modulus E (GPa)
GST-01-UCS-01	53.50	138.83	2.53	82.67	13.39
GST-01-UCS-02	53.52	138.92	2.53	75.18	11.57
GST-01-UCS-03	53.50	138.92	2.54	65.49	11.94
GST-01-UCS-04	53.49	138.95	2.54	76.03	12.56
GST-01-UCS-05	53.49	138.71	2.53	66.00	11.61
GST-01-UCS-06	53.46	138.85	2.51	72.24	11.39
GST-01-UCS-07	53.51	138.08	2.54	71.10	11.63
GST-01-UCS-08	53.50	137.55	2.56	79.51	13.02
GST-01-UCS-09	53.50	137.54	2.56	72.38	12.19
GST-01-UCS-10	53.49	138.24	2.53	67.71	12.21
Average Uniaxial Compressive Strength				72.83 ± 5.65 MPa	
Average Elastic Modulus				12.15 ± 0.67 GPa	

Table A.8 Results of uniaxial compressive strength tests of Phu Phan sandstone.

Specimen No.	Average Diameter D (mm)	Average Length L (mm)	Density ρ (g/cc)	Failure Stress σ_c (MPa)	Elastic Modulus E (GPa)
YST-01-UCS-01	53.52	137.93	2.25	81.92	18.81
YST-01-UCS-02	53.51	137.95	2.29	72.33	18.29
YST-01-UCS-03	53.52	137.03	2.29	71.59	17.91
YST-01-UCS-04	53.51	138.17	2.25	73.29	17.77
YST-01-UCS-05	53.52	137.40	2.25	83.50	19.61
YST-01-UCS-06	53.52	137.85	2.27	51.29	17.05
YST-01-UCS-07	53.52	137.08	2.25	49.51	10.78
YST-01-UCS-08	53.52	137.48	2.25	63.31	17.17
YST-01-UCS-09	53.51	136.61	2.25	60.64	19.02
YST-01-UCS-10	53.50	136.88	2.25	74.60	20.24
Average Uniaxial Compressive Strength				72.37 ± 8.53 MPa	
Average Elastic Modulus				18.43 ± 1.08 GPa	

Table A.9 Results of uniaxial compressive strength tests of Phra Wihan sandstone.

Specimen No.	Average Diameter D (mm)	Average Length L (mm)	Density ρ (g/cc)	Failure Stress σ_c (MPa)	Elastic Modulus E (GPa)
WST-01-UCS-01	53.52	137.68	2.32	77.40	14.79
WST-02-UCS-02	53.50	137.65	2.32	51.81	10.22
WST-03-UCS-03	53.51	136.96	2.33	78.38	15.08
WST-04-UCS-04	53.50	136.56	2.32	63.62	11.12
WST-05-UCS-05	53.52	136.60	2.33	69.77	14.63
WST-06-UCS-06	53.50	137.59	2.34	83.98	16.62
WST-07-UCS-07	53.51	137.03	2.33	75.89	15.17
WST-08-UCS-08	53.52	136.47	2.33	70.77	13.86
WST-09-UCS-09	53.52	138.01	2.33	73.08	15.18
WST-10-UCS-10	53.51	137.42	2.32	68.21	12.65
Average Uniaxial Compressive Strength				71.29 ± 8.96 MPa	
Average Elastic Modulus				13.93 ± 2.00 GPa	

Table A.10 Results of uniaxial compressive strength tests of Sao Khua sandstone.

Specimen No.	Average Diameter D (mm)	Average Length L (mm)	Density ρ (g/cc)	Failure Stress σ_c (MPa)	Elastic Modulus E (GPa)
RST-01-UCS-01	53.69	137.23	2.33	45.43	8.45
RST-01-UCS-02	53.75	137.68	2.33	66.78	11.31
RST-01-UCS-03	53.76	136.92	2.32	64.34	11.77
RST-01-UCS-04	53.77	137.04	2.32	60.47	10.39
RST-01-UCS-05	53.73	136.84	2.33	71.71	11.97
RST-01-UCS-06	53.75	138.64	2.33	64.88	11.57
RST-01-UCS-07	53.80	137.58	2.32	74.69	11.87
RST-01-UCS-08	53.76	138.10	2.32	66.12	11.33
RST-01-UCS-09	53.76	138.28	2.32	70.61	11.46
RST-01-UCS-10	53.73	137.03	2.33	50.54	9.87
Average Uniaxial Compressive Strength				67.45 ± 4.59 MPa	
Average Elastic Modulus				11.46 ± 0.50 GPa	

APPENDIX B

DIRECT SHEAR STRENGTH TEST RESULTS ON THE SAW CUT SURFACES

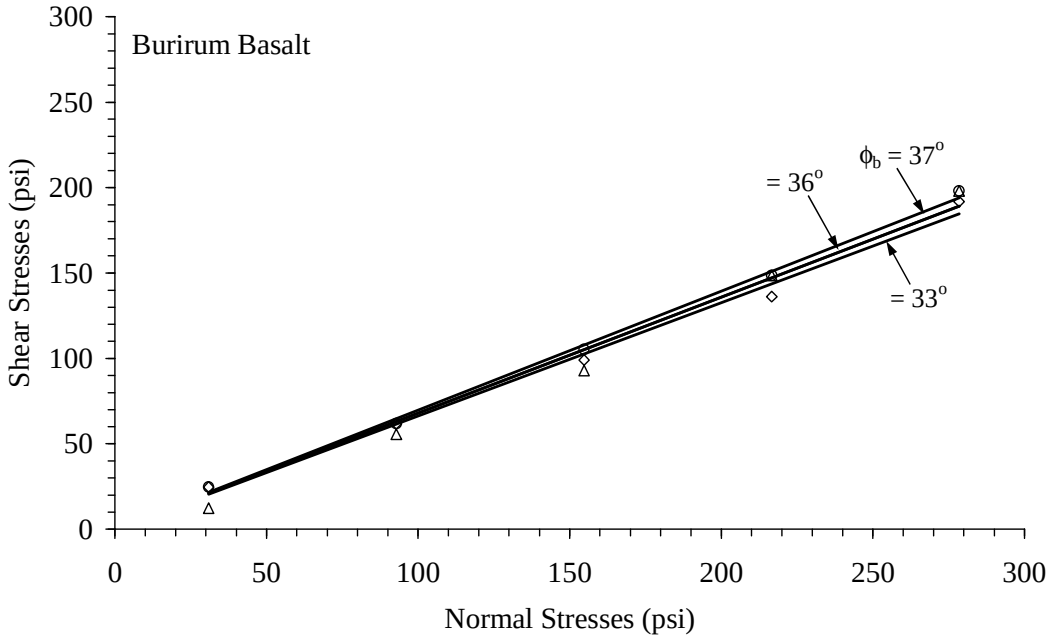

Figure B.1 Shear stresses plotted as a function of normal stresses for 3 specimens of Burirum basalt.

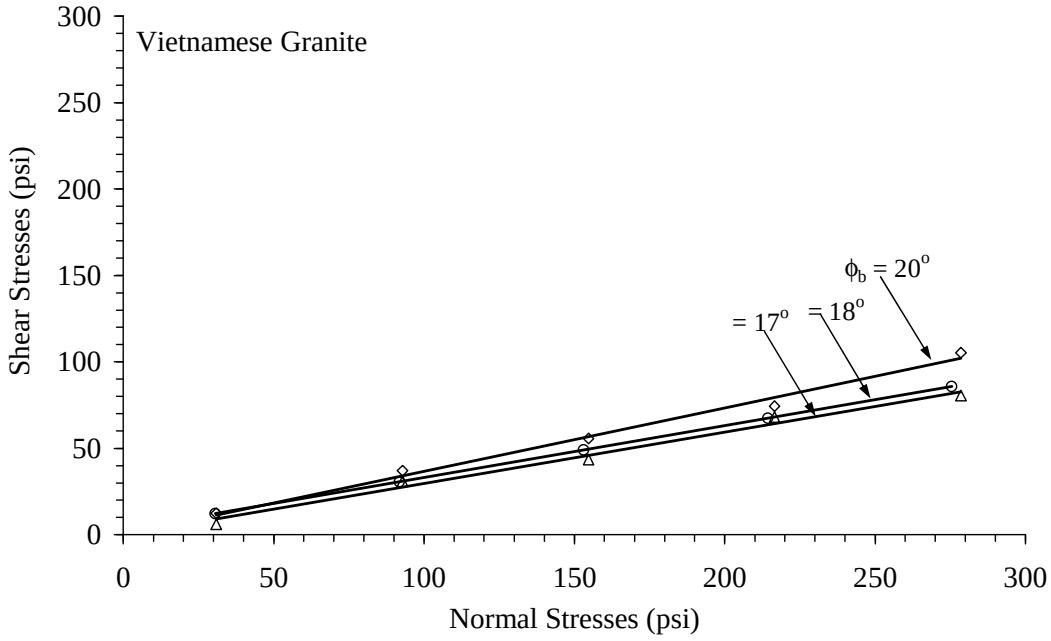

Figure B.2 Shear stresses plotted as a function of normal stresses for 3 specimens of Vietnamese granite.

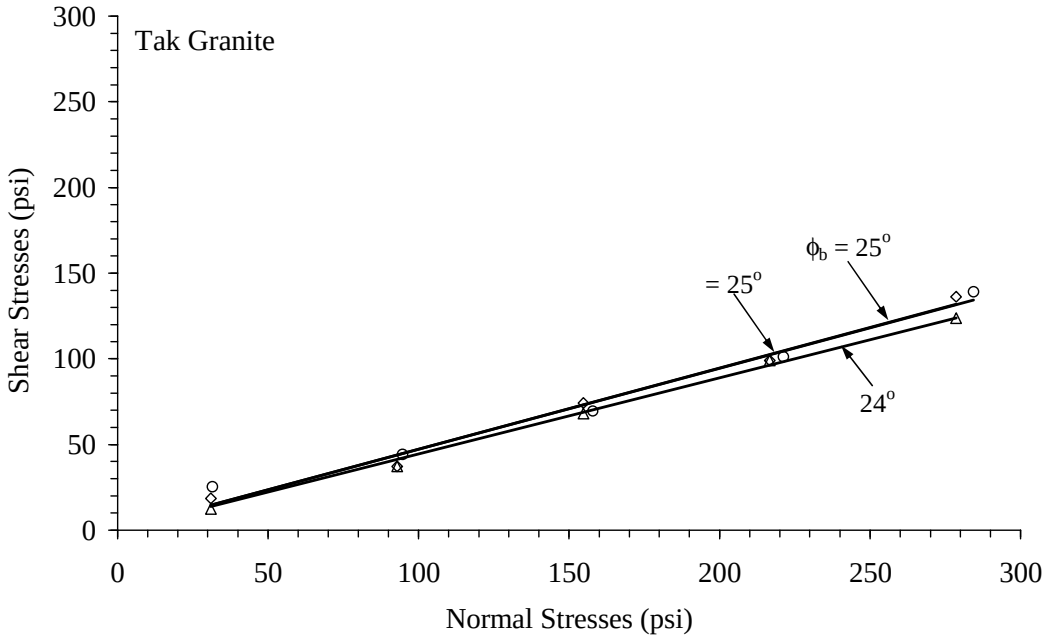

Figure B.3 Shear stresses plotted as a function of normal stresses for 3 specimens of Tak granite.

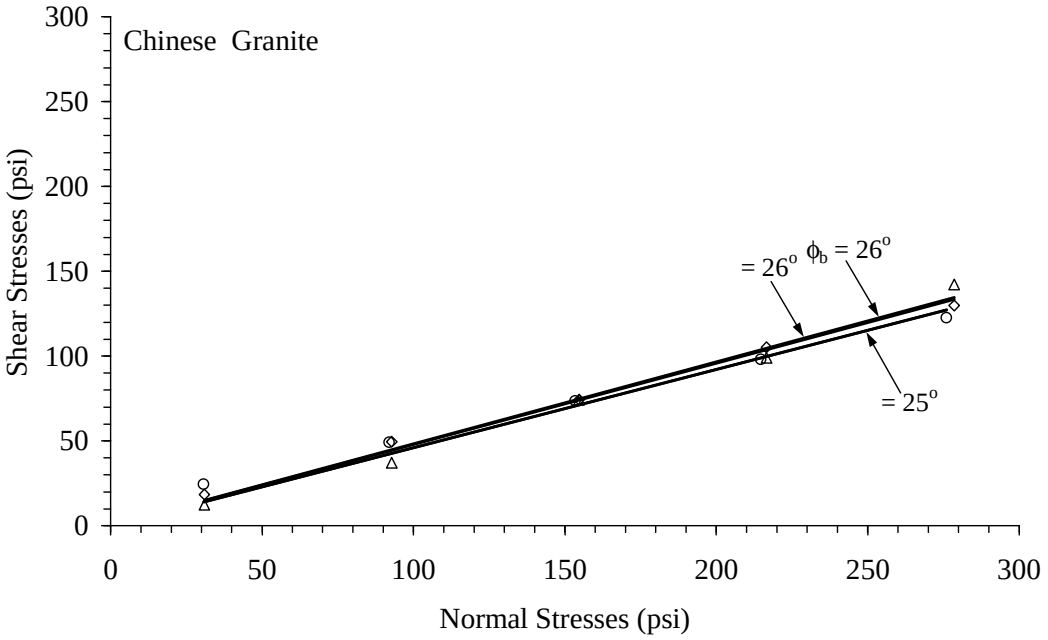

Figure B.4 Shear stresses plotted as a function of normal stresses for 3 specimens of Chinese granite.

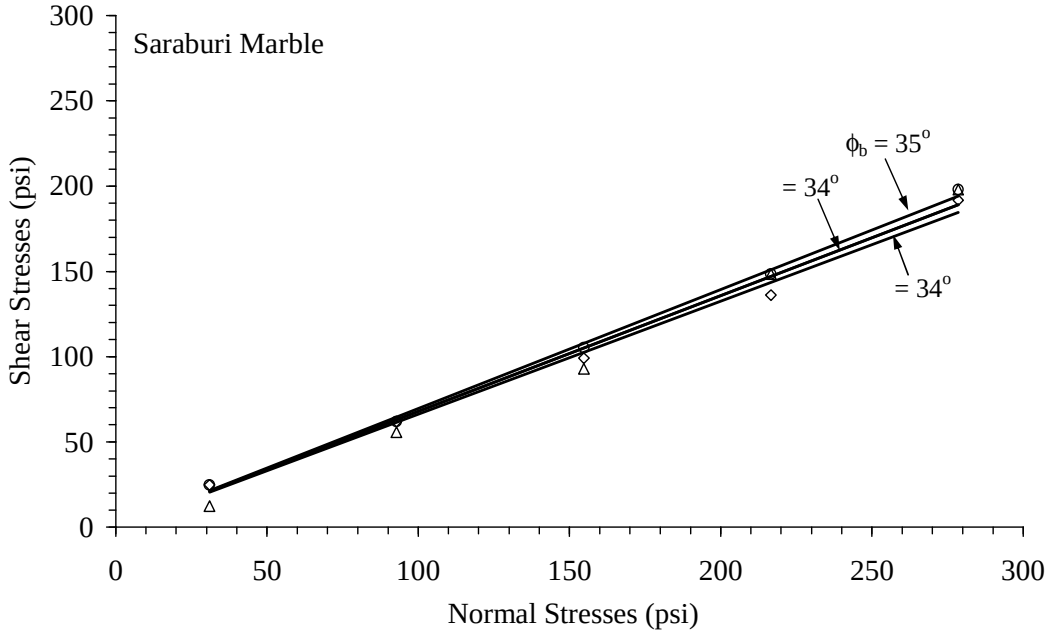

Figure B.5 Shear stresses plotted as a function of normal stresses for 3 specimens of Saraburi marble.

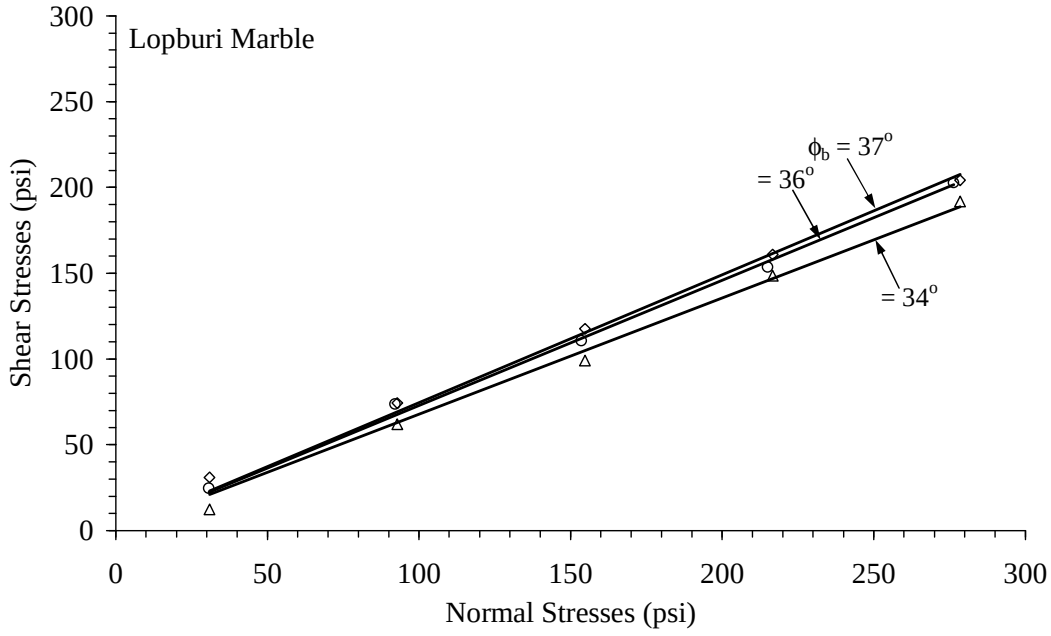

Figure B.6 Shear stresses plotted as a function of normal stresses for 3 specimens of Lopburi marble.

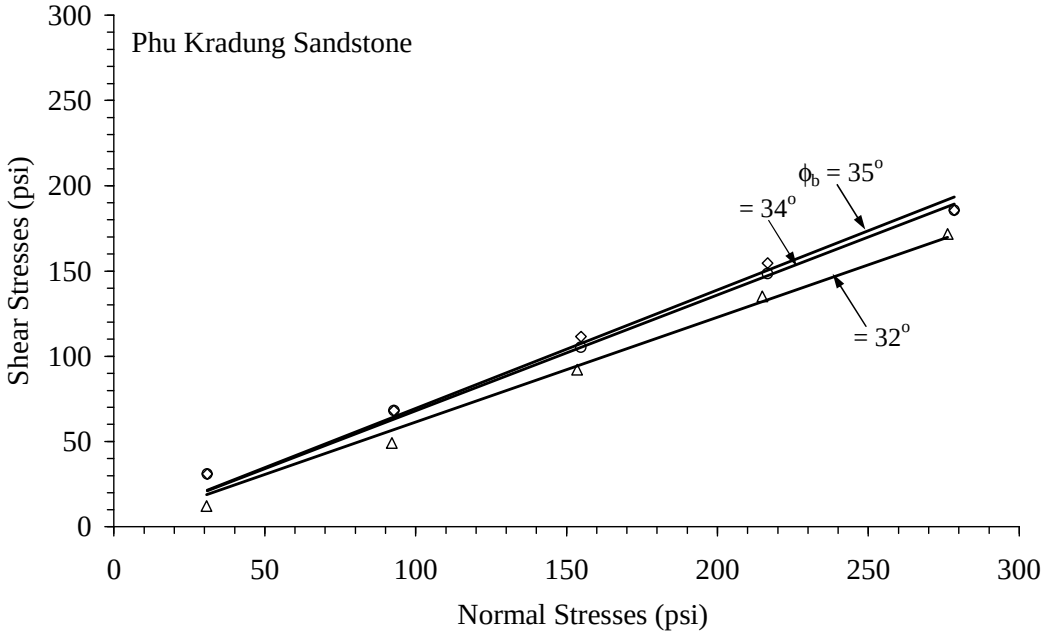

Figure B.7 Shear stresses plotted as a function of normal stresses for 3 specimens of Phu Kradung sandstone.

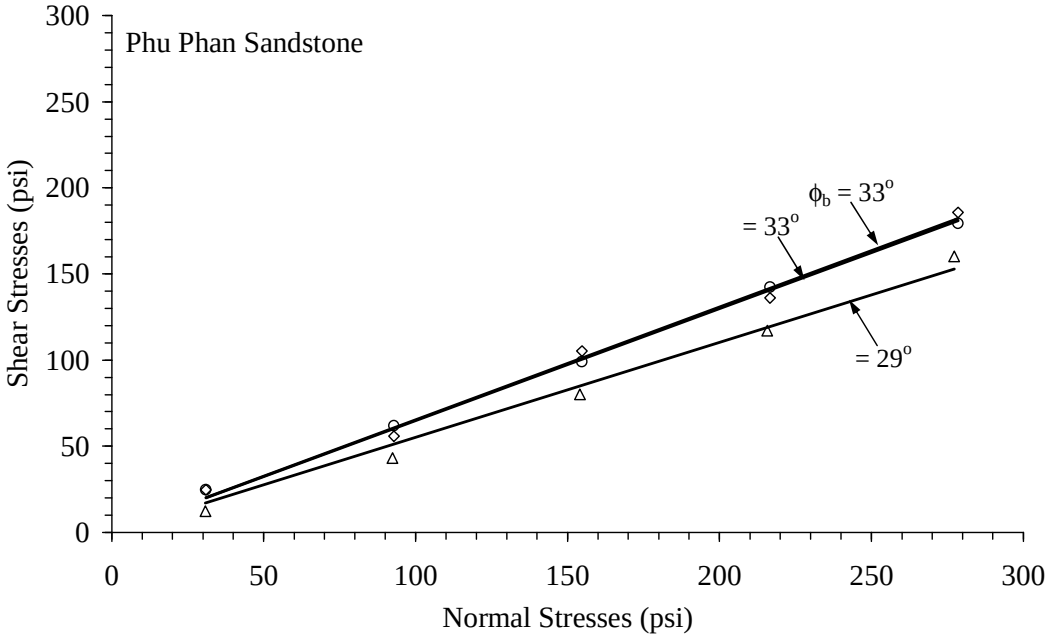

Figure B.8 Shear stresses plotted as a function of normal stresses for 3 specimens of Phu Phan sandstone.

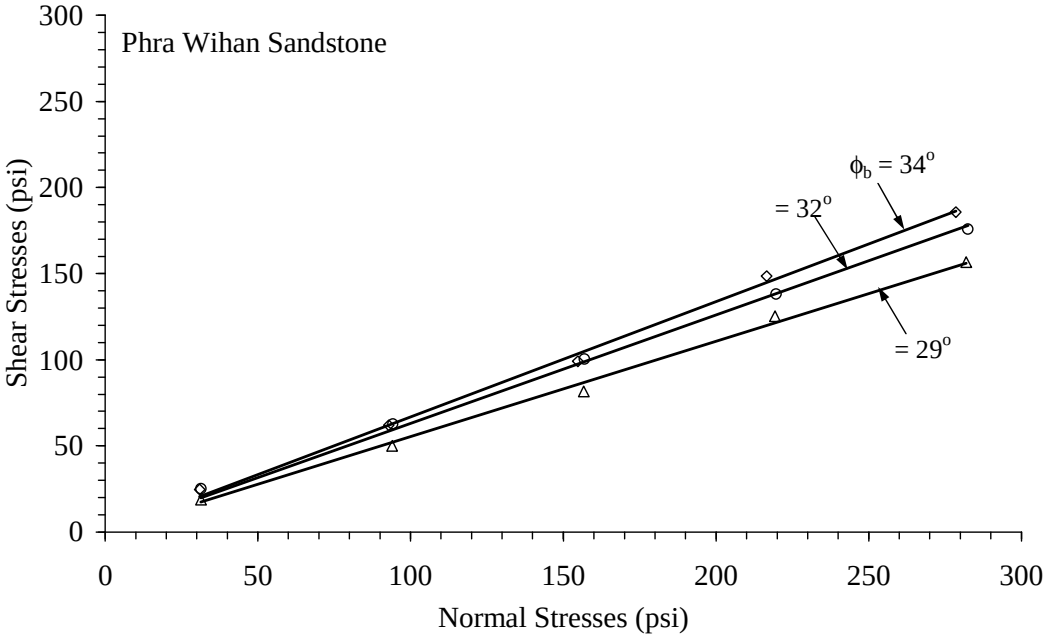

Figure B.9 Shear stresses plotted as a function of normal stresses for 3 specimens of Phra Wihan sandstone.

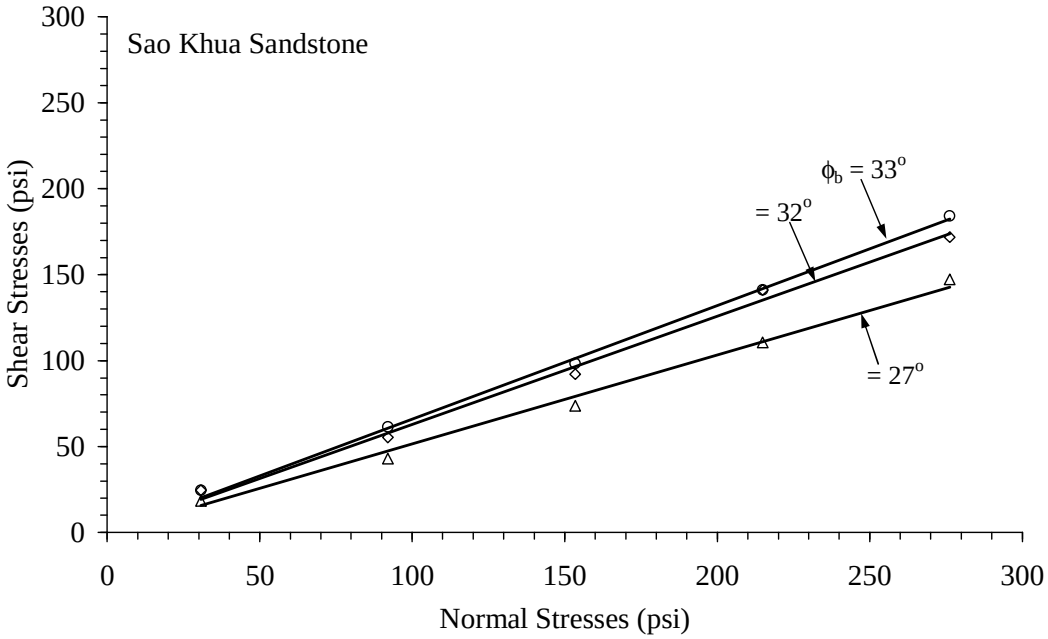

Figure B.10 Shear stresses plotted as a function of normal stresses for 3 specimens of Sao Khua sandstone.

APPENDIX C

FORCE-DISPLACEMENT CURVES FROM DIRECT SHEAR TESTS ON ROUGH JOINTS

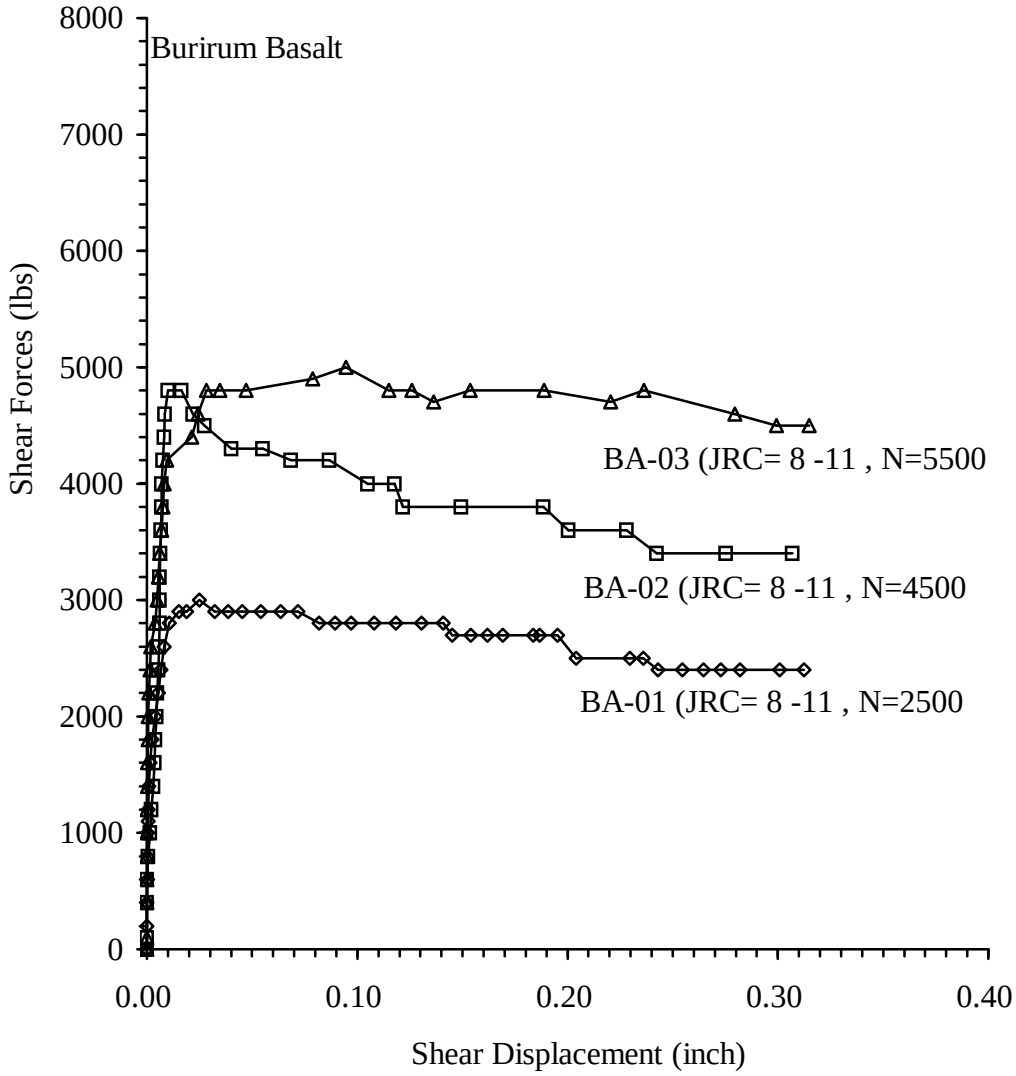

Figure C.1 Shear force plotted against shear displacement of Burirum basalt.

JRC = Joint Roughness Coefficient, N = Normal Load

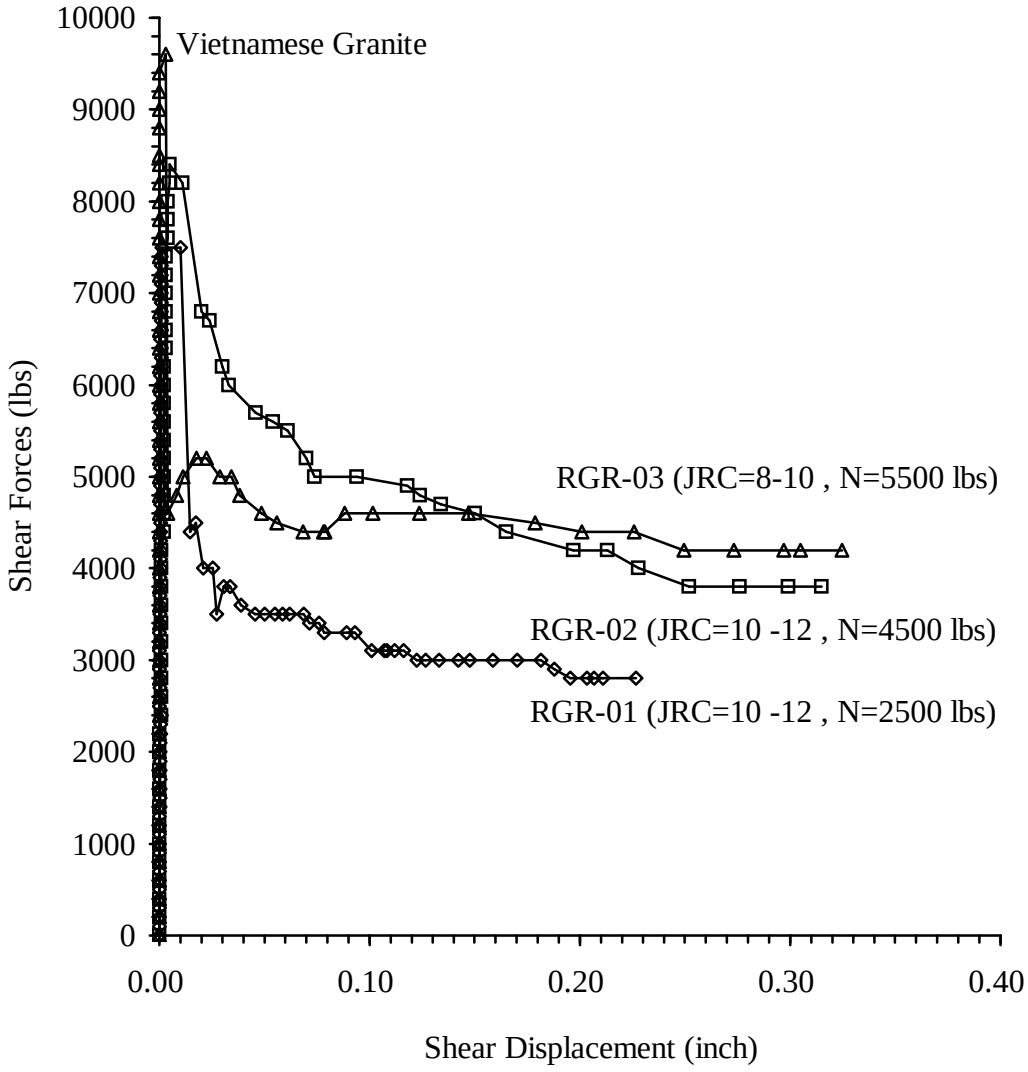

Figure C.2 Shear force plotted against shear displacement of Vietnamese Granite.

JRC = Joint Roughness Coefficient, N = Normal Load

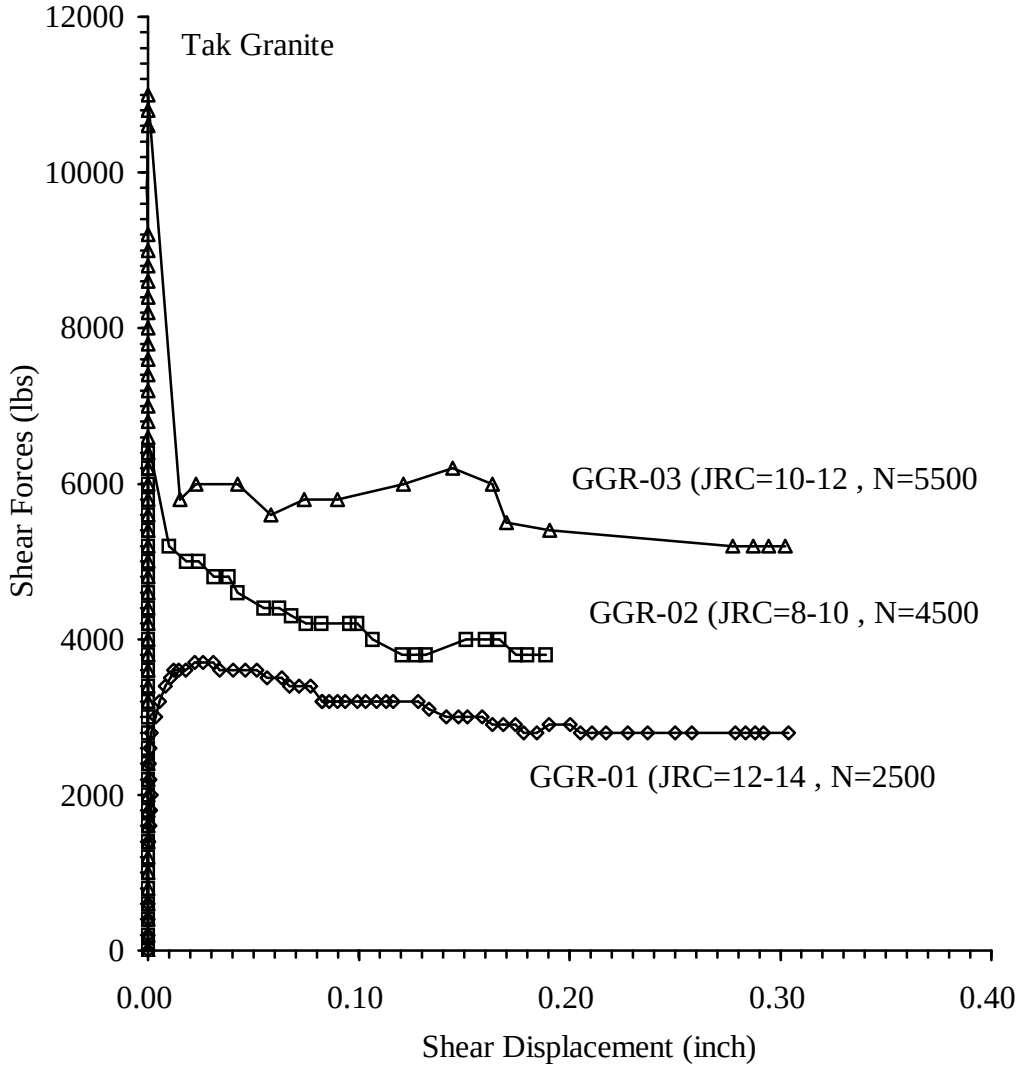

Figure C.3 Shear force plotted against shear displacement of Tak Granite.

JRC = Joint Roughness Coefficient, N = Normal Load

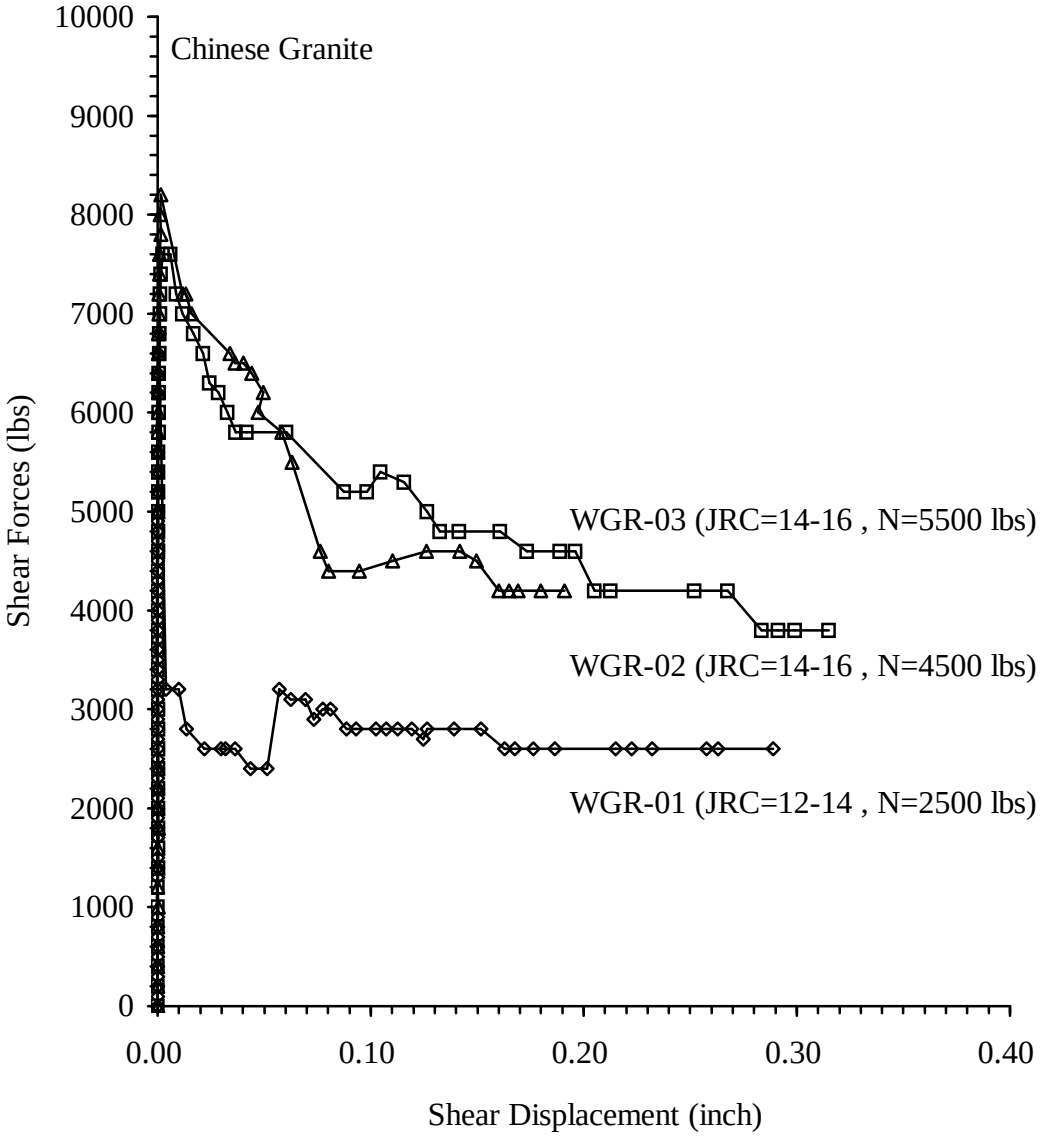

Figure C.4 Shear force plotted against shear displacement of Chinese granite.

JRC = Joint Roughness Coefficient, N = Normal Load

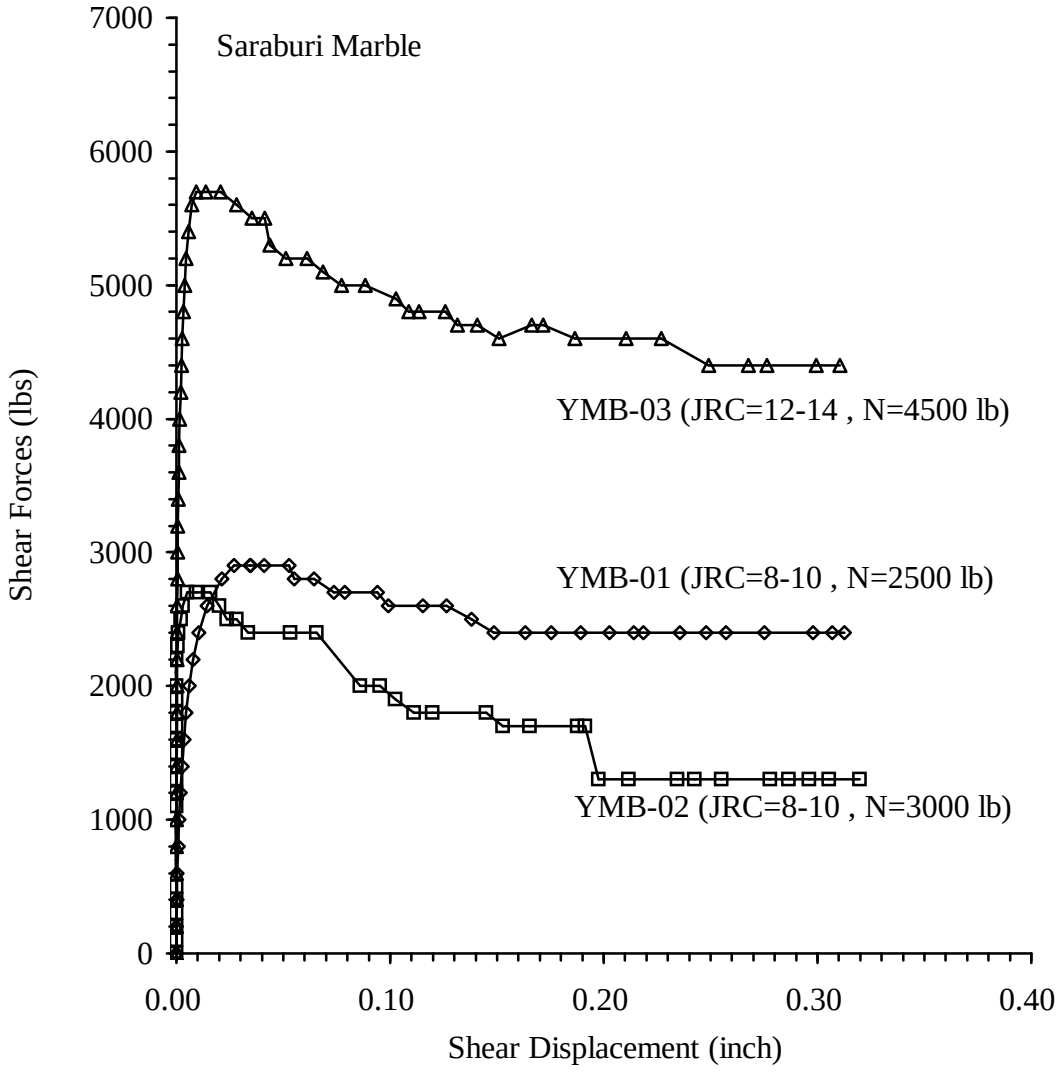

Figure C.5 Shear force plotted against shear displacement of Saraburi Marble.

JRC = Joint Roughness Coefficient, N = Normal Load

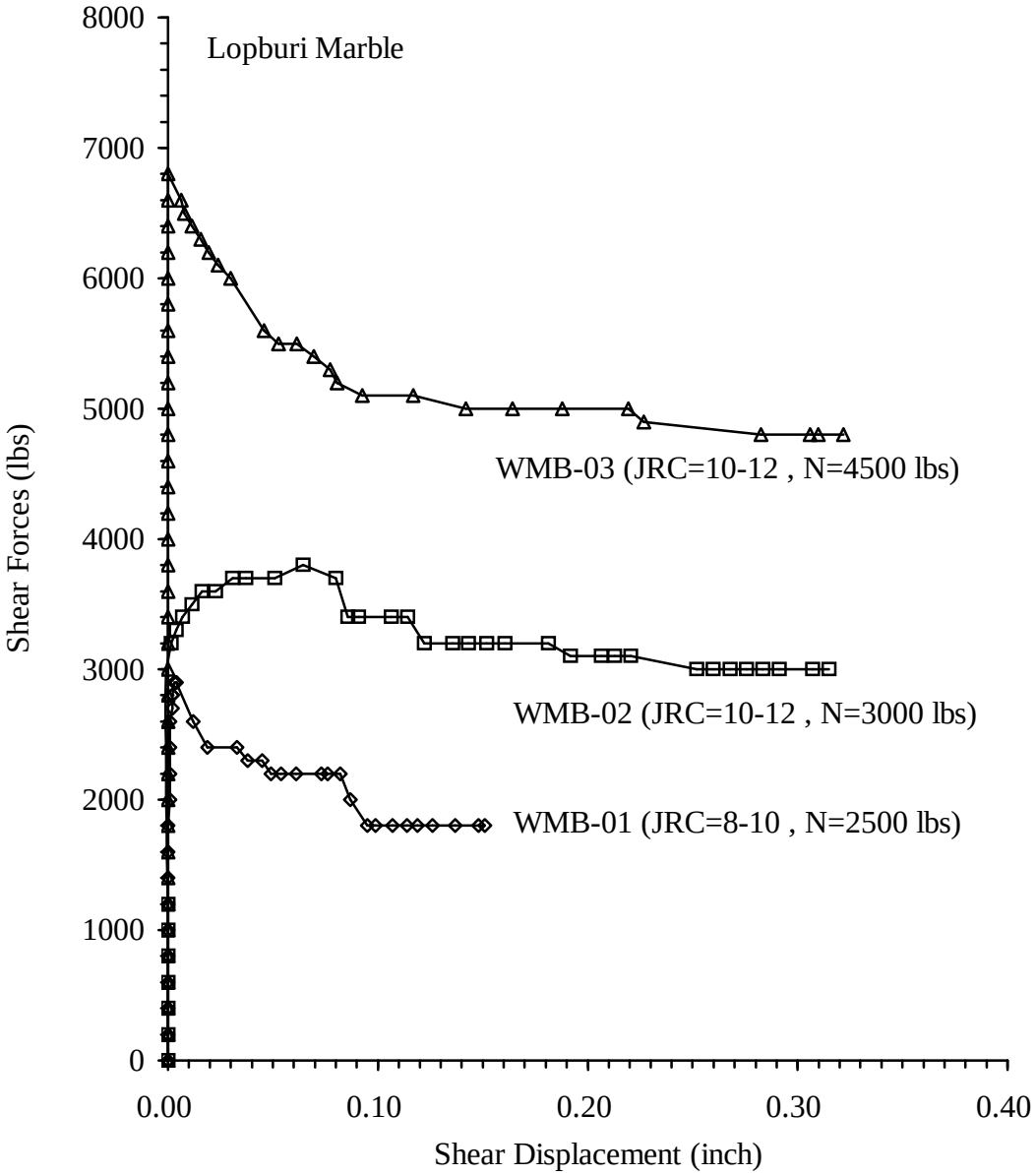

Figure C.6 Shear force plotted against shear displacement of Lopburi Marble.

JRC = Joint Roughness Coefficient, N = Normal Load

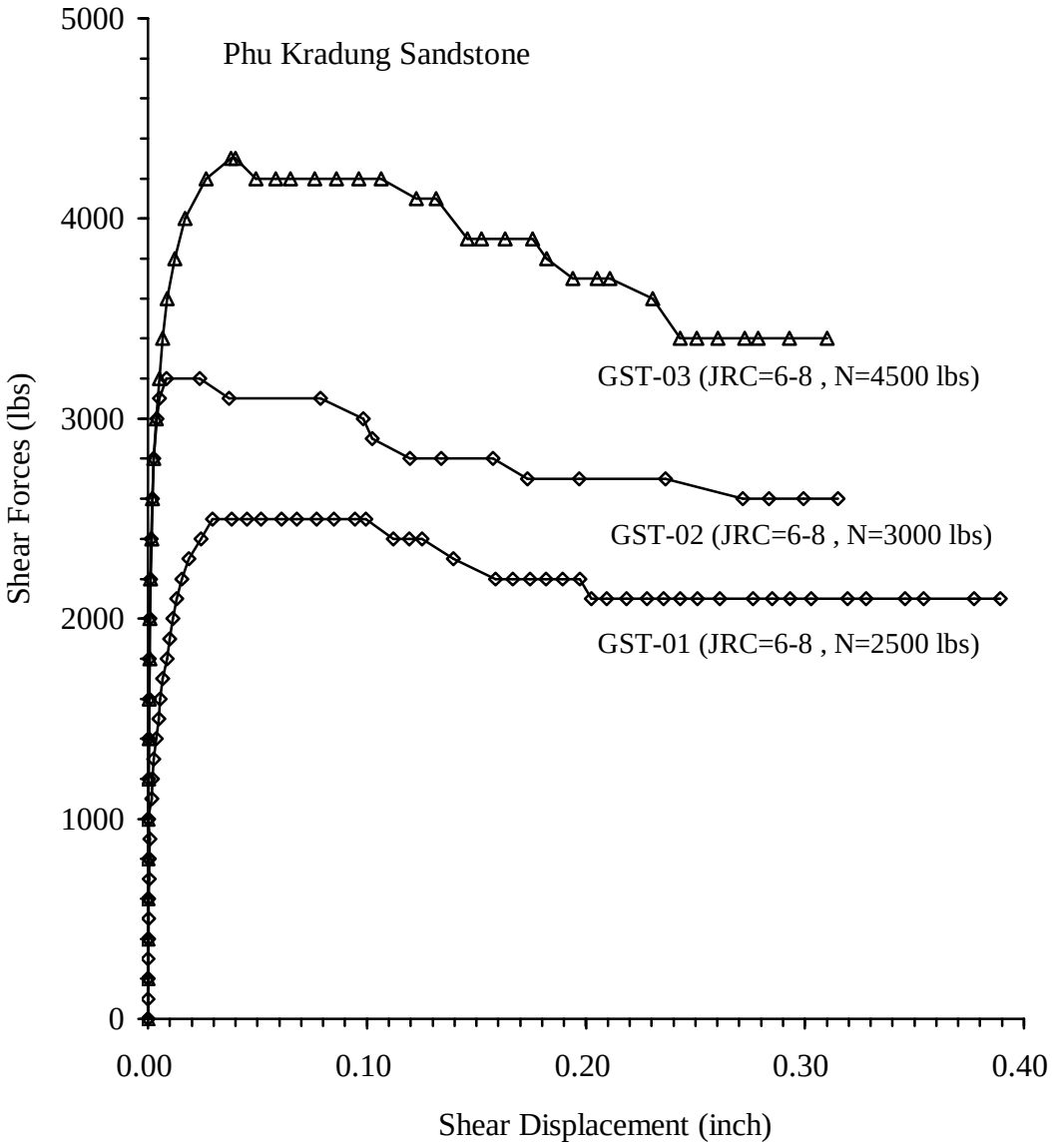

Figure C.7 Shear force plotted against shear displacement of Phu Kradung Sandstone.

JRC = Joint Roughness Coefficient, N = Normal Load

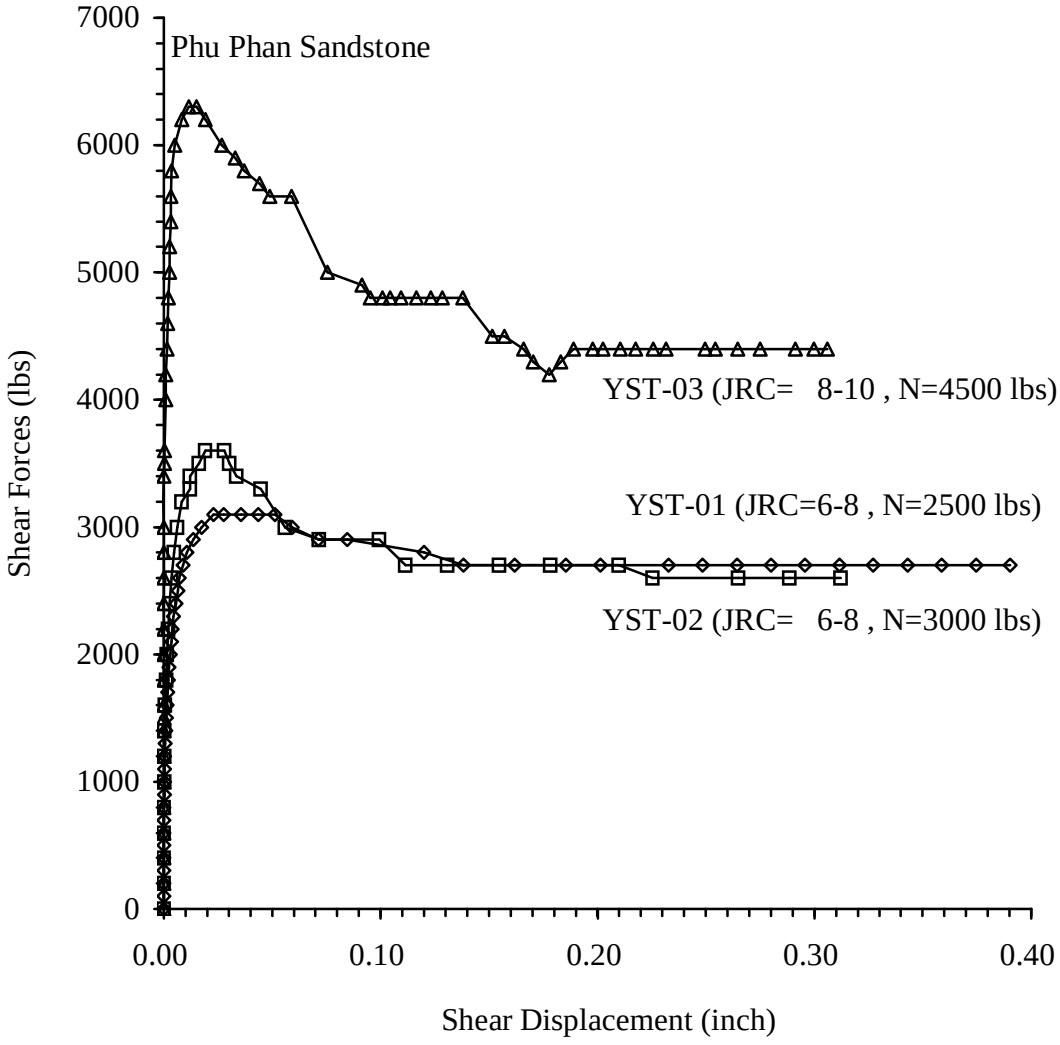

Figure C.8 Shear force plotted against shear displacement of Phu Phan Sandstone.

JRC = Joint Roughness Coefficient, N = Normal Load

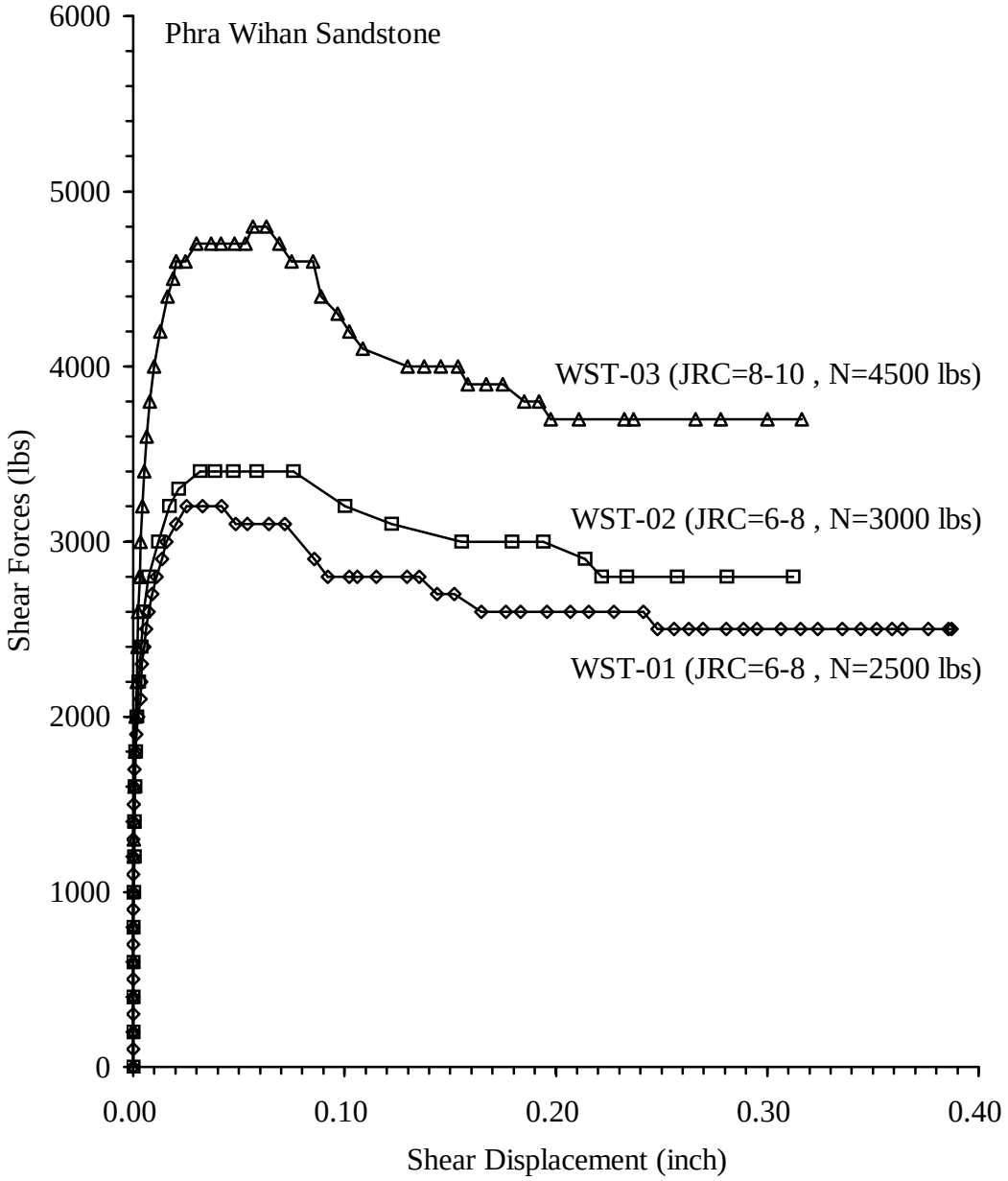

Figure C.9 Shear force plotted against shear displacement of Phra Wihan Sandstone.

JRC = Joint Roughness Coefficient, N = Normal Load

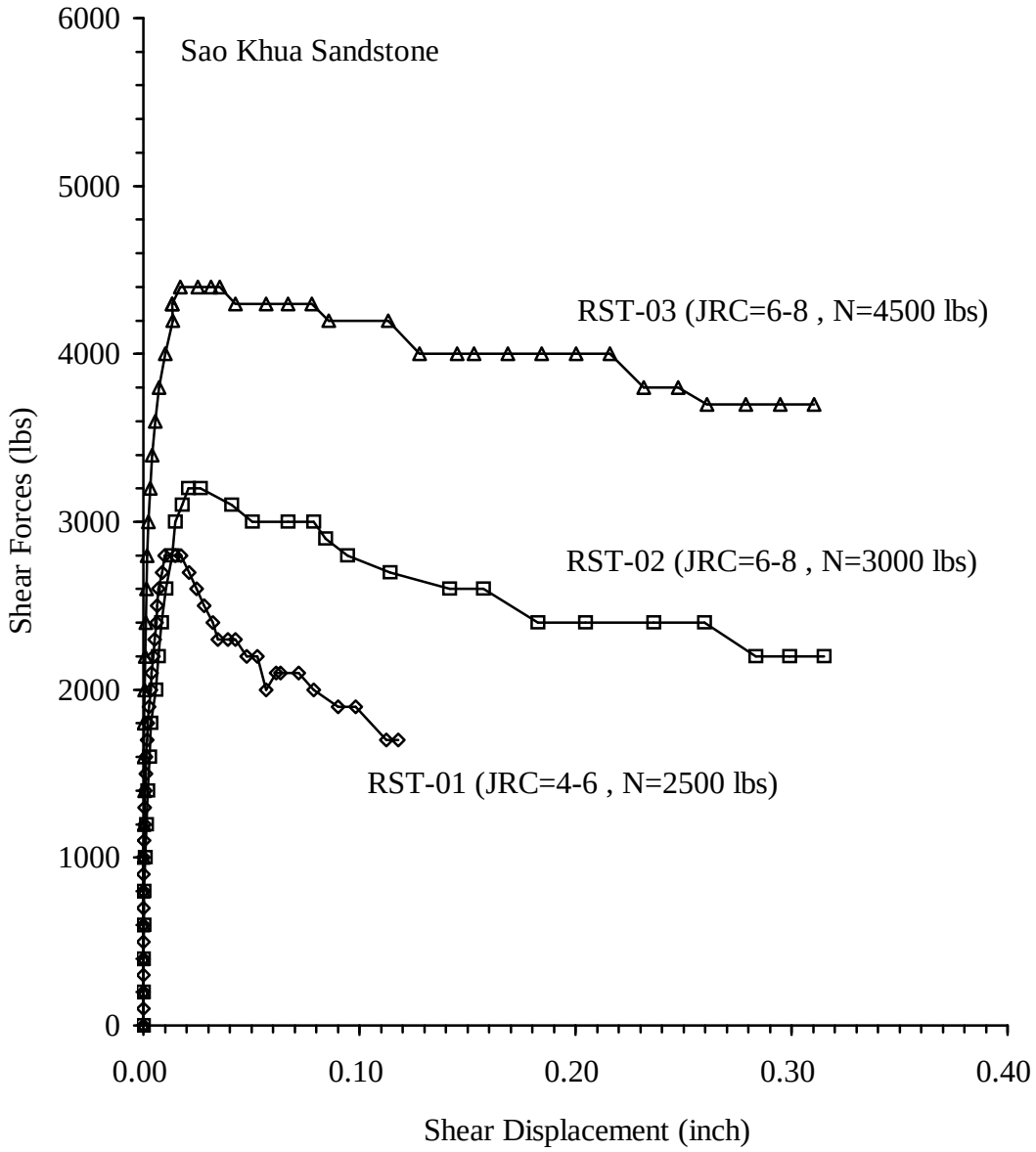

Figure C.10 Shear force plotted against shear displacement of Sao Khua Sandstone.

JRC = Joint Roughness Coefficient, N = Normal Load

BIOGRAPHY

Mr. Rutthapol Kemthong was born on March 14, 1973 in Nakhon Nayok province, Thailand. He received his Bachelor's Degree in Engineering (Civil Engineering) form Rajamangala University of Technology Isan in 1996. After graduation, he has been employed under the position of site engineer by Siphaya Construction Co., Ltd. He served in position of lecturer at Faculty of Industrial Technology, Nakhon Ratchasima Rajabhat University in 1999. He continued with his graduate studies in the Geological Engineering Program, Institute of Engineering, Suranaree University of Technology.